FINAL REPORT

CO_2 LASER MODELING

Contract No. NAS8-36955, D.O. 130

Prof. Barry Johnson, Principal Investigator

Prepared for

Marshall Space Flight Center
National Aeronautics and Space Administration
Huntsville, AL 35812

Prepared by

Center for Applied Optics
University of Alabama in Huntsville
Huntsville, AL 35899

July 1992

THIS REPORT CONTAINS LAWS CONTRACTOR SPECIFIC INFORMATION
AND IS COMPETITION SENSITIVE

Table of Contents

1 CO_2 Laser Kinetics Modeling

1.1 Introduction

This chapter presents results from the modeling of the CO_2 laser kinetics undertaken during the year. An overview of the model is provided by the viewgraphs in Appendix 2.

1.2 The Boltzmann Equation

When a discharge is formed, the electrons in the discharge move at much higher velocities than the molecules and ions present. In the case of a brief pulsed discharge of a few microseconds, the ions and molecules are essentially stationary and only the electron velocity distribution need be considered. Additionally at the pressures under consideration here, the mean free path between collisions for the electrons is small compared to the discharge volume. For elastic electron-molecule collisions, the large mass difference of the colliding particles results in small energy transfers compared to the collision energy of the electrons, and also results in large electron deflections. This, together with the small mean free path mean that the velocity distribution of the electrons is almost independent of the direction of the velocity. This makes the calculation task much easier.

When an electron collides with a molecule energy can be transfered to the molecule such that:-

a) the molecule momentum changes.

b) one or a combination of the vibrational states of the molecule is/are excited.

c) electrons bound to the molecule become excited.

d) the molecule is ionised.

Figures 1.1-1.11 show electron collision cross-sections for these processes for the CO_2 molecule. There are several cross-sections for excitation of the 0n0 + n00 CO_2 vibrational levels, each represents a different loss process.

As the gas mixture also contains He and N_2 electron collision cross-sections for these are also required by the Boltzmann solver.

CO2 Momentum Transfer Cross-Section From Electron Collision

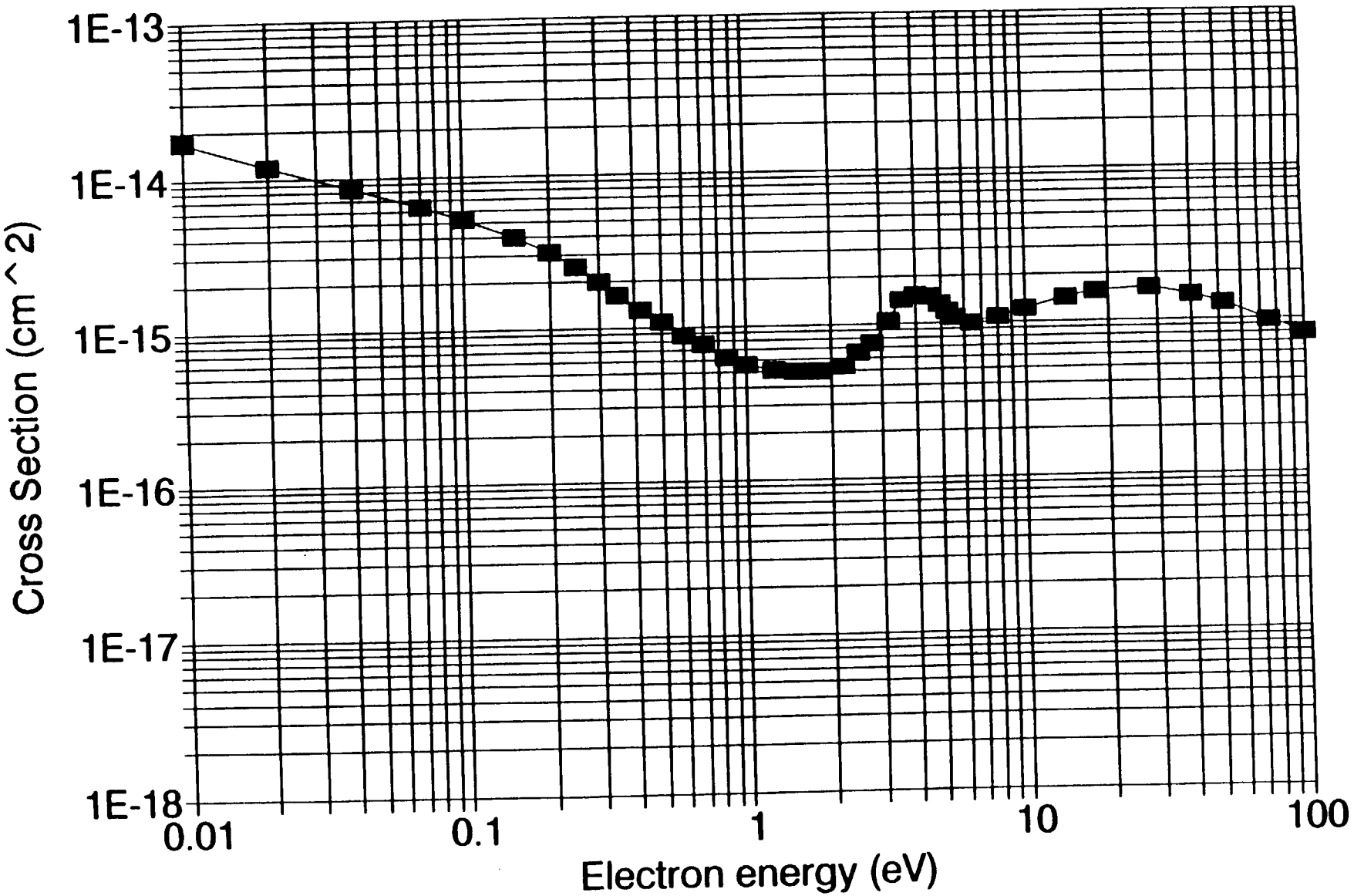

CO2 010 Level Excitation Cross-Section From Electron Collision

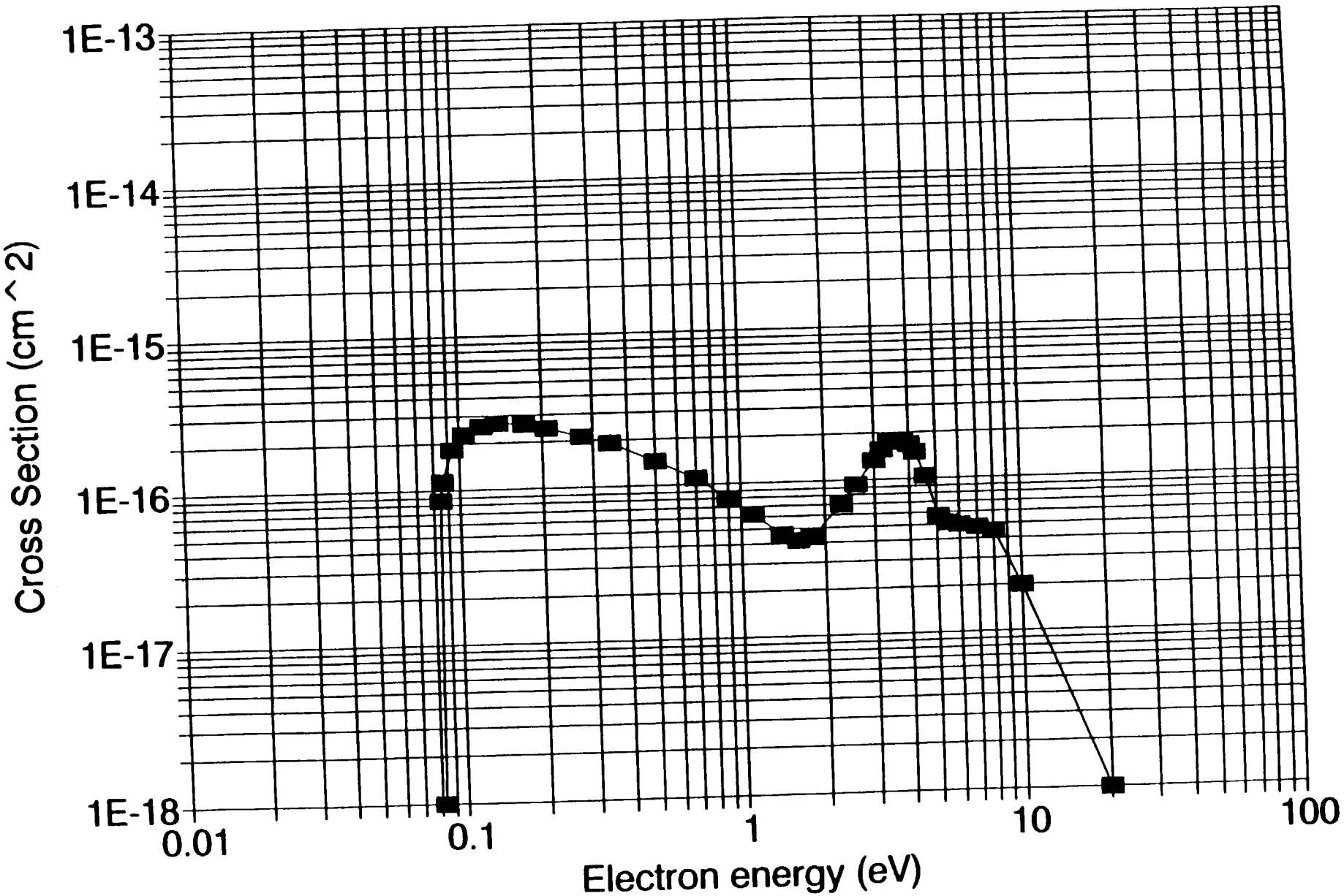

Fig 1.2

CO2 100 + 020 Level Excitation Cross-Section From Electron Collision

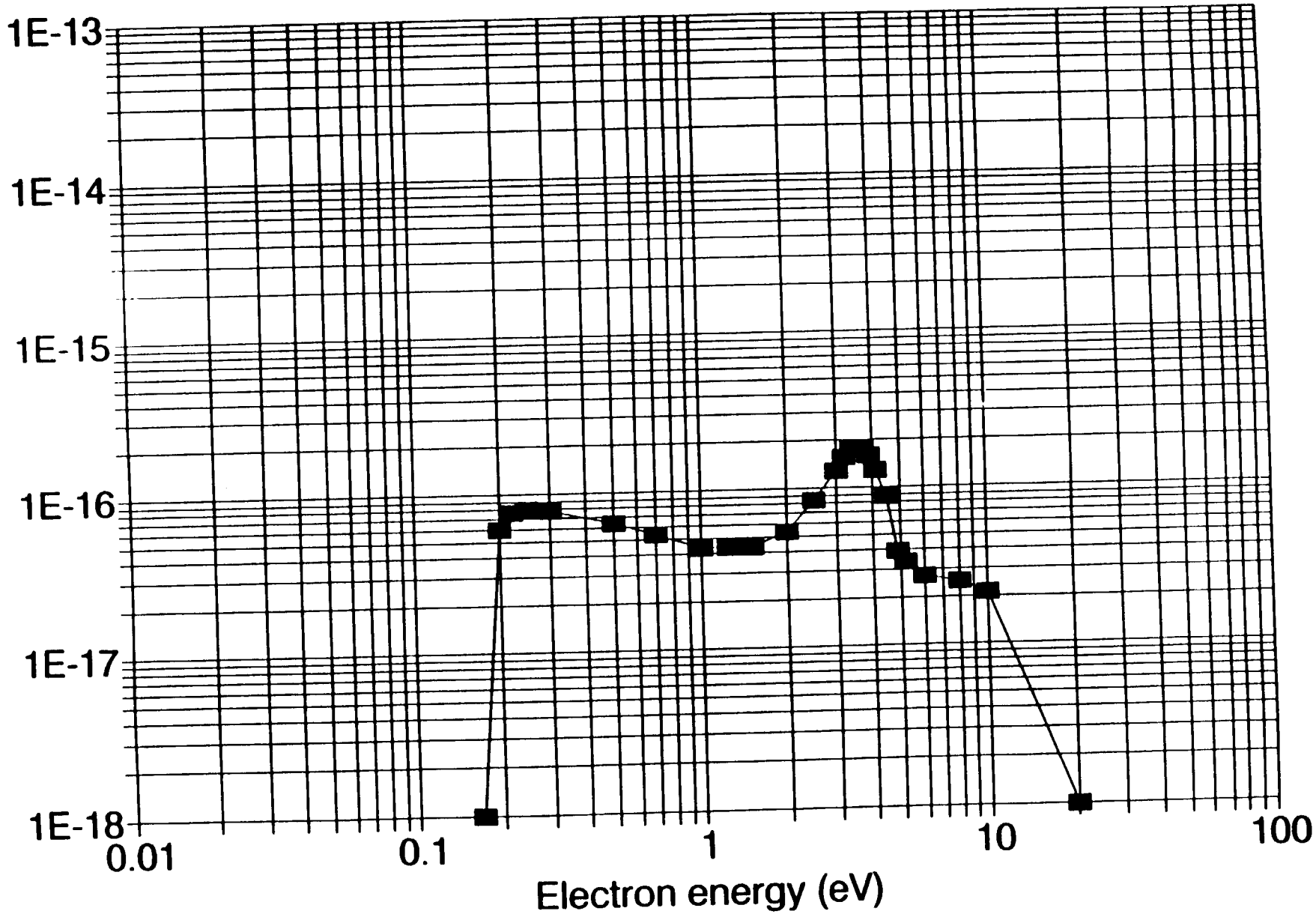

Fig 1.3 4

CO2 001 Level Excitation Cross-Section From Electron Collision

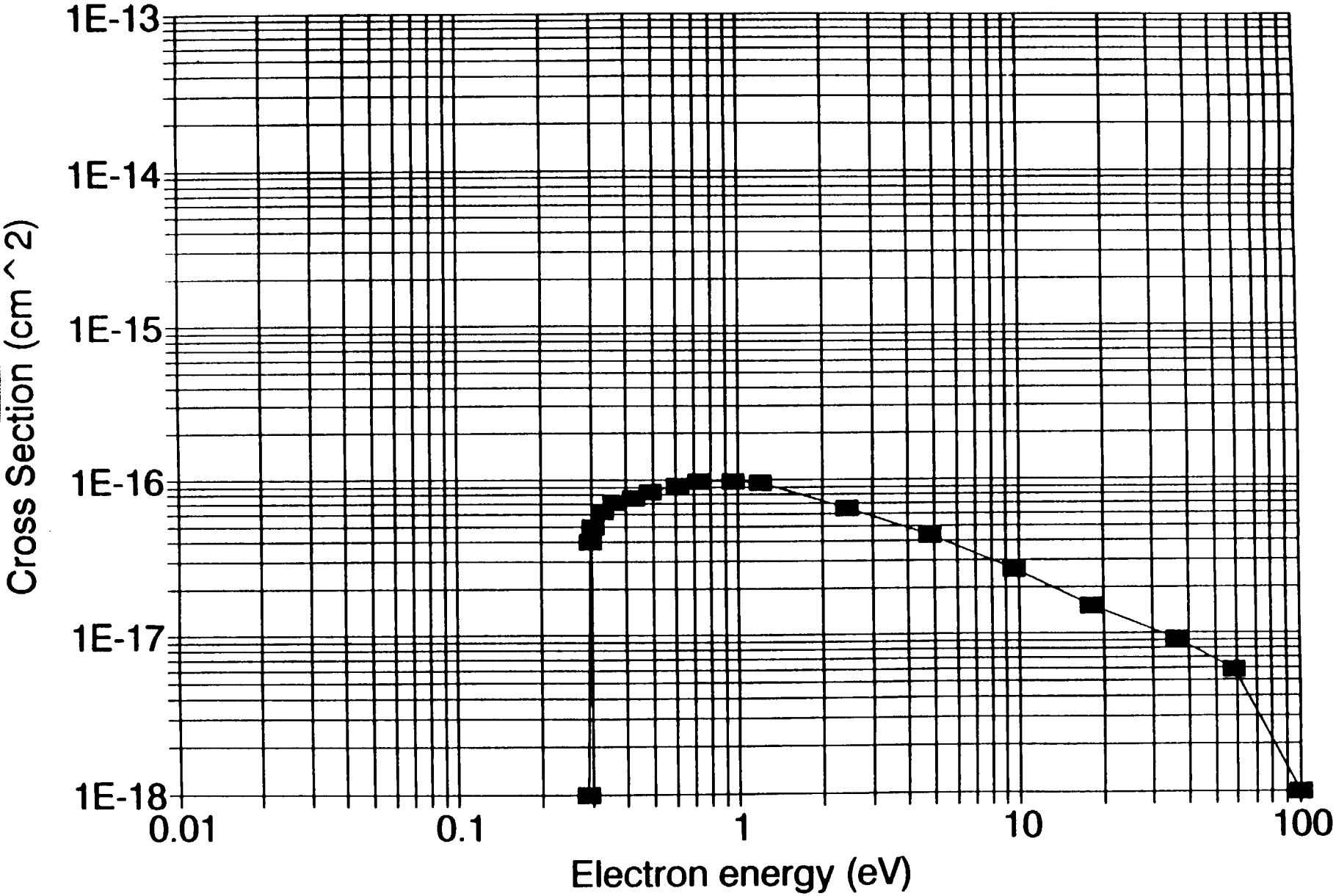

Fig 1.4

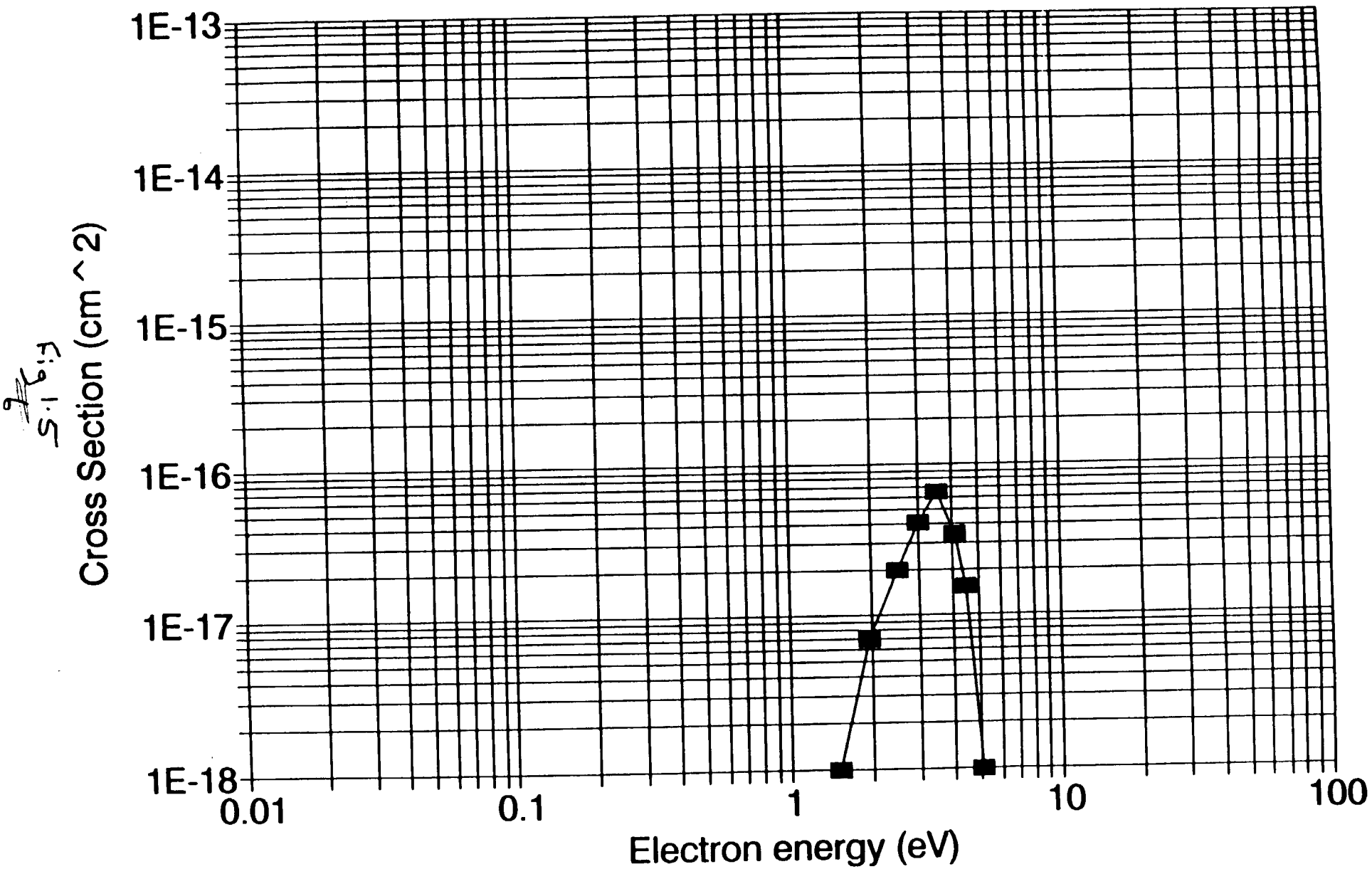
CO2 0n0 + n00 Level Excitation
Cross-Section From Electron Collision
1E-13
1E-14
1E-15
1E-16
1E-17
1E-18
Cross Section (cm ^ 2)
0.01
0.1
1
10
100
Electron energy (eV)

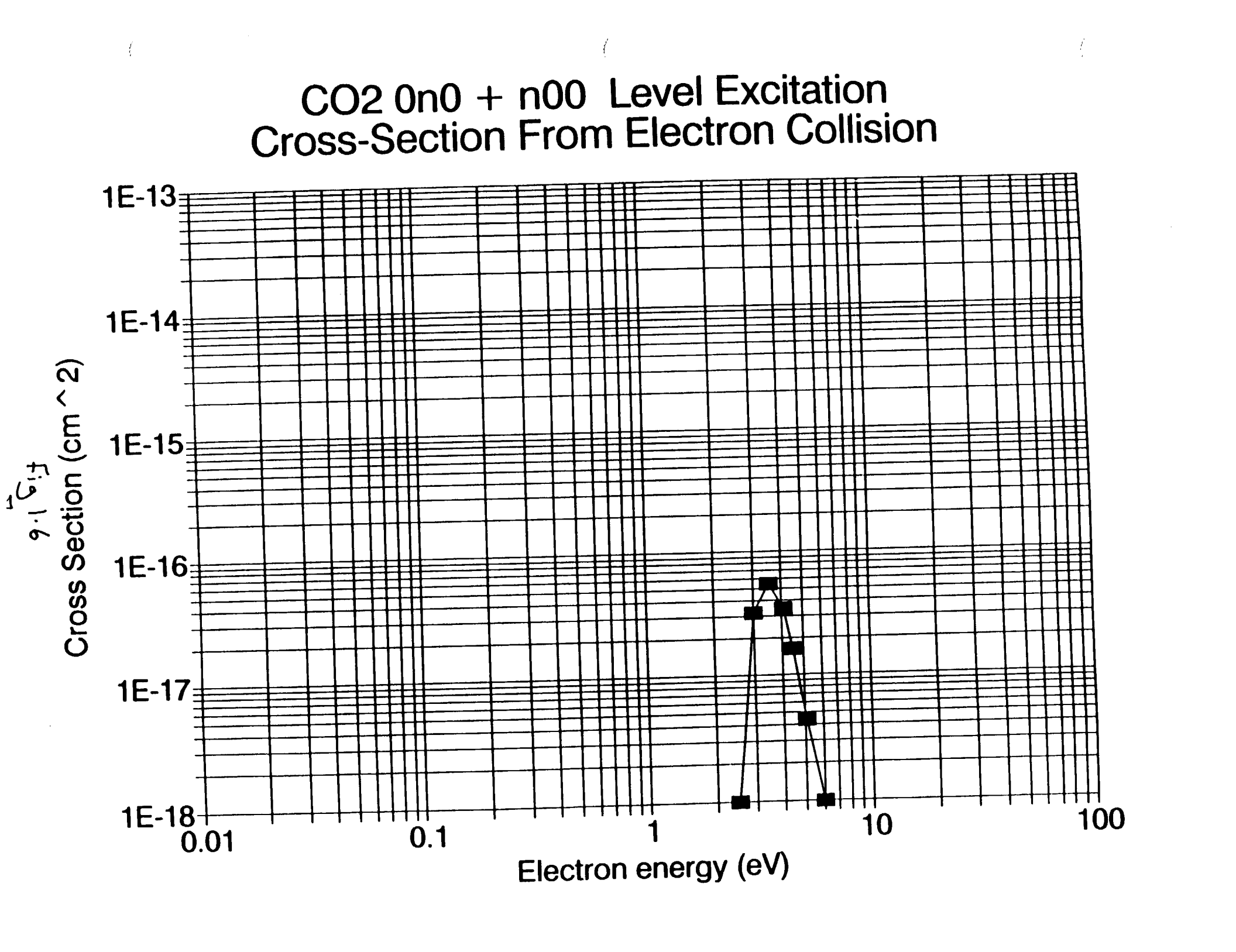
CO2 0n0 + n00 Level Excitation
Cross-Section From Electron Collision
1E-13
1E-14
1E-15
1E-16
1E-17
1E-18
Cross Section (cm^2)
0.01
0.1
1
10
100
Electron energy (eV)

CO2 0n0 + n00 Level Excitation Cross-Section From Electron Collision

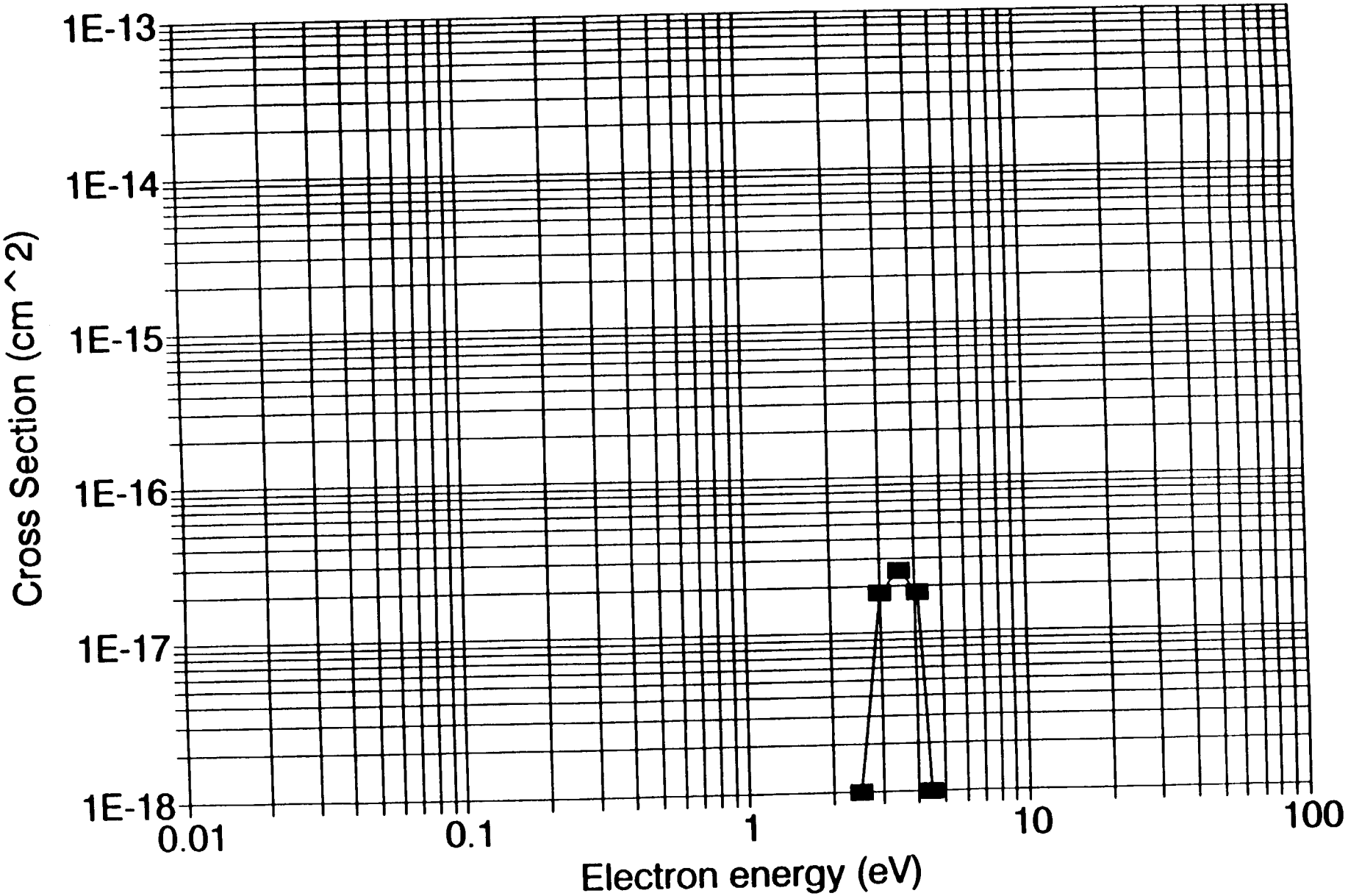

Fig 1.7a

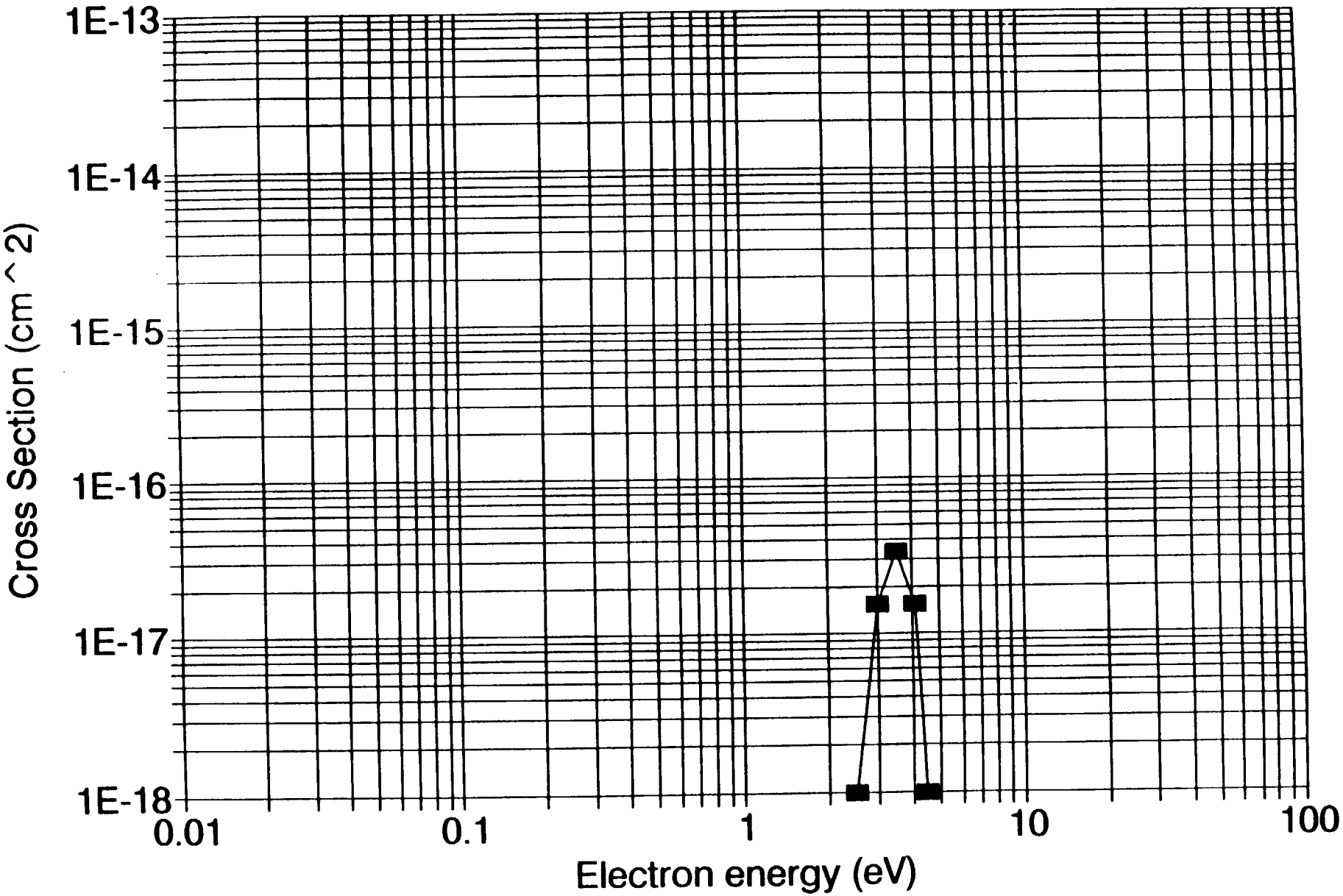
CO2 0n0 + n00 Level Excitation
Cross-Section From Electron Collision
1E-13
1E-14
1E-15
1E-16
1E-17
1E-18
Cross Section (cm ^ 2)
0.01
0.1
1
10
100
Electron energy (eV)

CO2 Electronic Excitation Cross-Section From Electron Collision

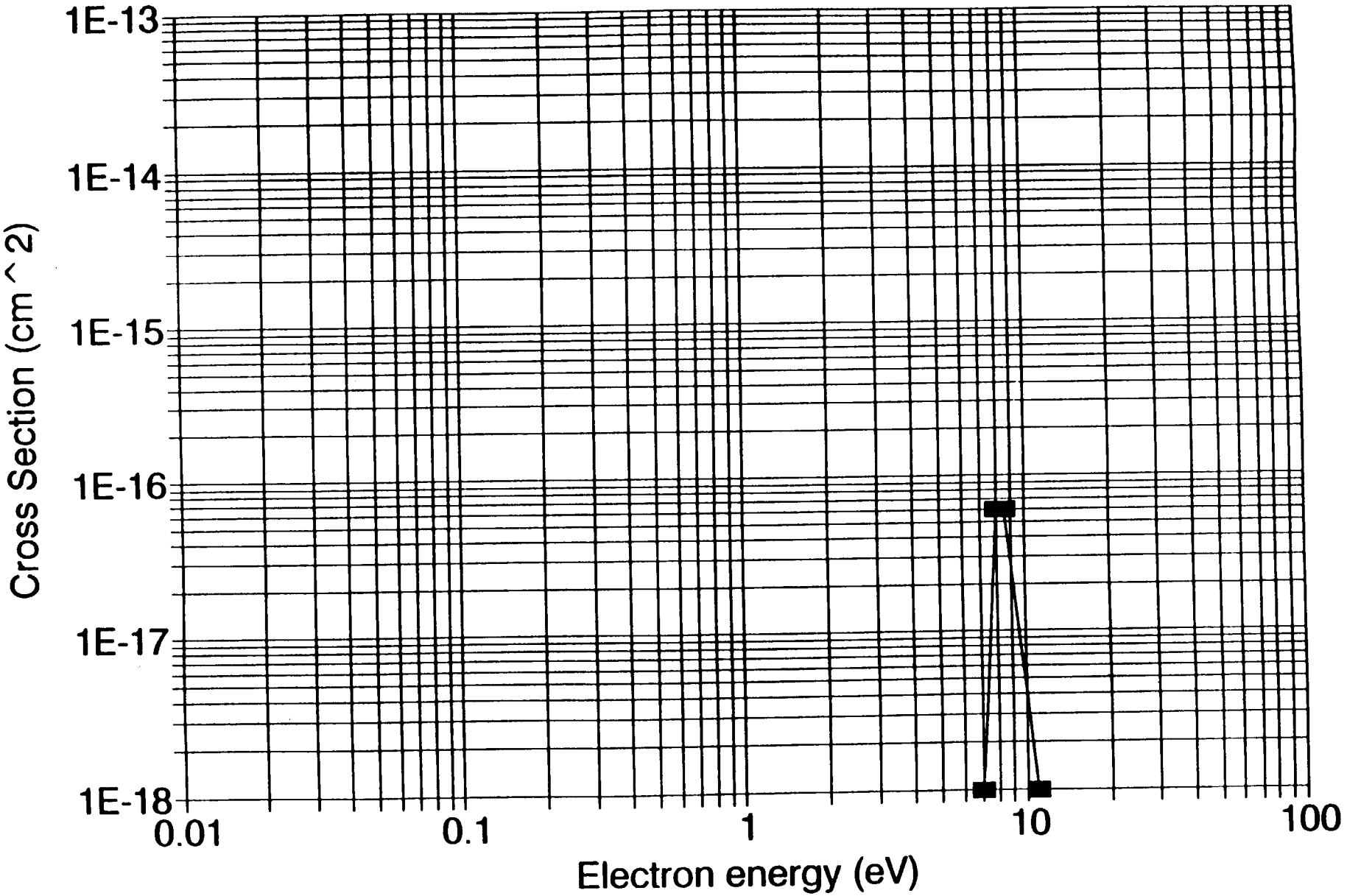

Fig 1.9

CO2 Ionisation Cross-Section From Electron Collision

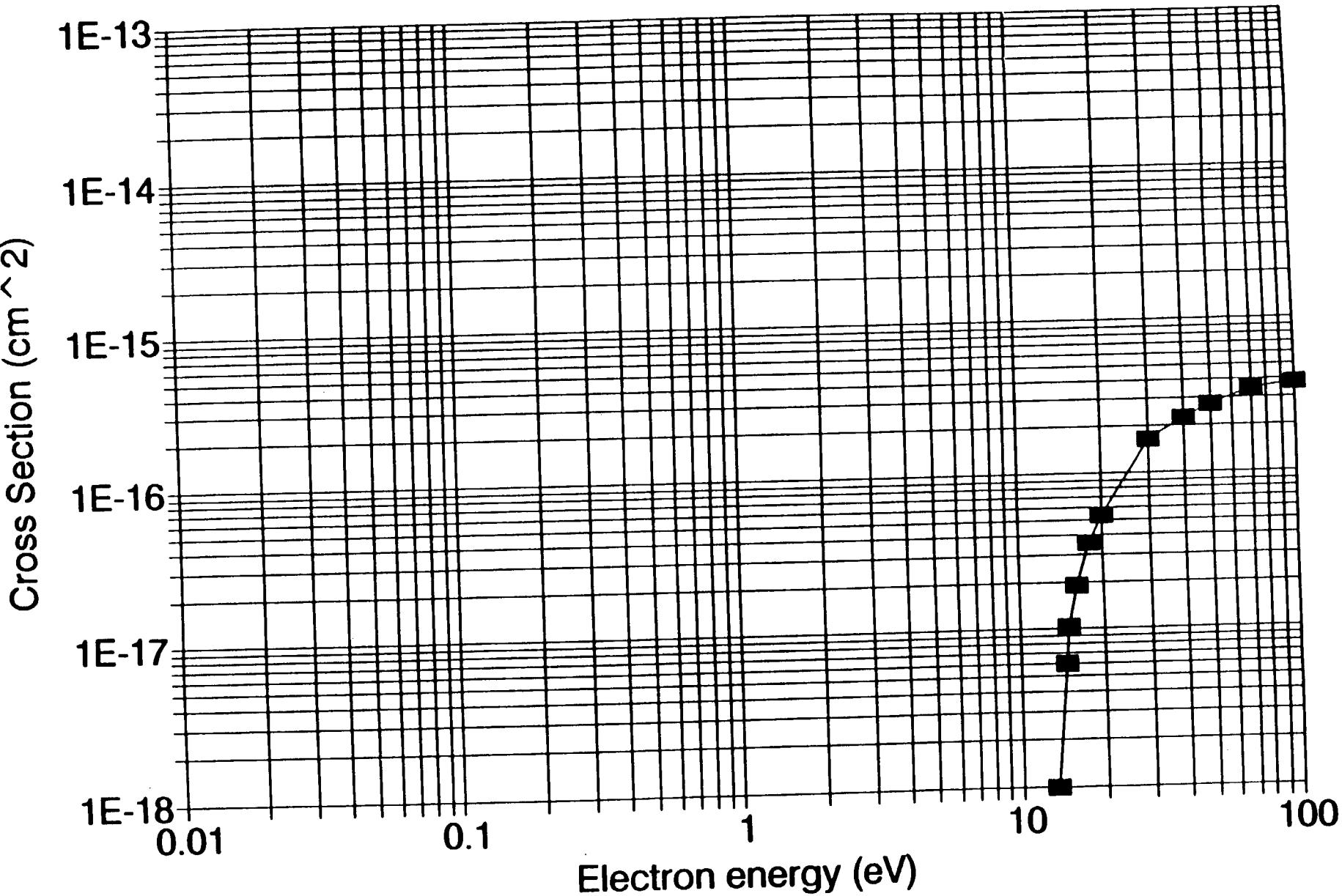

Fig 1.10

CO2 Electronic Excitation
Cross-Section From Electron Collision

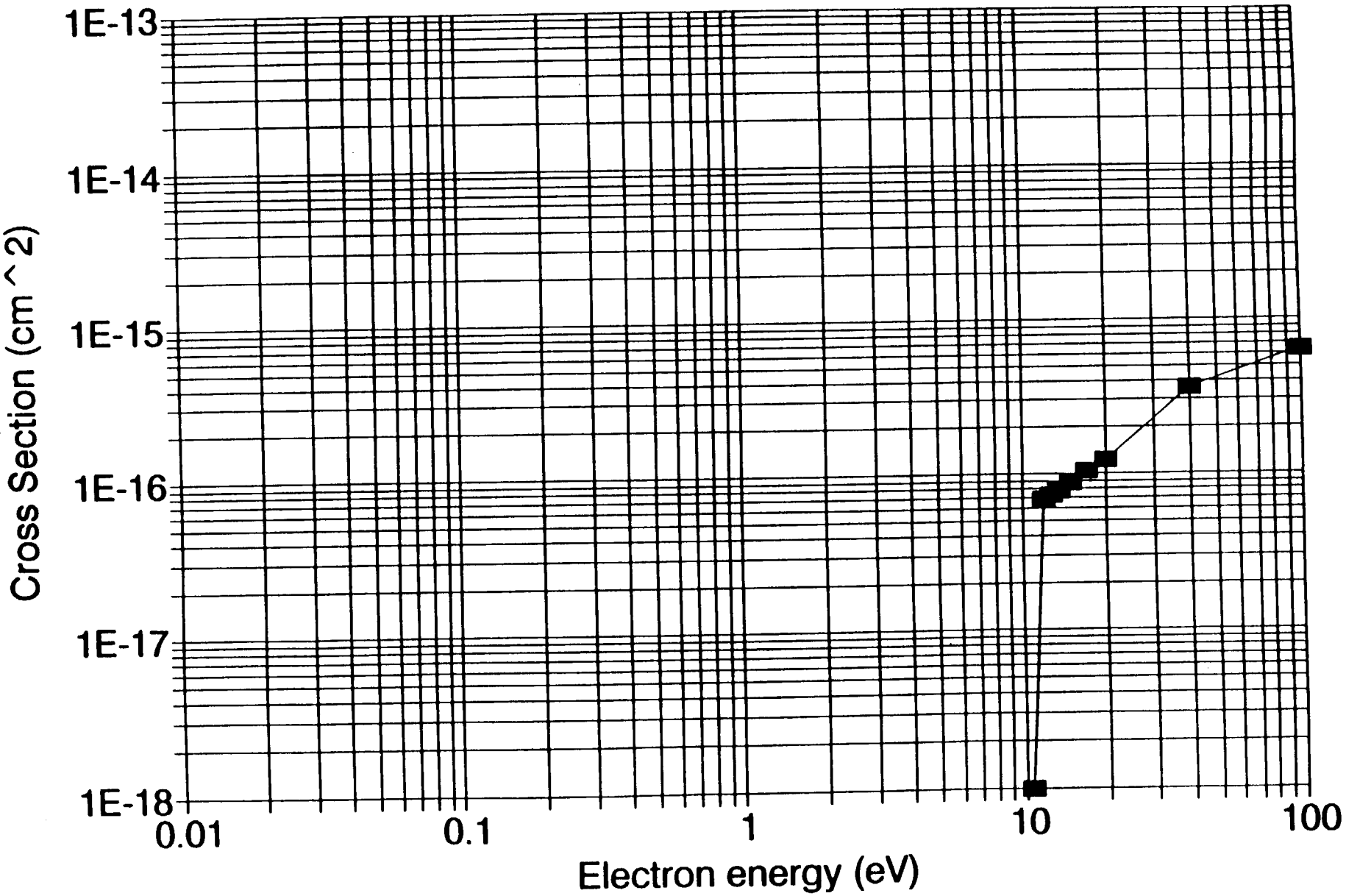

Fig 1.11

12

Once all the cross-sections have been obtained the Boltzmann equation is solved to obtain the effective excitation rates of the various molecular levels for various values of the applied field, E/N. Figures 1.12-1.15 show results for four different CO_2 laser gas mixes. RP001 and RP010 are the excitation rates for the upper and lower laser levels. RPNV is the nitrogen vibrational level excitation rate, IONIZE and ATTACH are the electron ionisation and attachment rates, VDRIFT is the electron drift velocity, ENERGY is the peak energy of the electron distribution curve and EBAR is the average electron energy.

BOLTZMANN CODE SOLUTION

CO2 1
N2 1
He 2

E/N (Vcm^2)	RP001 (cm^3/s)	RP010 (cm^3/s)	RP100 (cm^3/s)	RP0n0 (cm^3/s)	RPNV (cm^3/s)	IONIZE (cm^3/s)	ATTACH (cm^3/s)	VDRIFT (cm/s)	ENERGY (eV)	EBAR (eV)
1E-17	1.79E-15	2.85E-10	6.22E-13	0	3.19E-18	0	0	576000	0.0273	0.0414
2E-17	2.57E-12	1.05E-09	3.43E-11	6.89E-23	5.61E-15	0	0	1140000	0.039	0.0606
3E-17	3.48E-11	2.05E-09	1.6E-10	3.98E-18	1.1E-13	0	0	1780000	0.0499	0.0827
4E-17	1.52E-10	2.91E-09	4.31E-10	1.19E-15	6.15E-13	0	0	2160000	0.078	0.12
5E-17	4.07E-10	3.64E-09	6.71E-10	3.28E-14	2.28E-12	0	5.84E-30	2810000	0.0966	0.158
6E-17	8.24E-10	4.06E-09	9.8E-10	2.9E-13	9.92E-12	0	1.63E-26	3230000	0.133	0.217
7E-17	1.26E-09	4.29E-09	1.38E-09	1.33E-12	3.91E-11	0	4.07E-24	3560000	0.181	0.291
8E-17	1.78E-09	4.37E-09	1.59E-09	3.81E-12	1.16E-10	0	2.54E-22	3780000	0.236	0.369
9E-17	2.29E-09	5.09E-09	1.86E-09	9.26E-12	2.87E-10	7.25E-32	6.95E-21	4180000	0.29	0.467
1E-16	2.81E-09	5.24E-09	2.03E-09	1.55E-11	5.15E-10	2.3E-29	8.3E-20	4570000	0.329	0.538
1.5E-16	4.17E-09	5.09E-09	2.5E-09	1.1E-10	3.24E-09	3.9E-22	1.04E-16	5200000	0.589	0.834
2E-16	4.71E-09	4.95E-09	3E-09	4.37E-10	7.29E-09	9.61E-19	2.72E-15	5810000	0.785	1.02
2.5E-16	4.9E-09	5.12E-09	3.47E-09	1.13E-09	1.19E-08	8.59E-17	1.78E-14	6540000	0.917	1.17
3E-16	5.25E-09	5.49E-09	4.05E-09	2.33E-09	1.73E-08	1.76E-15	5.92E-14	6930000	1.1	1.39
3.5E-16	5.57E-09	5.97E-09	4.73E-09	3.68E-09	2.03E-08	1.54E-14	1.37E-13	6330000	1.52	1.69
4E-16	5.48E-09	6.43E-09	4.96E-09	4.58E-09	2.19E-08	6.17E-14	2.24E-13	8740000	1.26	1.81
5E-16	5.6E-09	7.08E-09	5.65E-09	5.67E-09	2.45E-08	5.25E-13	4.64E-13	10200000	1.52	2.32
6E-16	5.77E-09	7.67E-09	6.24E-09	7.93E-09	1.96E-08	2.2E-12	6.99E-13	9250000	2.26	2.92
7E-16	5.75E-09	8.07E-09	6.46E-09	8.51E-09	2.45E-08	6.09E-12	8.63E-13	11900000	2.19	3.34
8E-16	5.76E-09	8.16E-09	6.55E-09	7.61E-09	2.83E-08	1.19E-11	8.57E-13	13300000	2.37	3.67

Fig 1.12

BOLTZMANN CODE SOLUTION

CO2 1
N2 1
He 3

E/N (Vcm^2)	RP001 (cm^3/s)	RP010 (cm^3/s)	RP100 (cm^3/s)	RP0n0 (cm^3/s)	RPNV (cm^3/s)	IONIZE (cm^3/s)	ATTACH (cm^3/s)	VDRIFT (cm/s)	ENERGY (eV)	EBAR (eV)
1E-17	1.41E-14	4.07E-10	2E-12	0	2.78E-17	0	0	667000	0.0296	0.0446
2E-17	8.34E-12	1.41E-09	7.11E-11	3.71E-21	2.03E-14	0	0	1290000	0.0449	0.0689
3E-17	8.34E-11	2.59E-09	2.78E-10	6.23E-17	2.83E-13	0	0	1940000	0.0615	0.0993
4E-17	3E-10	3.48E-09	6.38E-10	9.08E-15	1.41E-12	0	7.51E-32	2360000	0.096	0.148
5E-17	7.03E-10	4.19E-09	9.39E-10	1.62E-13	6.48E-12	0	2.07E-27	2950000	0.125	0.203
6E-17	1.27E-09	4.53E-09	1.28E-09	1.03E-12	3.12E-11	0	2.03E-24	3320000	0.174	0.281
7E-17	1.81E-09	4.66E-09	1.67E-09	3.68E-12	1.11E-10	4.59E-35	2.43E-22	3570000	0.235	0.374
8E-17	2.36E-09	4.65E-09	1.87E-09	8.86E-12	2.88E-10	1.72E-31	8.41E-21	3760000	0.301	0.465
9E-17	2.86E-09	5.1E-09	2.1E-09	1.87E-11	6.2E-10	1.07E-28	1.4E-19	3990000	0.369	0.569
1E-16	3.33E-09	5.16E-09	2.25E-09	2.96E-11	1.01E-09	1.46E-26	1.15E-18	4290000	0.413	0.638
1.5E-16	4.44E-09	5E-09	2.67E-09	2.1E-10	4.88E-09	2.06E-20	4.74E-16	4960000	0.671	0.911
2E-16	4.87E-09	5.02E-09	3.22E-09	8.12E-10	9.87E-09	1.63E-17	7.42E-15	5650000	0.857	1.1
2.5E-16	5.02E-09	5.38E-09	3.81E-09	1.88E-09	1.49E-08	7.69E-16	3.59E-14	6460000	0.993	1.3
3E-16	5.34E-09	5.92E-09	4.52E-09	3.42E-09	2.01E-08	1.02E-14	9.72E-14	6860000	1.21	1.58
3.5E-16	5.61E-09	6.51E-09	5.23E-09	4.85E-09	2.23E-08	6.54E-14	1.92E-13	6670000	1.59	1.95
4E-16	5.55E-09	6.93E-09	5.46E-09	5.77E-09	2.34E-08	2.2E-13	2.89E-13	8540000	1.45	2.13
5E-16	5.64E-09	7.52E-09	6.05E-09	6.52E-09	2.5E-08	1.39E-12	5.17E-13	9980000	1.77	2.71
6E-16	5.76E-09	7.96E-09	6.44E-09	8.42E-09	1.93E-08	4.79E-12	7.04E-13	9810000	2.44	3.33
7E-16	5.74E-09	8.24E-09	6.59E-09	8.78E-09	2.31E-08	1.17E-11	8.33E-13	11900000	2.52	3.81
8E-16	5.73E-09	8.25E-09	6.61E-09	7.74E-09	2.68E-08	2.13E-11	7.99E-13	13400000	2.71	4.16

Fig 1-13

BOLTZMANN CODE SOLUTION

CO2 1
N2 1
He 8

E/N (Vcm^2)	RP001 (cm^3/s)	RP010 (cm^3/s)	RP100 (cm^3/s)	RP0n0 (cm^3/s)	RPNV (cm^3/s)	IONIZE (cm^3/s)	ATTACH (cm^3/s)	VDRIFT (cm/s)	ENERGY (eV)	EBAR (eV)
1E-17	1.5E-12	1.07E-09	3.06E-11	1.27E-25	3.78E-15	0	0	937000	0.0406	0.0599
2E-17	1.15E-10	2.85E-09	3.61E-10	3.78E-17	3.63E-13	0	0	1650000	0.0732	0.11
3E-17	5.48E-10	4.18E-09	8.74E-10	3.08E-14	2.89E-12	0	8.26E-30	2210000	0.117	0.183
4E-17	1.26E-09	4.82E-09	1.4E-09	7.89E-13	2.5E-11	0	8.17E-25	2530000	0.186	0.289
5E-17	2.1E-09	5.11E-09	1.76E-09	4.75E-12	1.49E-10	0	7.48E-22	2820000	0.262	0.413
6E-17	2.85E-09	5.07E-09	2.05E-09	1.46E-11	4.95E-10	2.65E-29	6.36E-20	2990000	0.353	0.54
7E-17	3.39E-09	4.93E-09	2.32E-09	3.36E-11	1.13E-09	4.12E-26	1.33E-18	3110000	0.446	0.655
8E-17	3.81E-09	4.8E-09	2.46E-09	6.51E-11	2.04E-09	8.16E-24	1.2E-17	3260000	0.525	0.746
9E-17	4.12E-09	4.9E-09	2.61E-09	1.23E-10	3.25E-09	4.73E-22	6.67E-17	3380000	0.607	0.834
1E-16	4.38E-09	4.9E-09	2.73E-09	2.01E-10	4.46E-09	1.06E-20	2.41E-16	3620000	0.654	0.891
1.5E-16	4.98E-09	5.19E-09	3.39E-09	1.33E-09	1.24E-08	8.78E-17	9.4E-15	4490000	0.897	1.18
2E-16	5.24E-09	5.9E-09	4.37E-09	3.33E-09	1.86E-08	6.31E-15	4.79E-14	5300000	1.13	1.54
2.5E-16	5.34E-09	6.7E-09	5.23E-09	5.14E-09	2.25E-08	7.51E-14	1.17E-13	6140000	1.37	1.97
3E-16	5.56E-09	7.37E-09	5.94E-09	6.66E-09	2.47E-08	3.92E-13	1.99E-13	6660000	1.71	2.48
3.5E-16	5.68E-09	7.84E-09	6.38E-09	7.46E-09	2.39E-08	1.28E-12	2.8E-13	7100000	2.09	2.97
4E-16	5.66E-09	8.04E-09	6.47E-09	8.04E-09	2.35E-08	2.92E-12	3.56E-13	8240000	2.19	3.3
5E-16	5.66E-09	8.18E-09	6.61E-09	7.58E-09	2.29E-08	9.98E-12	4.76E-13	9750000	2.66	4.04
6E-16	5.66E-09	8.18E-09	6.52E-09	8.52E-09	1.67E-08	2.32E-11	5.32E-13	10800000	3.24	4.74
7E-16	5.62E-09	8.1E-09	6.43E-09	8.3E-09	1.81E-08	4.36E-11	5.74E-13	12300000	3.58	5.35
8E-16	5.57E-09	7.94E-09	6.32E-09	7.14E-09	2.11E-08	6.78E-11	5.14E-13	13900000	3.86	5.81

Fig 1-14

BOLTZMANN CODE SOLUTION

CO2 1
N2 2
He 3

E/N (Vcm^2)	RP001 (cm^3/s)	RP010 (cm^3/s)	RP100 (cm^3/s)	RP0n0 (cm^3/s)	RPNV (cm^3/s)	IONIZE (cm^3/s)	ATTACH (cm^3/s)	VDRIFT (cm/s)	ENERGY (eV)	EBAR (eV)
1E-17	5.41E-14	5.4E-10	4.52E-12	1.64E-31	1.13E-16	0	0	746000	0.0321	0.0479
2E-17	1.78E-11	1.75E-09	1.17E-10	2.35E-20	4.59E-14	0	0	1400000	0.0508	0.0772
3E-17	1.42E-10	3.03E-09	3.96E-10	1.98E-16	5.02E-13	0	0	2020000	0.0723	0.115
4E-17	4.44E-10	3.9E-09	8.09E-10	1.91E-14	2.23E-12	0	0	2410000	0.112	0.172
5E-17	9.47E-10	4.54E-09	1.14E-09	2.6E-13	9E-12	0	3.86E-29	2900000	0.148	0.238
6E-17	1.58E-09	4.79E-09	1.46E-09	1.33E-12	3.47E-11	0	6.15E-26	3180000	0.203	0.326
7E-17	2.14E-09	4.84E-09	1.83E-09	4.09E-12	1.02E-10	0	1.05E-23	3360000	0.271	0.424
8E-17	2.68E-09	4.78E-09	2.01E-09	8.71E-12	2.35E-10	0	4.82E-22	3500000	0.339	0.515
9E-17	3.16E-09	5.09E-09	2.21E-09	1.69E-11	4.72E-10	4.22E-31	1.04E-20	3610000	0.417	0.616
1E-16	3.56E-09	5.11E-09	2.33E-09	2.32E-11	7.08E-10	7.91E-29	9.86E-20	3870000	0.459	0.675
1.5E-16	4.48E-09	4.92E-09	2.61E-09	9.47E-11	3.01E-09	3.9E-22	7.29E-17	4510000	0.694	0.895
2E-16	4.9E-09	4.79E-09	2.99E-09	3.21E-10	6.11E-09	6.52E-19	1.61E-15	4970000	0.9	1.05
2.5E-16	4.96E-09	4.94E-09	3.32E-09	7.93E-10	9.57E-09	4.96E-17	9.48E-15	5850000	0.982	1.15
3E-16	5.25E-09	5.23E-09	3.79E-09	1.72E-09	1.45E-08	1.02E-15	3.17E-14	6310000	1.14	1.33
3.5E-16	5.6E-09	5.61E-09	4.4E-09	2.9E-09	1.74E-08	9.52E-15	7.6E-14	5590000	1.61	1.61
4E-16	5.44E-09	6.04E-09	4.55E-09	3.58E-09	1.9E-08	3.82E-14	1.2E-13	8270000	1.24	1.67
5E-16	5.55E-09	6.64E-09	5.19E-09	4.63E-09	2.15E-08	3.5E-13	2.55E-13	10200000	1.41	2.1
6E-16	5.77E-09	7.31E-09	5.93E-09	7.06E-09	1.81E-08	1.65E-12	4.16E-13	8630000	2.27	2.75
7E-16	5.73E-09	7.75E-09	6.14E-09	7.68E-09	2.39E-08	4.75E-12	5.16E-13	11900000	2.03	3.12
8E-16	5.75E-09	7.86E-09	6.27E-09	6.96E-09	2.7E-08	9.36E-12	5.15E-13	13500000	2.21	3.43

Fig. 1.15

2 Gas Lifetimes in Pulsed CO_2 Lasers

2.1 Introduction

There are many potential factors that may limit the lifetime of pulsed CO_2 lasers. Perhaps the most serious limitation is that of gas lifetime. This chapter surveys available published data on lifetimes of sealed pulsed CO_2 lasers in an attempt to estimate the likelyhood of obtaining the 10^9 pulse lifetime required by LAWS.

2.2 CO_2 Dissociation

In a sealed laser the CO_2 loss caused by dissociation in the discharge results in a reduction in energy over time. The main source of this dissociation is by single electron collision[3.1-3.5],

$$CO_2 + e \rightarrow CO + O + e \qquad (3.1)$$

The dissociation leads to the formation of CO and O_2 over many pulses and under ideal conditions an equilibrium distribution would eventually be formed. Unfortunately there are several fast attachment processes which cause elctrons in the discharge to attach to the oxygen to form a negative ion. These attachment processes occur by collision with a third body, M and during the early stages of the discharge pulse may create a negative-ion density comparable to the electron density. The three body attachment reaction given by:-

$$e + O_2 + M \rightarrow O_2^- + M \qquad (3.2)$$

is particularly important and is followed by the rapid formation of more complex CO^-_4 and CO^-_3 cluster ions.

$$O_2^- + CO_2 + M \rightarrow CO_4^- + M \qquad (3.3)$$

$$CO_4^- + O \rightarrow CO_3^- + O_2 \qquad (3.4)$$

$$CO_4^- + H \rightarrow CO_3^- + OH \qquad (3.5)$$

$$CO_3^- + O \rightarrow O_2^- + CO_2 \qquad (3.6)$$

The equations (3.3-3.6) are a simplified representation of a closed loop which causes significant CO_2 loss from the system during the discharge. Similar reactions occur for the formation of NO^-_2 and NO^-_3 ions. If these negative ion concentrations become too large they can result in attachment instabilities and lead to discharge arcing[3.6]. The key to limiting the negative ion concentration is to limit the oxygen

production, arising from the dissociation of CO_2 in equation (3.1). Typically (1/2 - 2)% O_2 will cause arcing[3.5,3.7-3.10] in the discharge.

2.3 Catalysts

In order to obtain extended lifetimes from sealed CO_2 lasers catalysts have been included in the gas system to assist in the recombination of the O_2 and CO. The catalysts fall into two main types, homogenoeous gas catalysts and heterogeneous solid catalysts. Table 3.1 summarises the reports for each type of catalyst, together with a discussion of each of the catalyst types. The table consists of the following parameters:-

Pulse energy. The pulse energy provides an indication of the size of the laser. Ideally the more important parameter is the energy loading of the device as this directly determines the degree of dissociation per pulse. Unfortunately many of the authors omitted this information. It should be noted that the output for the RSRE devices (Stark et al.) is given as a peak power. This is because their experiments were aimed at obtaining high peak powers, however from other data available the pulse energy can be estimated to be <100 mJ. All of the reports have a pulse energy < 1 J, compared to the LAWS contractor proposals of 10 - 20 J.

PRF. The higher the pulse rate the greater the rate of dissociation and hence the recombination rate of the catalyst must be higher than for an equivalent laser running at a lower pulse rate. This can indicate either the use of a more efficient catalyst or the use of a larger quantity. In order to obtain results within a reasonable time period most of these tests were conducted at pulse rates $\geq$ 10 Hz.

CO2 Concentration. The concentration is the CO_2 partial pressure as a percentage of the total pressure. The higher the CO_2 concentration the greater the amount of dissociation per pulse. Most of the lasers reported use a CO_2 concentration equal to or greater than that of the LAWS device.

Life. The lifetime achieved by each of the lasers is given together with the cause of the test termination.

Catalyst. The type and quantity of catalyst used.

Group	Year	Energy (mJ)	PRF (Hz)	CO_2 (%)	Life (pulses)	Catalyst	Cause of test termination
Stark et al.(3.11)	1975	110	2	15	$2x10^6$	CO, H_2	Not indicated
Stark et al.(3.16)	1978	80	1	40	$>3x10^5$	Pt wire @ 1100°C	Terminated
Smith et al.(3.4)	1978	~100	1	20	$>10^5$	5-20% CO	Gas failure
Pace et al.(3.5)	1978	250	30	11	$2x10^6$	0.7% H_2, 4% CO	Terminated
Norris et al.(3.27)	1979	20	1-5	25	$\sim 2x10^6$	15% CO	Terminated
Marchetti et al.(3.25)	1982	50	4	20	$>10^6$	TPA	Terminated
Pace et al.(3.28)	1982	70	2	15	$\sim 2.5x10^6$	SnO_2-Pt @ 20°C	
Stark et al.(3.9)	1983	1MW pk	100	>50	$>2.5x10^6$	40g SnO_2-Pd @ 20°C	Not indicated
Stark et al.(3.10)	1983	1MW pk	30	50	$>2x10^7$	135g SnO_2-Pd/Pt @ 20°C + 1% CO	Damage to ZnSe O/C.
Stark et al.(3.29)	1984	0.5MW pk	30	>40	$8x10^6$	2% CO, 0.1% H_2	Damage to Ge O/C.
Smith et al.(3.19)	1984	20 45	10	25 45	$\sim 10^7$ $\sim 10^6$	15% CO 22.5% CO, 3% H_2 no He + Hopcalite @ 140°C	Terminated Terminated
Marchetti et al.(3.12)	1985	20	400	20	$2.2x10^7$ $>7x10^5$	15mbar H_2 H_2O	Terminated Terminated
Baranov et al.(3.24)	1986	900	400	25	$\sim 10^7$	3Kg Hopcalite @ 100°C	Gas failure
Upchirch et al.(3.17)	1989	?	10	?	$1x10^6$	150g of 2% Pt/SnO_2	Terminated

Table 3.1. Notable sealed TEA carbon dioxide lasers.

2.3.1 Homogeneous Catalysts

The three gases CO, H_2 and H_2O have been used as catalysts (Table 3.1.) to obtain longer lifetimes in sealed TEA CO_2 lasers. A summary of the output energy decline with pulse number when these gases are used is preceded by a brief reason for the use of each of these gases.

2.3.1.1 Carbon Monoxide Addition

The three body recombination equation

$$CO + O + M \rightarrow CO_2 + M \qquad (3.7)$$

is enhanced when CO is added to the initial gas mix and this leads to a relative decrease in the CO_2 dissociation per pulse(3.2,3.3) and thus an increase in gas life.

2.3.1.2 Hydrogen Addition

Within the discharge atomic and molecular hydrogen can be expected to react with any oxygen present to form the OH radical(3.5,3.11,3.13,3.14).

$$H_2 + O \rightarrow OH + H \quad (3.8)$$

$$O + H \rightarrow OH \quad (3.9)$$

The OH and CO molecules then recombine to form CO_2,

$$CO + OH \rightarrow CO_2 + H \quad (3.10)$$

From equation (3.10) it can be seen that the addition of both CO and H_2 could further reduce CO_2 dissociation and this has been found to be the case [3.11].

2.3.1.3 Water Addition

As water is a liquid at room temperature only quantities less than the saturated vapour pressure (23 mb at 20°C) can be added. The normal addition technique involves bubbling the gas mixture through a pool of water during the laser filling procedure [3.12]. Within the discharge the water readily decomposes to H^- ions and OH radicals.

$$H_2O + e \rightarrow H^- + OH \quad (3.11)$$

The OH radical is then available for recombination with the CO (equation (3.10)).

2.3.1.4 Discussion

When these gaseous catalysts are used there is a general tendency for the output energy to rapidly drop to ~(70 - 95) % of the initial energy within 10^4 - 10^5 pulses. However, after this point the energy appears to remain constant. The best result obtained is that of Smith et al.[3.19] who achieved ~95 % of the initial energy after ~10^7 pulses with the addition of CO only.

The main disadvantage of adding H_2 and H_2O to the gas mixture is that they lead to an increase in the negative ion density in the discharge, particularly for H_2O[3.2,3.5,3.15] resulting in discharge arcing. With efficient preionisation however this problem can be overcome[3.12]. Of the three additives a theoretical analysis[3.3] suggested that H_2O is the best additive, provided the discharge instability can be avoided, and that CO was the least effective of the three additives. At present the experimental evidence is insufficient to confirm or invalidate this analysis.

2.3.2 Solid Catalysts

The use of solid catalysts has received considerable interest and reports of longlife using them are summarised in Table 3.1. Several different catalysts have been used.

2.3.2.1 Platinum and Palladium

Catalysts involving Pt and Pd are the most popular of the heterogeneous catalysts. The first use of such a technique was by Stark et al.[3.15,3.16] who used a platinum wire catalyst heated to 1100°C. The basic problem with this early technique was the amount of heat required to maintain the Pt wire at the high temperatures required for the catalytic action to occur efficiently. This heat had to be subsequently removed before the gas re-entered the discharge chamber. This problem has led to the development of more effective low temperature Pd/Pt catalysts on a SnO_2 support structure. Due to the proprietary nature of many of these types of catalyst, reports tend to be vague with regard to the exact composition and the energy output dependence on number of pulses.

Using these catalysts lifetimes of ~10^7 pulses have been obtained, however due to optics damage the energy at this point is not reported. Upchurch et al.[3.17] have reported lifetimes of ~10^6 pulses with > 96 % of the initial energy. This was obtained using a commercial laser that had not been designed for longlife sealed operation.

2.3.2.2 Hopcalite

Hopcalite is a commercially available catalyst consisting of ~ 60% MnO_2 and ~ 40% CuO which has successfully been used in a high CO_2 concentration, He free long life discharge laser[3.18]. Helium free gas mixtures[3.14,3.19,3.20] of the N_2:CO_2:H_2 type enable high peak and average powers to be obtained from small volumes. The small quantity of hydrogen in such mixtures ensures rapid depopulation of the 010 CO_2 level and aids the uniformity and effectiveness of the preionisation-[3.21]. In the sealed laser the hopcalite, heated to (130 - 200)°C, was accompanied by CO which was required for efficient operation[3.22]. Recently, Baranov et al.[3.23] have shown that fresh hopcalite catalyst releases oxygen. The addition of CO therefore acts to counter this oxygen release as describe above and also reduces the hopcalite to prevent the subsequent release of oxygen.

Lifetimes of ~10^7 pulses[3.23] have been reported but with no indication of available pulse energy at this point.

2.3.2.3 Tripropylamine (TPA)

Also included in the table is a report by Marchetti et al.[3.24] of a long life sealed laser using tripropylamine (TPA) as an additive. In early TEA CO_2 lasers discharge instabilities were a common problem and as TPA is an easily ionisable additive, it was occasionally added to the gas mixture to increase the electron density and hence discharge stability. During the discharge the TPA breaks down and some of the compounds formed deposit themselves in the discharge chamber. Marchetti et al.[3.25] postulated that this compound acted as a catalyst and demonstrated this by preconditioning a laser head before testing it with a TPA free gas mix. The compound formed by the break down of the TPA has not been identified in the literature. Thus allthough TPA is added as a gas (ie homogeneous) component the compound responsible for the catalytic action is a solid and hence heterogeneous.

A pulse life of >10^6 pulses has been reported[3.24]. The energy output fell rapidly to ~70 % after ~10^4 pulses and then slowly increased to ~80 % at 10^6 pulses.

2.4 Discussion

Homogeneous catalysts were the initial catalysts[3.11] used to obtain longlife sealed off operation of TEA CO_2 lasers with low CO_2 concentrations (< 20 %). At higher concentrations of CO_2 they were found to be inadequate and a switch to heterogeneous catalysts occured. During this period the dominant preionisation method used was various types of bare spark preionisation. This preionisation technique produces essentially complete dissociation in the region of the sparks and hence a very active catalyst is required. In the recent past, more efficient and 'gentler' preionisation techniques such as corona and x-ray preionisers have been used. These produce dissociation equilibria equivalent to or lower than the main discharge pulse. This has enabled the homogeneous catalysts to be used with high CO_2 concentrations. This improvement coupled together with a greater understanding of both the mechanisms involved and the need to use suitably inert materials within the laser head have led to the homogeneous catalyst results being on a par with those of the heterogeneous catalysts.

The need for the correct choice of materials can be highlighted by the report of many of the authors of a greyish or whitish deposit forming in the laser during these life tests. These deposits are oxides of the materials used to form the electrodes and preionisers. Some have reported a slow reduction in the output energy as a consequence of these deposits. If these oxides form, there is a reduction of the CO_2 concentration within the laser chamber and this could account for the gradual change in output. One benefit of this deposit is that it appears to assist discharge stability. This occurs because the layer of oxides forming on the electrodes acts as a ballasting mechanism. A laser using many small inductively ballasted electrode segments to form each electrode has greater discharge stability than a conventional electrode structure. The disadvantage of such schemes is a reduction in the discharge energy deposition efficiency.

In general there appears to be little to choose between the various systems and even the best report of ~95 % energy at $\sim 10^7$ pulses would result in ~0 % energy at ~2.5 x 10^8 pulses (assuming a linear extrapolation), ie short of the LAWS lifetime requirement. If a LAWS requirement of 50 % energy at 10^9 pulses was to be specified, this would require 99.5% energy at 10^7 pulses. This variation in pulse energy would be indestinguishable from the normal fluctuations in pulse energy. Allthough the results of this survey do not appear promising under first considerations, it should be noted that:-

a) Most of the experimenters listed did not construct ideal lasers from a cleanliness perspective. Most of the reports are simply a try it and see approach. Therefore it does not appear difficult to obtain lifetimes of 10^6 - 10^7 pulses.

b) The assumption of a linear scaling law out to 10^9 pulses may be invalid as indicated by the change of dissociation rate at 10^4 for the homogeneous catalysts. The energy may increase again as indicated with the addition of TPA.

2.5 Summary

There are only a few reports of sealed TEA CO_2 laser operation and because of proprietary constraints many of these are sketchy. Most of the tests have terminated at $\sim 10^6$ - 10^7 pulses with no indication of the final failure mechanism. At this point it is difficult to draw any strong conclusions as to the feasability of obtaining 10^9 pulses from the LAWS device. Linear extrapolation of the results from the best test to date indicates 0 % energy would be reached at ~2.5 x 10^8 pulses. Assuming a 50% energy requirement at 10^9 pulses gives 99.5 % energy at 10^7 pulses. It should be noted that there is

sufficient evidence to question the validity of the linear extrapolation. Only longlife tests beyond 10^7 pulses will provide a reliable indicator of final lifetime.

2.6 References

(3.1) A.L.S. Smith and J.N. Austin, J. Phys. D: Appl. Phys., **7**, 314 (1974).

(3.2) H. Shields, A.L.S. Smith and B. Norris, J. Phys. D: Appl. Phys., **9**, 1587 (1976).

(3.3) H. Hokazono and H. Fujimoto, J. Appl. Phys., **62**, 5, 1585 (1987).

(3.4) A.L.S. Smith and B. Norris, J. Phys. D: Appl. Phys., **11**, 1949 (1978).

(3.5) P.W. Pace and M. Lacombe, IEEE J. Quant. Electron., **QE-14**, 263 (1978).

(3.6) W.L. Nighan, Phys. Rev. A, **15**, 1701 (1977).

(3.7) I. Chis, A. Ciura, V. Draganescu, D. Dragulinescu, D. Grigorescu, C. Grigoru, M.L. Pascu, V.G. Velculescu, M. Abrudean, D. Axente, A. Bâldea and M. Gligan, J. Phys. E: Sci. Instrum., **21**, 393 (1988).

(3.8) D.S. Stark and M.R. Harris, J. Phys. E: Sci. Instrum., **21**, 715 (1988).

(3.9) D.S. Stark, A. Crocker and G.J. Steward, J. Phys. E: Sci. Instrum., **16**, 158 (1983).

(3.10) D.S. Stark, A. Crocker and N.A. Lowde, J. Phys. E: Sci. Instrum., **16**, 1069 (1983).

(3.11) D.S. Stark, P.H. Cross and H. Foster, IEEE J. Quant. Electron., **QE-11**, 774 (1975).

(3.12) R. Marchetti, E. Penco and G. Salvetti, IEEE J. Quant. Electron., **QE-21**, 11, 1766 (1985).

(3.13) W.J. Wittemann, Phillips Tech. Rev., **28**, 287 (1967).

(3.14) A.L.S. Smith and P.G. Browne, J. Phys. D: Appl. Phys., **7**, 1652 (1974).

(3.15) D.S. Stark and M.R. Harris, J. Phys. E: Sci. Instrum., **11**, 317 (1978).

(3.16) D.S. Stark, P.H. Cross and M.R. Harris, J. Phys. E: Sci. Instrum., **11**, 311 (1978).

(3.17) B.T. Upchurch, D.R. Schryer, G.M. Wood and R.V. Hess, Proc. SPIE, **1062**, 287 (1989)

(3.18) A.L.S. Smith, J.P. Sephton and G. Scott, J. Phys. E: Sci. Instrum., **17**, 591 (1984).

(3.19) P.E. Dyer and B.L. Tait, J. Phys. E: Sci. Instrum., **16**, 467 (1983).

(3.20) P.E. Dyer and B.L. Tait, Appl. Phys. Lett., **41**, 506 (1982).

(3.21) T.F. Deutsch, Appl. Phys. Lett., **20**, 8, 315 (1972).

(3.22) R.B. Gibson, A. Javan and K. Boyer, Appl. Phys. Lett., **32**, 726 (1978).

(3.23) V.Yu. Baranov, G.F. Drokov, V.A. Kuz'menko , V.S. Meghevov and V.V. Pigul'skaya, Sov. J. Quant. Electron., **16**, 5, 645 (1986).

(3.24) R. Marchetti, E. Penco, E. Armandillo and G. Salvetti, Appl. Phys. Lett., **41**, 7, 601 (1982).

(3.25) R. Marchetti, E. Penco, M. Cavaioli and G. Salvetti, Poster Paper WM15, CLEO, (1985).

(3.26) B.Norris and A.L.S. Smith, Appl. Phys. Lett., **34**, 6, 385 (1979).

(3.27) P. Pace, P. Mathieu and J. Cruickshank, Rev. Sci. Instrum., **53**, 12, 1861 (1982).

(3.28) D.S. Stark and A. Crocker, Opt. Commun., **48**, 5, 337 (1984).

3 Frequency Chirp and Laser Pulse Spectral Analysis

This chapter contains results of modeling of the anticipated LAWS laser pulse spectrum. Results for three different pulse shapes are presented. Each of the pulse shapes has a FWHM of 3.1 μs and an energy of 20 J. For each pulse the laser induced medium perturbation (limp) frequency chirp was calculated assuming a 1:1:3 CO_2:N_2:He gas mixture at 500 torr pressure with a 4.5 cm discharge cross-section and a 4 m cavity length. The three pulse shapes used were:-

a) a square pulse - considered the optimum pulse shape for LAWS.

b) a square pulse with a tail added. The relaxation time on the tail is chosen to match the kinetics of the laser gas mix.

c) pulse (b) with a gain switch spike included. This pulse is representative of the actual output of the LAWS laser.

For each case the laser pulse shape, integrated energy, frequency chirp and electric field are plotted as a function of time. The power spectrum and distribution of energy within the power spectrum are then plotted. Each pulse is plotted both with and without frequency chirp. These results are plotted in figures 3.1-6.

It can be seen that the effect of the frequency chirp is to broaden the spectrum, particularly for those pulses with a decay tail. This is because most of the frequency chirp occurs in the tail of the pulse.

A figure of merit for LAWS can be considered to be the energy in some bandwidth about the center of the frequency spectrum. This is shown for various pulse widths and gas pressures in figures 3.7-9. The pulse tail decay times of 4,3 and 2 μs represent gas pressures of ~0.5, 0.75 and 1 atms. respectively. It can be seen that the lower gas pressure results in more energy in a given bandwidth.

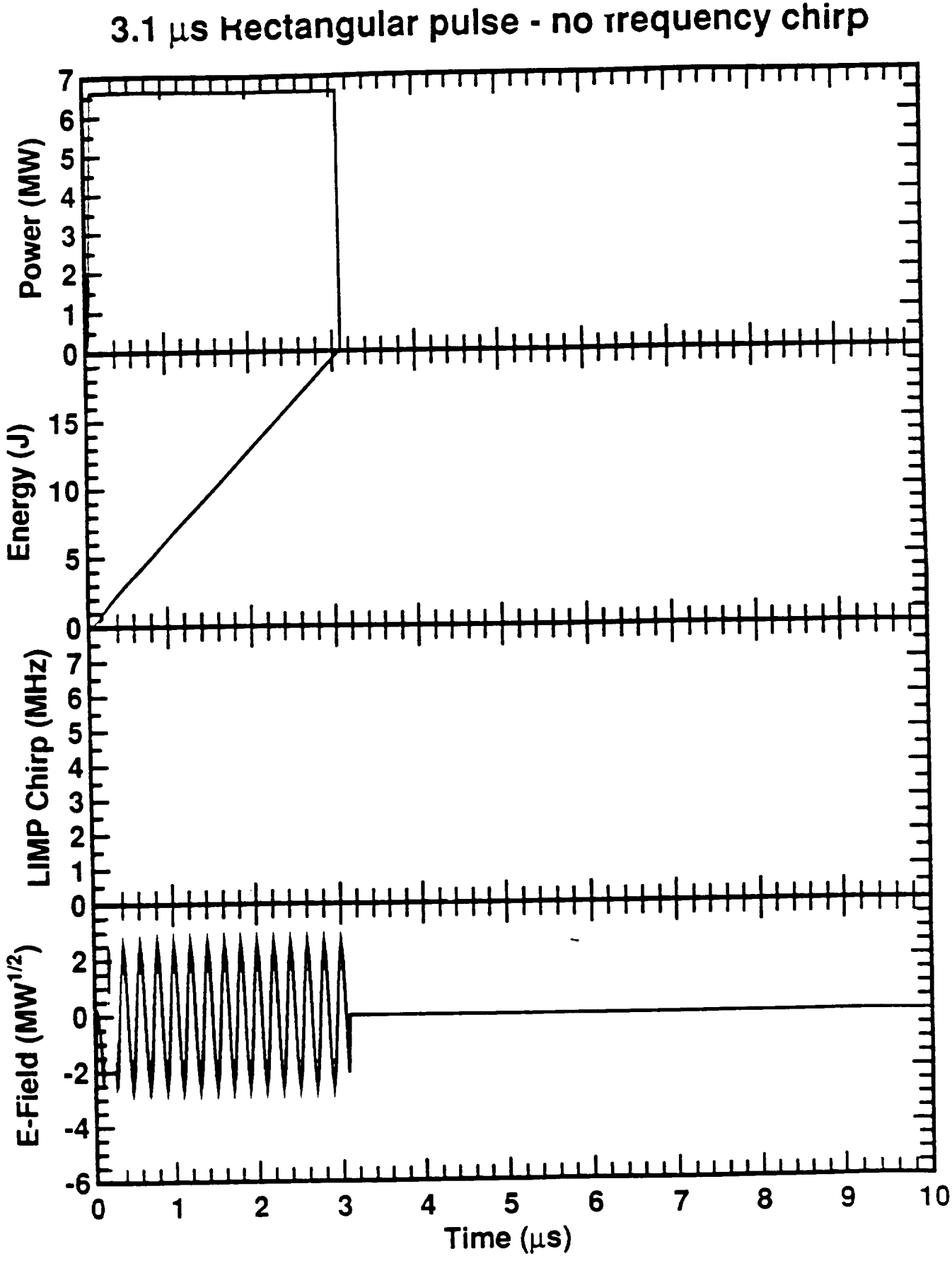
3.1 μs Rectangular pulse - no frequency chirp
Power (MW)
Energy (J)
LIMP Chirp (MHz)
E-Field (MW^1/2)
Time (μs)

Fig 3.1a

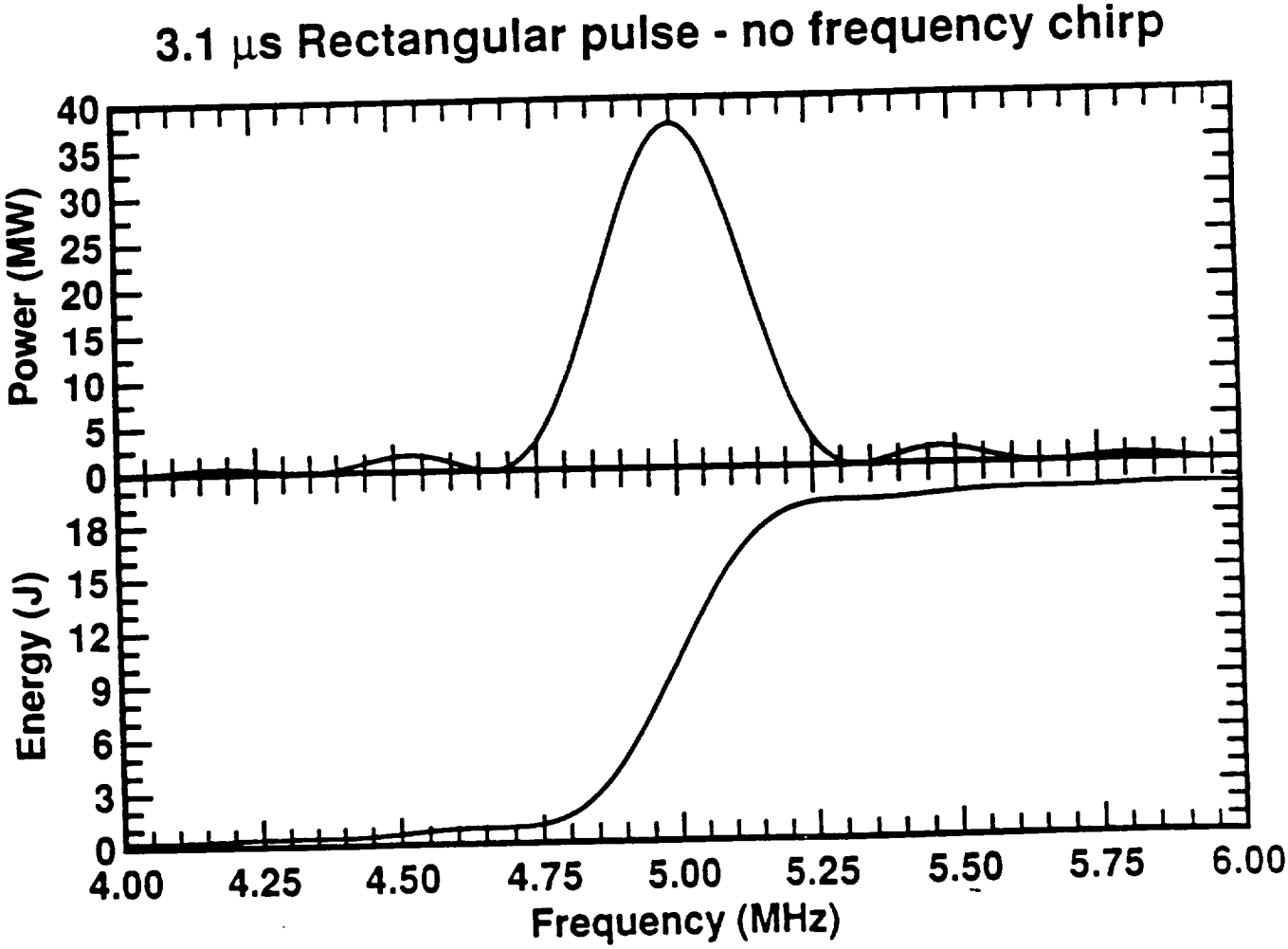
3.1 μs Rectangular pulse - no frequency chirp
Power (MW)
40
35
30
25
20
15
10
5
0
Energy (J)
18
15
12
9
6
3
0
4.00
4.25
4.50
4.75
5.00
5.25
5.50
5.75
6.00
Frequency (MHz)

Fig 3.1b

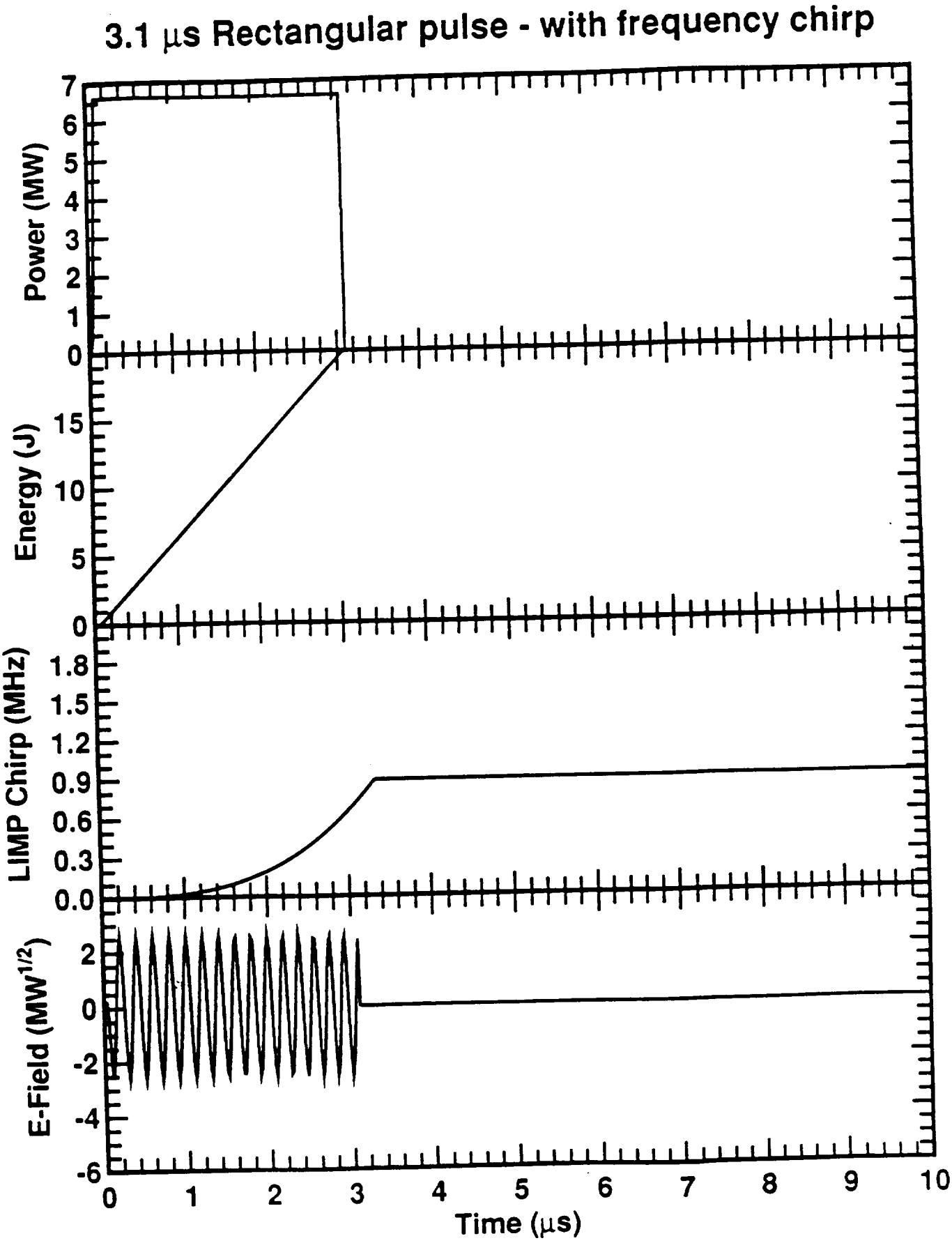
3.1 μs Rectangular pulse - with frequency chirp
Power (MW)
Energy (J)
LIMP Chirp (MHz)
E-Field (MW^1/2)
Time (μs)

Fig 3.2a

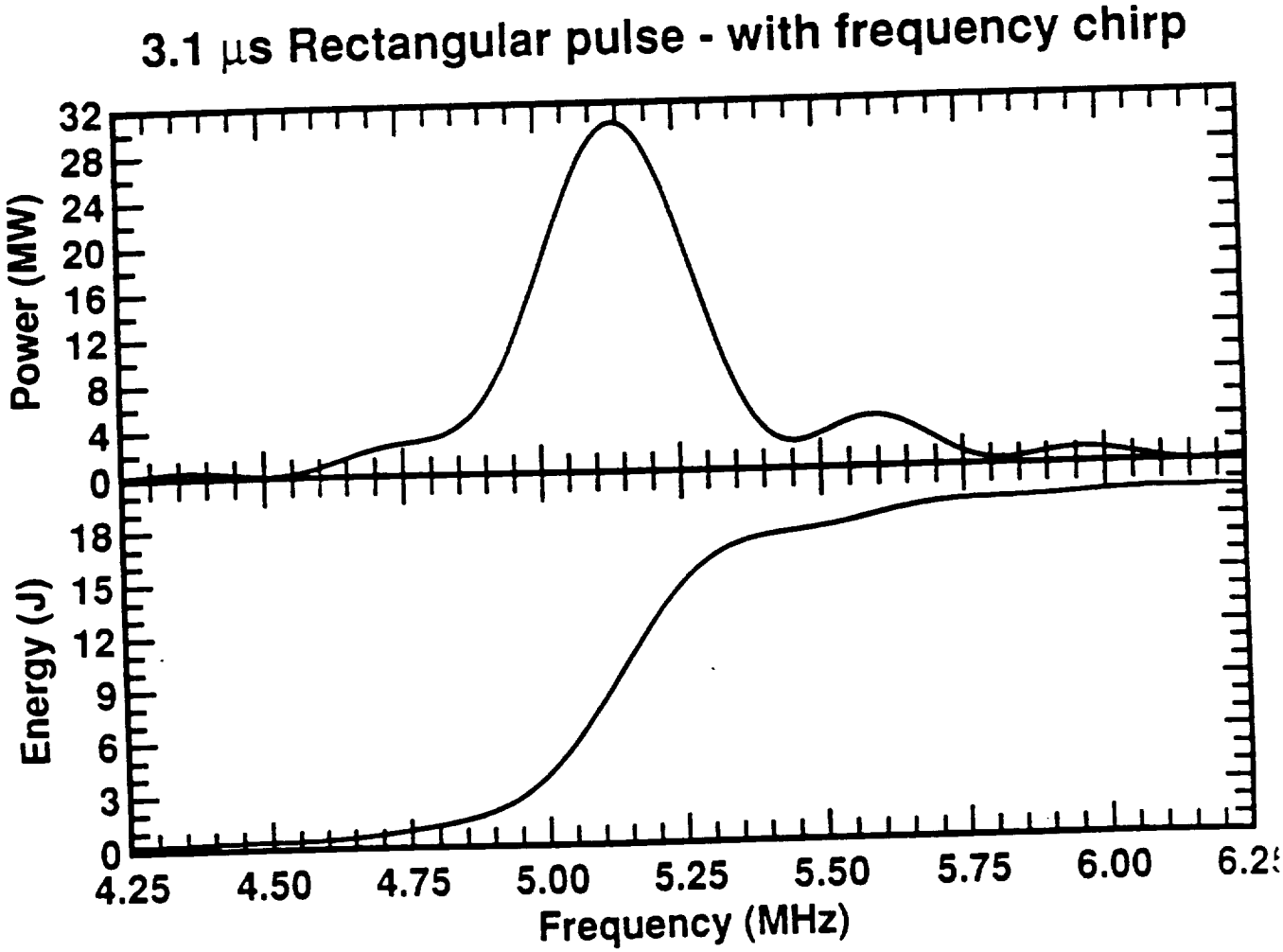
3.1 μs Rectangular pulse - with frequency chirp
Power (MW)
32
28
24
20
16
12
8
4
0
Energy (J)
18
15
12
9
6
3
0
4.25
4.50
4.75
5.00
5.25
5.50
5.75
6.00
Frequency (MHz)

Fig 3.2b

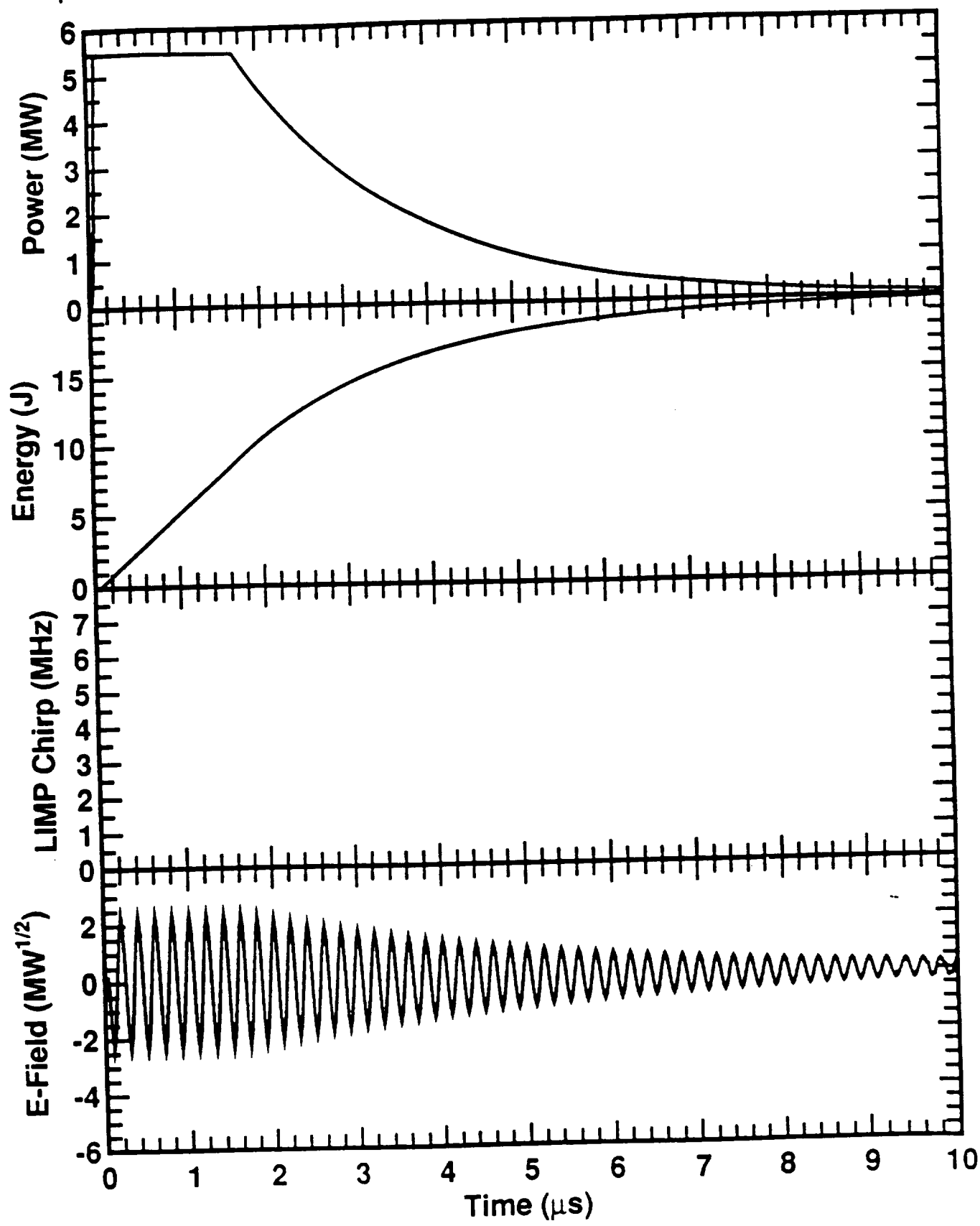
3.1 μs FWHM pulse and 4 μs tail decay - no frequency chi
Power (MW)
Energy (J)
LIMP Chirp (MHz)
E-Field (MW^1/2)
Time (μs)

Fig 3.3a

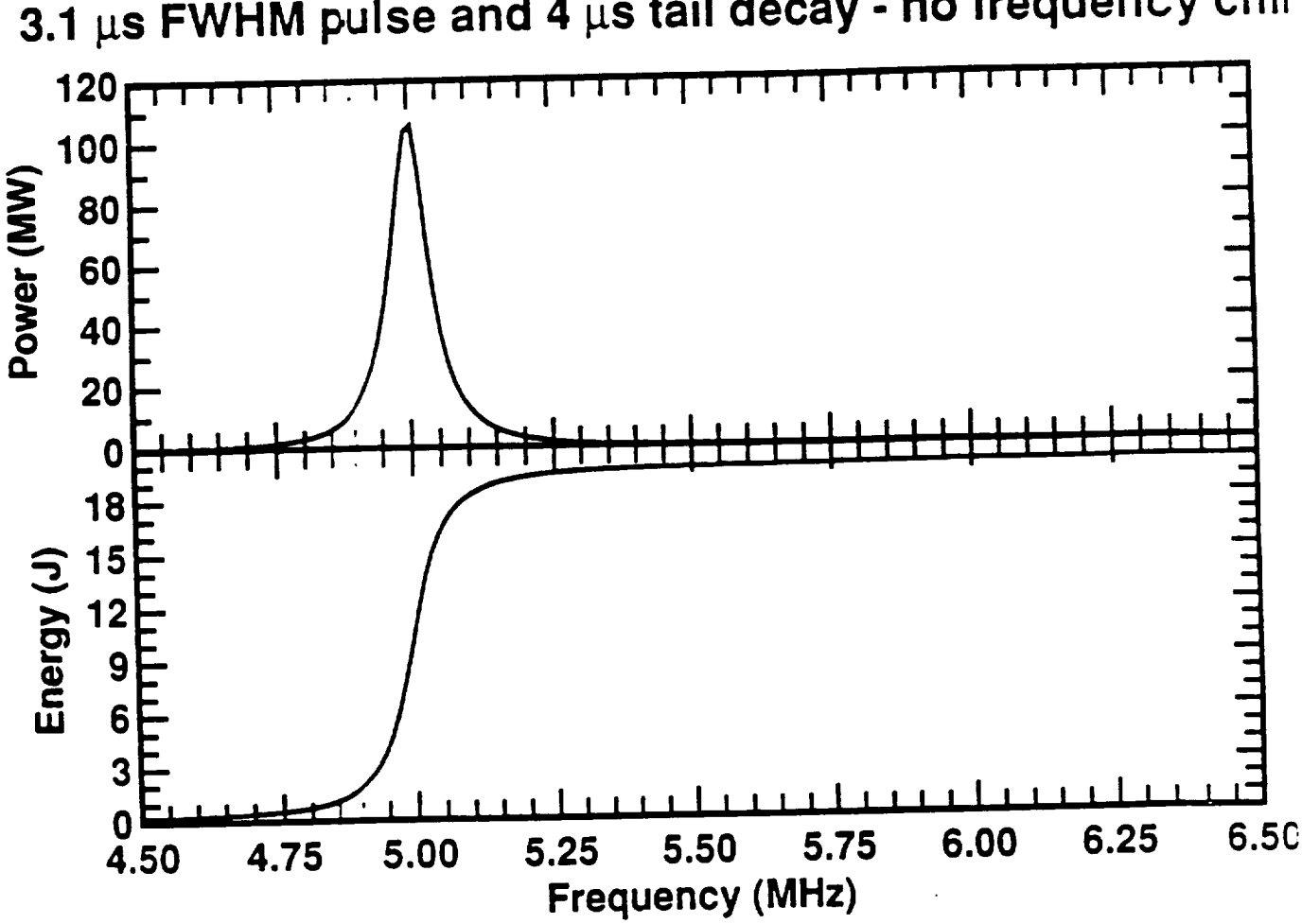
3.1 μs FWHM pulse and 4 μs tail decay - no frequency chi
Power (MW)
120
100
80
60
40
20
0
Energy (J)
18
15
12
9
6
3
0
4.50
4.75
5.00
5.25
5.50
5.75
6.00
6.25
6.50
Frequency (MHz)

Fig 3.36

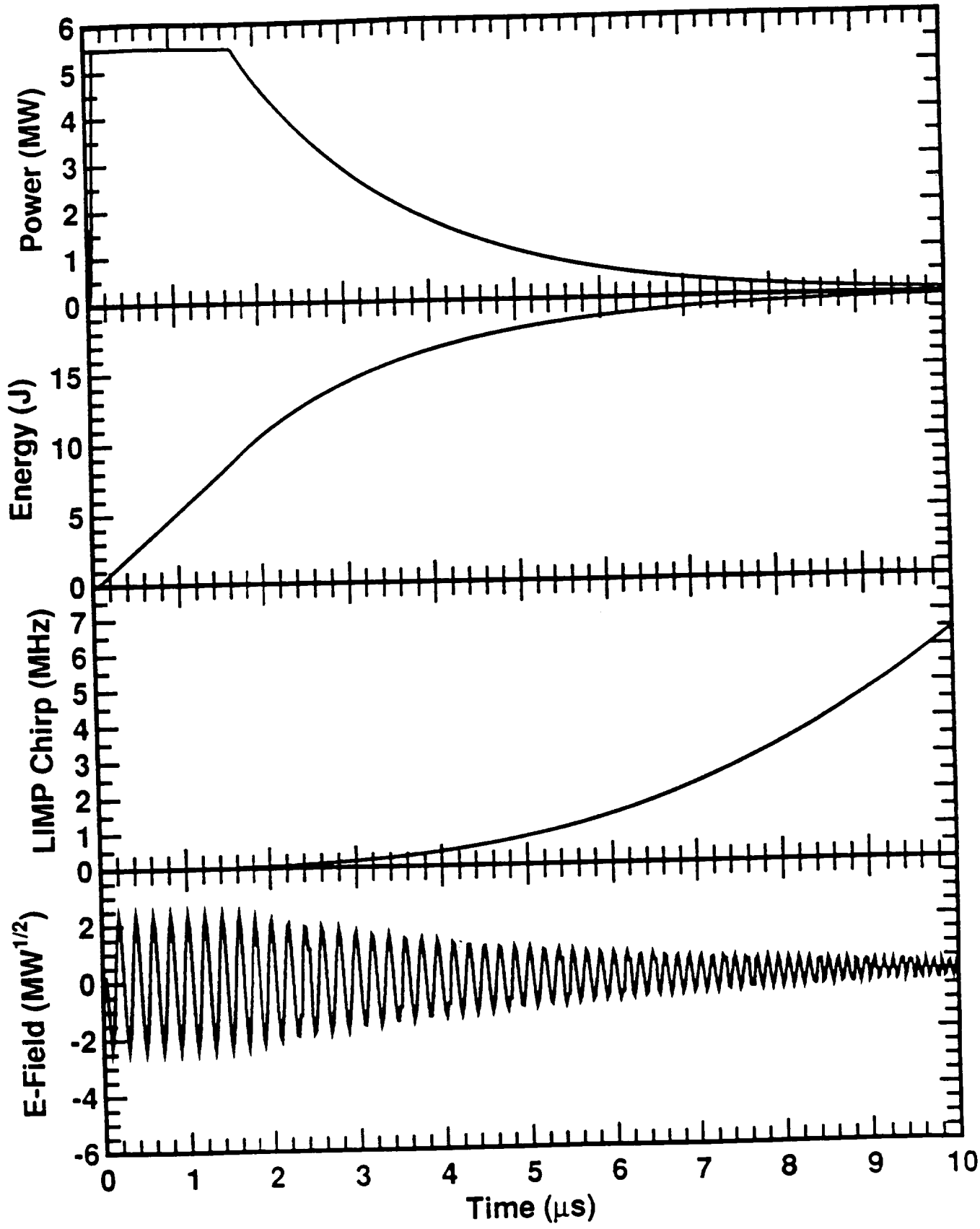
3.1 μs FWHM pulse and 4 μs tail decay - with frequency ch
Power (MW)
Energy (J)
LIMP Chirp (MHz)
E-Field (MW^1/2)
Time (μs)

Fig 3.4a

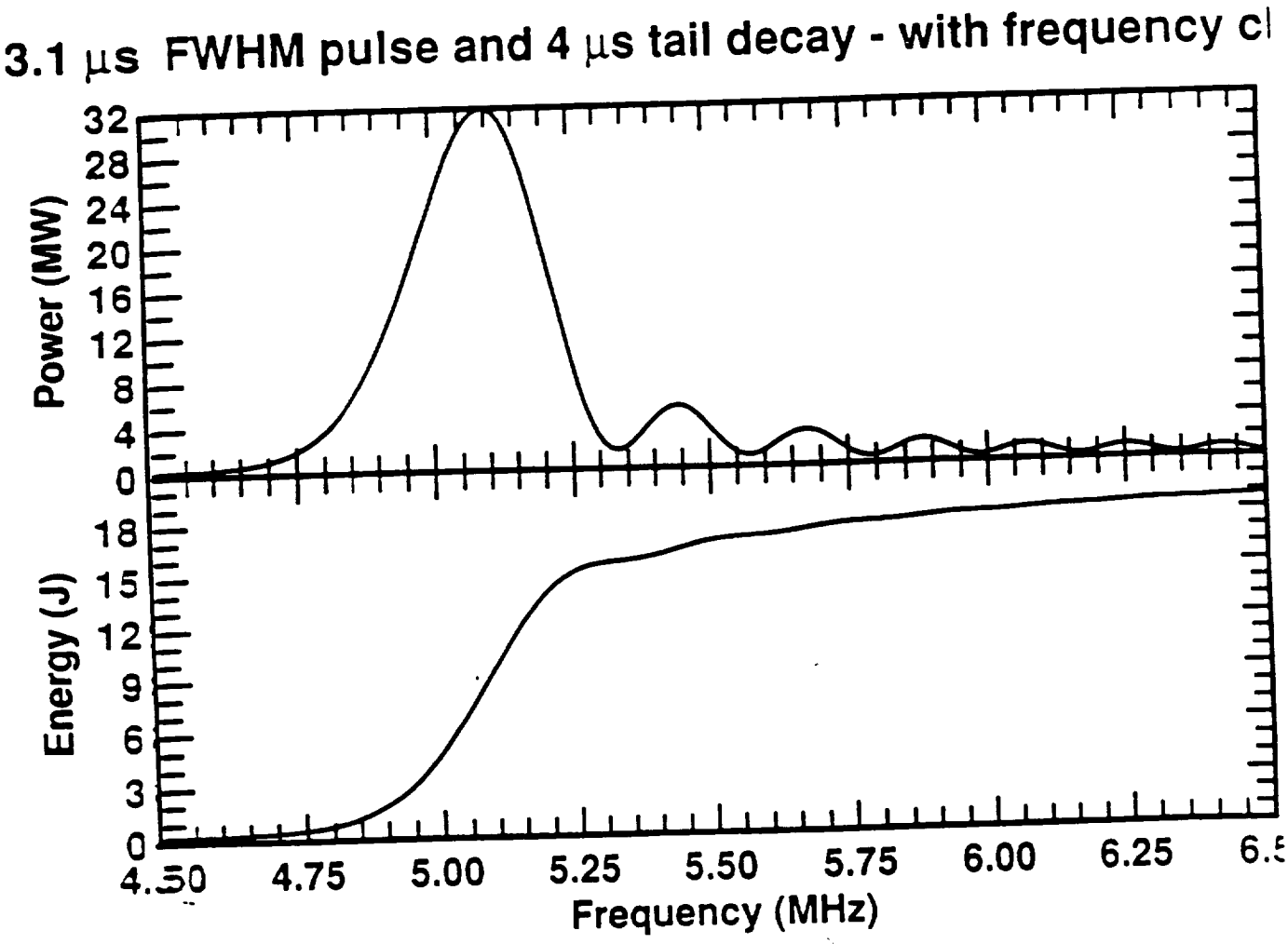
3.1 μs FWHM pulse and 4 μs tail decay - with frequency cl
Power (MW)
32
28
24
20
16
12
8
4
0
Energy (J)
18
15
12
9
6
3
0
4.50
4.75
5.00
5.25
5.50
5.75
6.00
6.25
Frequency (MHz)

Fig 3.4b

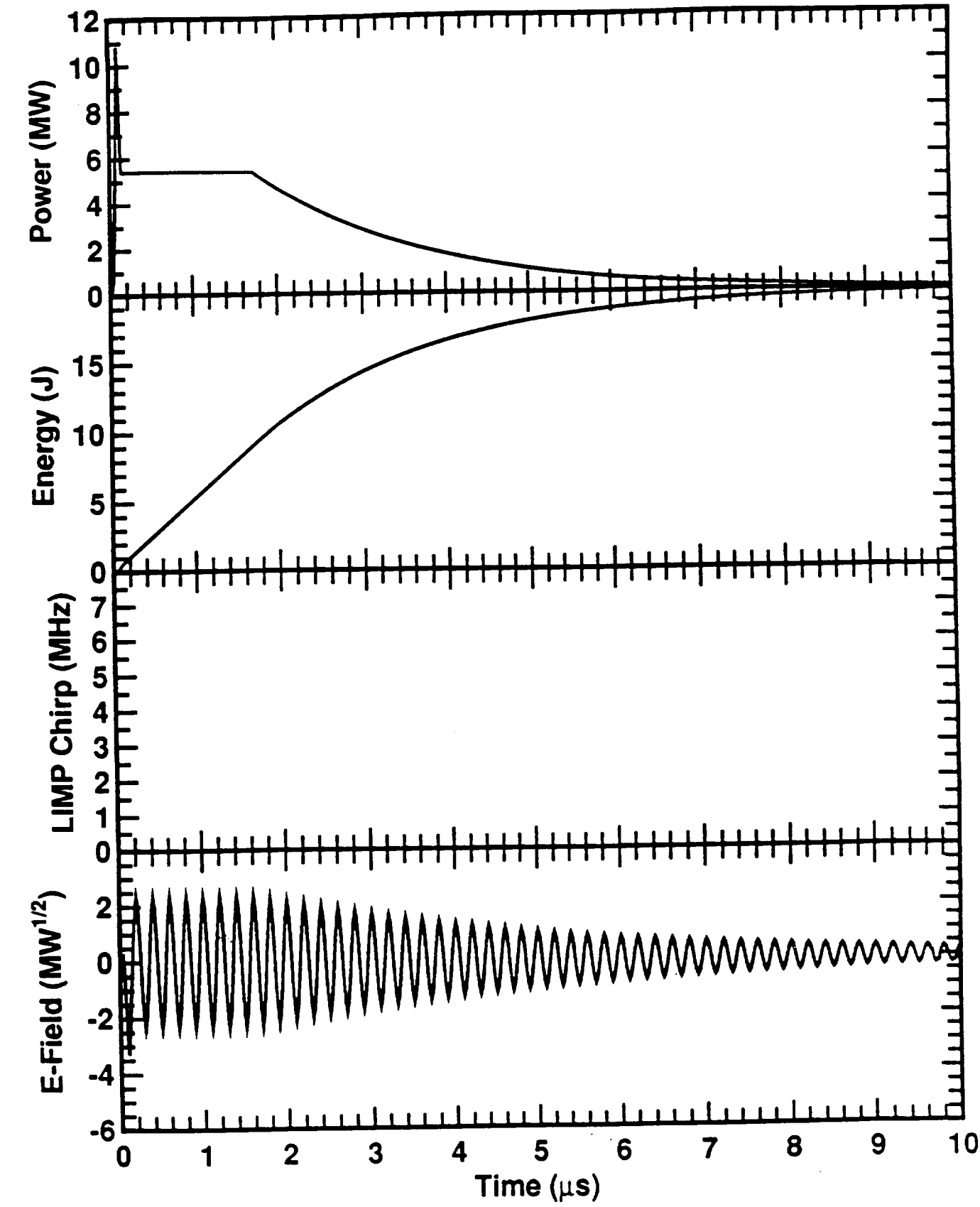
3.1 μs FWHM pulse, GSS and 4 μs tail decay - no frequency ch
Power (MW)
Energy (J)
LIMP Chirp (MHz)
E-Field (MW^1/2)
Time (μs)

Fig 3.5a

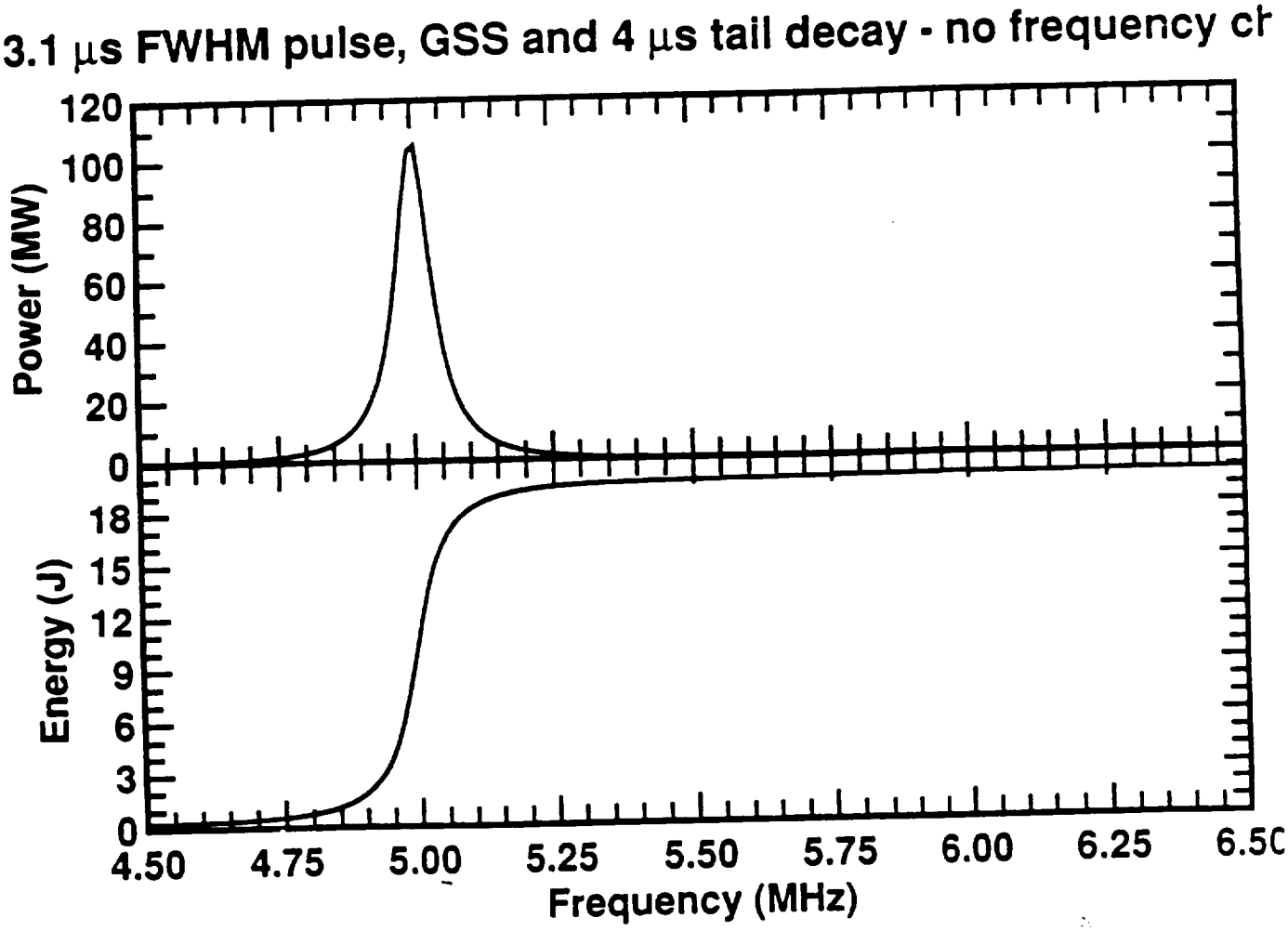
3.1 μs FWHM pulse, GSS and 4 μs tail decay - no frequency ch
Power (MW)
120
100
80
60
40
20
0
Energy (J)
18
15
12
9
6
3
0
4.50
4.75
5.00
5.25
5.50
5.75
6.00
6.25
6.50
Frequency (MHz)

Fig 3.5b

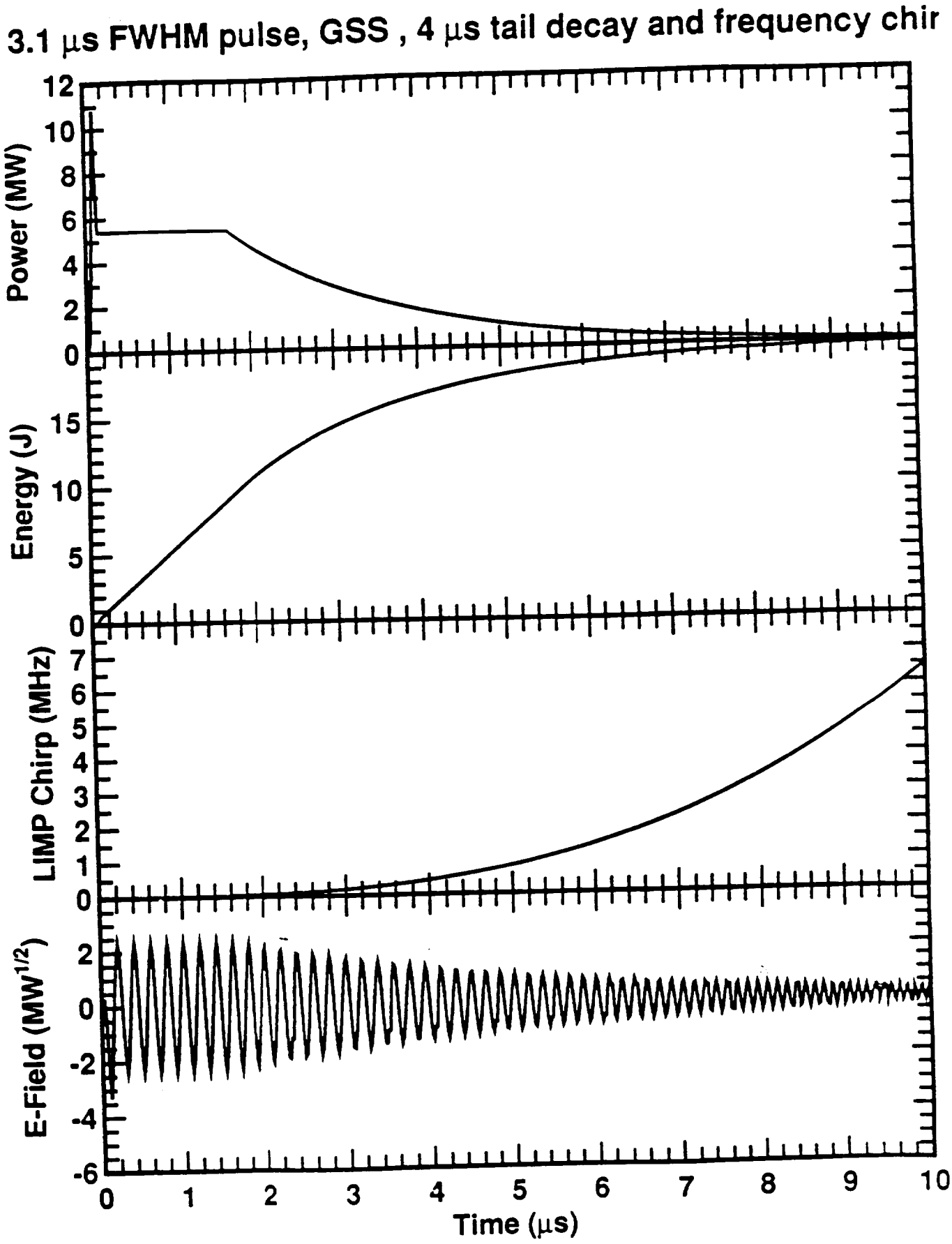
3.1 μs FWHM pulse, GSS , 4 μs tail decay and frequency chir
Power (MW)
Energy (J)
LIMP Chirp (MHz)
E-Field (MW^1/2)
Time (μs)

Fig 3.6a

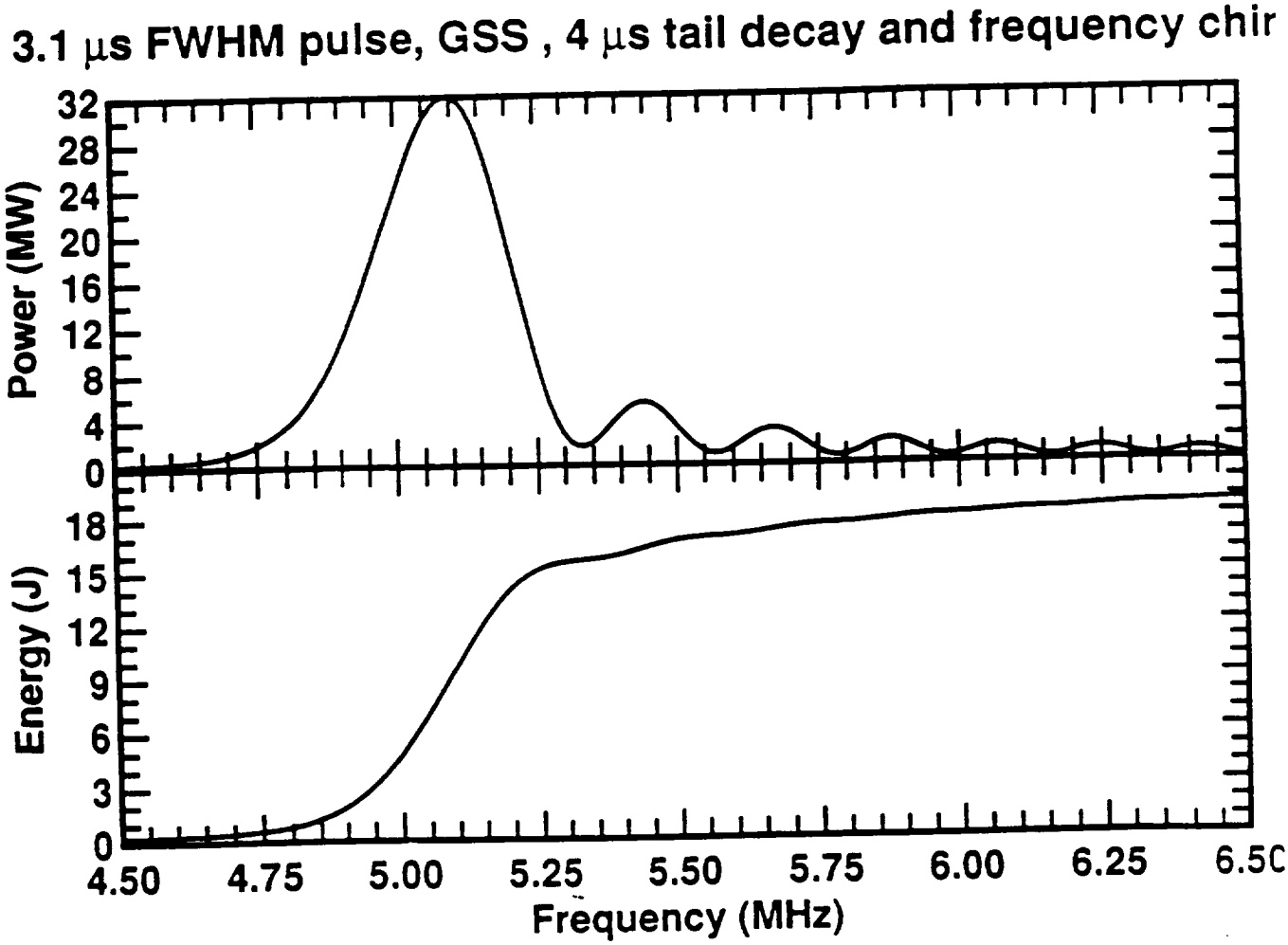
3.1 μs FWHM pulse, GSS , 4 μs tail decay and frequency chir
Power (MW)
32
28
24
20
16
12
8
4
0
Energy (J)
18
15
12
9
6
3
0
4.50
4.75
5.00
5.25
5.50
5.75
6.00
6.25
6.50
Frequency (MHz)

Fig 3.6b

Energy in a given frequency bandwidth

Pulse tail decay time is 4us.

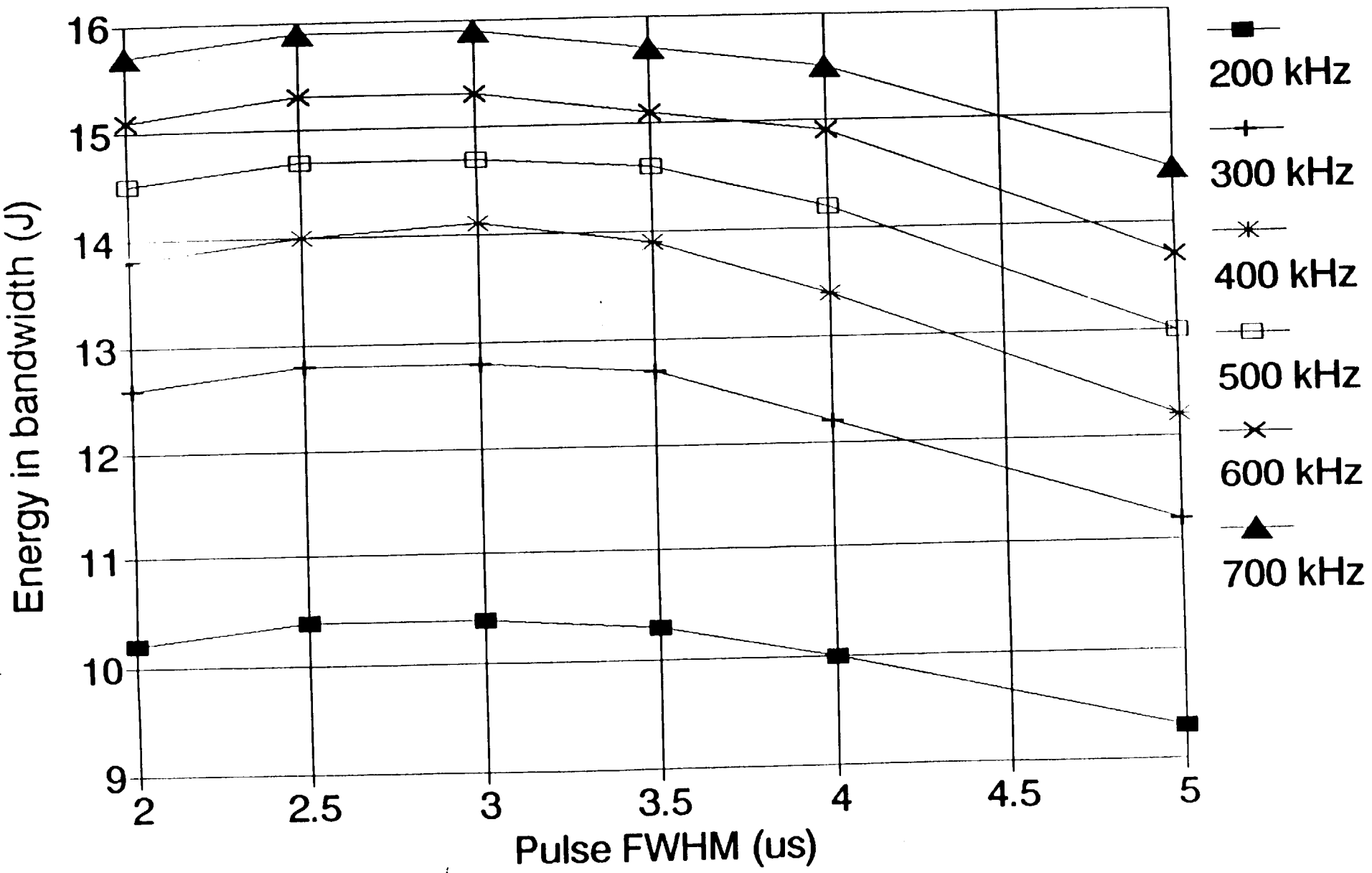

Fig 3.7

40

Energy in a given frequency bandwidth

Pulse tail decay time is 3us.

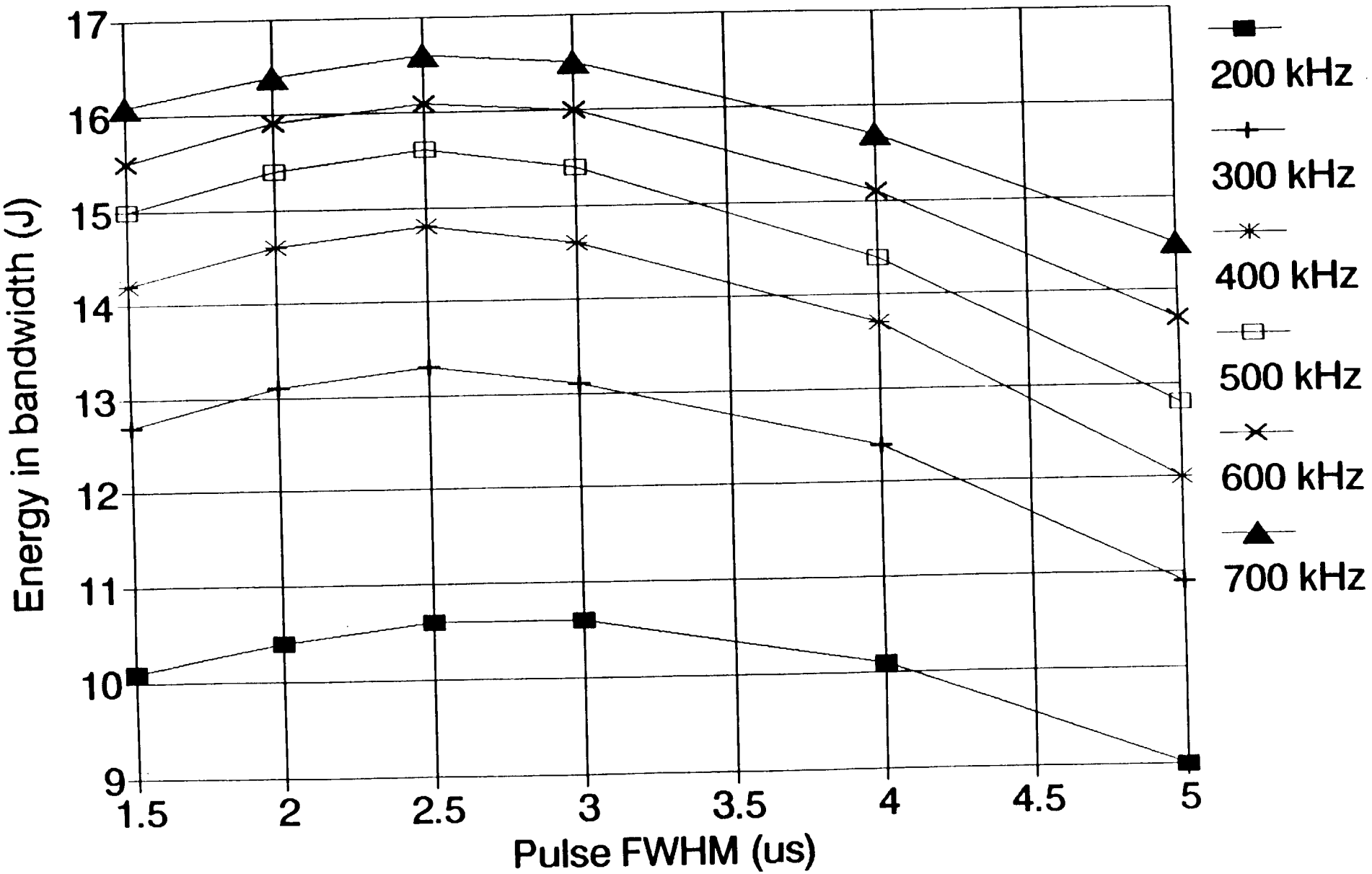

Fig 3.8

Energy in a given frequency bandwidth

Pulse tail decay time is 2us.

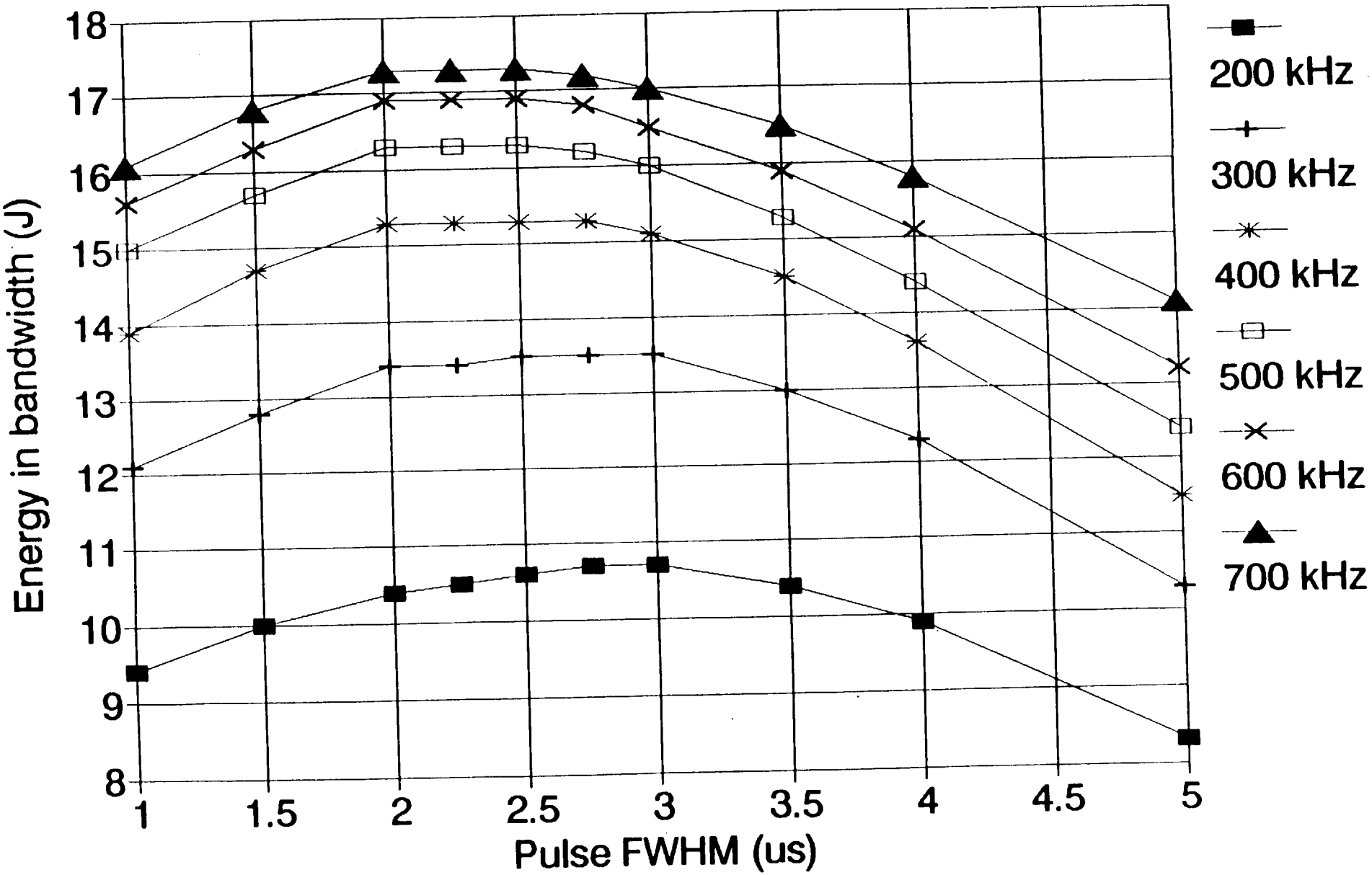

Fig 3.9

	Pulse energy (J)	20	1	2	4
Chamber	Length (cm)	121.92	27.26	38.55	54.52
	Diameter (cm)	60.96	28.83	34.28	40.77
	Cross-section (cm ^ 2)	2918.64	652.63	922.95	1305.25
	Volume (l)	355.84	17.79	35.58	71.17
Gas	Helium	3.00	3.00	3.00	3.00
	Nitrogen	1.00	1.00	1.00	1.00
	Carbon Dioxide	1.00	1.00	1.00	1.00
	Pressure (atm)	0.63	0.63	0.63	0.63
Discharge	Number	4.00			
	Length (m)	0.38			
	Total Length (m)	1.50	0.34	0.47	0.67
	Width (cm)	4.00	1.89	2.25	2.67
	Height (cm)	4.20	1.99	2.36	2.81
	Area (cm ^ 2)	16.80	3.76	5.31	7.51
	Volume (l)	2.52	0.13	0.25	0.50
	Electrode area (cm ^ 2)	600.00	63.44	106.70	179.44
	Electrode area ratio	1.00	0.11	0.18	0.30
	Striking voltage (kV)	34.00	16.08	19.12	22.74
	Glow voltage (kV)	21.00	9.93	11.81	14.04
	Electric field (kV/cm)	5.00	5.00	5.00	5.00
	Chamber length/discharge length	81.28	81.28	81.28	81.28
Resonator	Length (m)	3.00	3.00	3.00	3.00
	Beam width (cm)	4.00	1.89	2.25	2.67
	Beam height (cm)	4.00	1.89	2.25	2.67
	Beam area (cm ^ 2)	16.00	3.58	5.06	7.16
	Gain volume (l)	2.40	0.12	0.24	0.48
Pulse	Energy (J)	20.00	1.00	2.00	4.00
	FWHM (us)	3.00	3.00	3.00	3.00
	Freqency chirp in FWHM (kHz)	200	200	200	200
	Intensity (J/cm ^ 2)	1.25	0.28	0.40	0.56
	Energy density (J/l)	8.33	8.33	8.33	8.33
	Low average PRF (Hz)	4.60	4.60	4.60	4.60
	High average PRF (Hz)	10.00	10.00	10.00	10.00
	Maximum PRF (Hz)	16.00	16.00	16.00	16.00
Gas Loop (16 Hz)	Clearing ratio	3.00	3.00	3.00	3.00
	Flow rate (l/s)	115.20	5.76	11.52	23.04
	Flow ratio	1.00	0.05	0.10	0.20
	Flow velocity (m/s)	1.92	0.91	1.08	1.28
	Height shock	1.05	1.05	1.05	1.05
	Width shock	1.00	1.00	1.00	1.00
	Aperture area/Chamber area	0.01	0.01	0.01	0.01
	Muffler cross-section (cm ^ 2)	262.00	58.58	82.85	117.17
	Muffler area/Aperture area	7.80	7.80	7.80	7.80
	Recovery time (s)	0.06	0.06	0.06	0.06

	Sound speed (m/s)	472.00	472.00	472.00	472.00
	Acoustic transits	646.19	1366.53	1149.11	966.28
Electrical	Pulse energy (J)	20.00	1.00	2.00	4.00
	Intrinsic efficiency (%)	9.00	9.00	9.00	9.00
	Discharge energy/Stored energy	0.95	0.95	0.95	0.95
	Stored energy (J)	233.92	11.70	23.39	46.78
	PSU efficiency (%)	73.00	73.00	73.00	73.00
	1 Hz power (W)	320.44	16.02	32.04	64.09
	Low average PRF power (W)	1474.00	73.70	147.40	294.80
	High average PRF power (W)	3204.36	160.22	320.44	640.87
	Peak power (W)	5126.97	256.35	512.70	1025.39
Catalyst	No. of beds	2	2	2	2
	O2 production (std c.c./(s.kW))	1.00	1.00	1.00	1.00
	O2 produced (std. c.c./(s.kW))				
	@ Low average PRF	1.02	0.05	0.10	0.20
	@ High average PRF	2.22	0.11	0.22	0.44
	Catalyst safety margin	2	2	2	2
	Catalyst reactivity (cc/(g.s)	5	5	5	5
	O2 part. pressure req. (atm.)	1.00E-03	1.00E-03	1.00E-03	1.00E-03
	Catalyst mass required (kg)				
	@ Low average PRF	0.41	0.02	0.04	0.08
	@ High average PRF	0.89	0.04	0.09	0.18
	Catalyst fill (g/(g corderite))	0.20	0.20	0.20	0.20
	Mass of corderite (kg)				
	@ Low average PRF	2.04	0.10	0.20	0.41
	@ High average PRF	4.44	0.22	0.44	0.89
	Total catalyst mass (kg)				
	@ Low average PRF	2.45	0.12	0.25	0.49
	@ High average PRF	5.33	0.27	0.53	1.07
	Corderite density (kg/l)	0.50	0.50	0.50	0.50
	Catalyst volume (l)				
	@ Low average PRF	4.09	0.20	0.41	0.82
	@ High average PRF	8.89	0.44	0.89	1.78
HXchanger	Average Heat Load (W)				
	@ Low average PRF	0.93	0.05	0.09	0.19
	@ High average PRF	2.02	0.10	0.20	0.40
	Pulse energy (J)	20	1	2	4
PFN subsystem					
	Thyratron	3.27	3.27	3.27	3.27
	Thyratron heaters	0.91	0.91	0.91	0.91
	Thyratron grid filter	0.91	0.91	0.91	0.91
	Thyratron supt. base	0.68	0.68	0.68	0.68
	Thyratron resistor	1.13	1.13	1.13	1.13
	DC-DC converter	15.88	8.33	8.73	9.53
	PFN capacitors	22.68	1.13	2.27	4.54

Backup capacitors	9.07	0.45	0.91	1.81
PFN inductors	2.08	2.08	2.08	2.08
Charging diodes	1.83	0.92	1.03	1.22
Backup diodes	1.83	0.92	1.03	1.22
Cap. divider capacitors	0.42	0.42	0.42	0.42
Current transformers	2.99	2.99	2.99	2.99
Output voltage cap. divider	0.21	0.21	0.21	0.21
Output cable assembly	2.66	1.33	0.27	0.53
120VDC to 1kVDC, 10W	0.62	0.62	0.62	0.62
Inverse V sense & lockout cntrls	0.67	0.67	0.67	0.67
HV trigger generator	0.62	0.62	0.62	0.62
HV wiring conn. links	0.83	0.83	0.83	0.83
Cap. & PFN support str.	2.08	0.10	0.21	0.42
Cage	4.16	2.29	2.29	2.49
PSU heat exchanger	2.08	0.10	0.21	0.42
TOTAL PFN MASS	77.59	30.77	32.26	37.51
Flow subsystem				
Fan motor and couplings	7.71	4.05	4.24	4.63
Heat exchanger				
@ Low average PRF	1.38	0.07	0.14	0.28
@ High average PRF	2.99	0.15	0.30	0.60
Fan plus housing	2.72	0.14	0.27	0.54
Cathode	5.44	0.53	0.97	1.63
Anode & preioniser	9.98	1.40	1.77	2.98
Corona bar	2.22	0.24	0.40	0.66
Catalyst monolith				
@ Low average PRF	2.45	0.12	0.25	0.49
@ High average PRF	5.33	0.27	0.53	1.07
Flow loop walls				
End plates	3.58	0.89	1.13	1.60
Duct assembly	4.63	0.89	0.82	1.38
Muffler assembly	9.07	0.45	0.91	1.81
High voltage bushing				
Ceramic parts	3.18	3.18	3.18	3.18
Stainless steel parts	1.58	1.58	1.58	1.58
Copper parts	1.58	1.58	1.58	1.58
Fan motor heat exchanger	1.80	0.90	0.18	0.36
Laser thermal capacitor	13.57	0.68	1.36	2.71
TOTAL FLOW MASS				
@ Low average PRF	70.89	15.90	18.77	25.42
@ High average PRF	75.39	15.90	19.22	26.32
Optical subsystem				
Windows	0.61	0.14	0.19	0.27
Large mirrors	2.06	0.46	0.65	0.92
Large mirror mounts	2.99	0.67	0.95	1.34
Small mirrors	0.39	0.09	0.12	0.17
Small mirror mounts	0.68	0.15	0.22	0.30
Lens	0.10	0.02	0.03	0.05
Newport mount	0.45	0.45	0.45	0.45
PZT drive	0.91	0.91	0.91	0.91
Grating	0.07	0.02	0.02	0.03
Aerotech mount	1.13	1.13	1.13	1.13
Adapter	0.45	0.45	0.45	0.45

Output optical table	3.29	3.29	3.29	3.29
Folding optical table	1.88	1.88	1.88	1.88
TOTAL OPTICAL MASS	15.03	9.66	10.30	11.21
Support structure				
Pressure vessel	5.33	0.56	0.95	1.59
Flanges	3.95	1.85	2.22	2.64
End covers	5.63	1.26	1.78	2.52
Base mounts	0.78	0.37	0.44	0.52
TOTAL SUPPORT MASS	15.69	4.06	5.39	7.27
SUMMARY				
Pulse energy (J)	20	1	2	4
Optical subsystem	15.03	9.66	10.30	11.21
Laser flow subsystem				
@ Low average PRF	70.89	15.09	18.77	25.42
@ High average PRF	75.39	15.31	19.22	26.32
Pulse forming network	77.59	30.77	32.26	37.51
Control & instrumentation	4.50	4.50	4.50	4.50
Support structure	15.69	4.06	5.39	7.27
TOTAL LASER MASS				
@ Low average PRF	183.69	64.05	71.22	85.91
@ High average PRF	188.19	64.30	71.67	86.81

Pulse energy (J)	20	1	2	4
Laser PSU @ Low Average PRF	1474.00	73.70	147.40	294.80
Laser PSU @ High Average PRF	3204.36	160.22	320.44	640.87
Laser PSU @ Peak PRF	5126.97	256.35	512.70	1025.39
Fan Motors	50.00	26.25	27.50	30.00
Local Oscillator	30.00	30.00	30.00	30.00
Injection Oscillator	50.00	50.00	50.00	50.00
Controls	100.00	100.00	100.00	100.00
TOTAL LASER SYSTEM POWER				
@ Low average PRF	1704.00	279.95	354.90	504.80
@ High average PRF	3434.36	366.47	527.94	850.87
@ Peak PRF	5356.97	462.60	720.20	1235.39

LAWS LASER PARAMETERS

6	8	10	12	14	16	18	20
66.78	77.11	86.21	94.44	102.01	109.05	115.66	121.92
45.12	48.48	51.26	53.65	55.76	57.65	59.38	60.96
1595.60	1845.91	2063.79	2260.77	2441.91	2610.51	2768.86	2918.64
106.75	142.34	177.92	213.50	249.09	284.67	320.26	355.84
3.00	3.00	3.00	3.00	3.00	3.00	3.00	3.00
1.00	1.00	1.00	1.00	1.00	1.00	1.00	1.00
1.00	1.00	1.00	1.00	1.00	1.00	1.00	1.00
0.63	0.63	0.63	0.63	0.63	0.63	0.63	0.63
0.82	0.95	1.06	1.16	1.25	1.34	1.42	1.50
2.96	3.18	3.36	3.52	3.66	3.78	3.90	4.00
3.11	3.34	3.53	3.70	3.84	3.97	4.09	4.20
9.20	10.63	11.88	13.01	14.06	15.03	15.94	16.80
0.76	1.01	1.26	1.51	1.76	2.02	2.27	2.52
243.22	301.78	356.76	409.04	459.17	507.54	554.41	600.00
0.41	0.50	0.59	0.68	0.77	0.85	0.92	1.00
25.16	27.04	28.59	29.92	31.10	32.16	33.12	34.00
15.54	16.70	17.66	18.48	19.21	19.86	20.45	21.00
5.00	5.00	5.00	5.00	5.00	5.00	5.00	5.00
81.28	81.28	81.28	81.28	81.28	81.28	81.28	81.28
3.00	3.00	3.00	3.00	3.00	3.00	3.00	3.00
2.96	3.18	3.36	3.52	3.66	3.78	3.90	4.00
2.96	3.18	3.36	3.52	3.66	3.78	3.90	4.00
8.76	10.12	11.31	12.39	13.39	14.31	15.18	16.00
0.72	0.96	1.20	1.44	1.68	1.92	2.16	2.40
6.00	8.00	10.00	12.00	14.00	16.00	18.00	20.00
3.00	3.00	3.00	3.00	3.00	3.00	3.00	3.00
200	200	200	200	200	200	200	200
0.68	0.79	0.88	0.97	1.05	1.12	1.19	1.25
8.33	8.33	8.33	8.33	8.33	8.33	8.33	8.33
4.60	4.60	4.60	4.60	4.60	4.60	4.60	4.60
10.00	10.00	10.00	10.00	10.00	10.00	10.00	10.00
16.00	16.00	16.00	16.00	16.00	16.00	16.00	16.00
3.00	3.00	3.00	3.00	3.00	3.00	3.00	3.00
34.56	46.08	57.60	69.12	80.64	92.16	103.68	115.20
0.30	0.40	0.50	0.60	0.70	0.80	0.90	1.00
1.42	1.53	1.61	1.69	1.76	1.82	1.87	1.92
1.05	1.05	1.05	1.05	1.05	1.05	1.05	1.05
1.00	1.00	1.00	1.00	1.00	1.00	1.00	1.00
0.01	0.01	0.01	0.01	0.01	0.01	0.01	0.01
143.50	165.70	185.26	202.94	219.20	234.34	248.56	262.00
7.80	7.80	7.80	7.80	7.80	7.80	7.80	7.80
0.06	0.06	0.06	0.06	0.06	0.06	0.06	0.06

472.00	472.00	472.00	472.00	472.00	472.00	[illegible]	472.00
[illegible]73.13	812.54	768.45	734.21	706.46	683.26	[illegible]3.44	646.19
6.00	8.00	10.00	12.00	14.00	16.00	[illegible]00	20.00
9.00	9.00	9.00	9.00	9.00	9.00	9.00	9.00
0.95	0.95	0.95	0.95	0.95	0.95	[illegible]95	0.95
70.18	93.57	116.96	140.35	163.74	187.13	[illegible]0.53	233.92
73.00	73.00	73.00	73.00	73.00	73.00	[illegible]3.00	73.00
96.13	128.17	160.22	192.26	224.31	256.35	[illegible]8.39	320.44
442.20	589.60	737.00	884.40	1031.80	1179.20	1326.60	1474.00
961.31	1281.74	1602.18	1922.61	2243.05	2563.49	2883.92	3204.36
1538.09	2050.79	2563.49	3076.18	3588.88	4101.58	[illegible]614.28	5126.97
2	2	2	2	2	2	2	2
1.00	1.00	1.00	1.00	1.00	1.00	1.00	1.00
0.31	0.41	0.51	0.61	0.72	0.82	0.92	1.02
0.67	0.89	1.11	1.33	1.56	1.78	2.00	2.22
2	2	2	2	2	2	2	2
5	5	5	5	5	5	5	5
1.00E-03	1.00E-03	1.00E-03	1.00E-03	1.00E-03	1.00E-03	1.00E-03	1.00E-03
0.12	0.16	0.20	0.25	0.29	0.33	0.37	0.41
0.27	0.36	0.44	0.53	0.62	0.71	0.80	0.89
0.20	0.20	0.20	0.20	0.20	0.20	0.20	0.20
0.61	0.82	1.02	1.23	1.43	1.64	1.84	2.04
1.33	1.78	2.22	2.67	3.11	3.56	4.00	4.44
0.74	0.98	1.23	1.47	1.72	1.96	2.21	2.45
1.60	2.13	2.67	3.20	3.73	4.27	4.80	5.33
0.50	0.50	0.50	0.50	0.50	0.50	0.50	0.50
1.23	1.64	2.04	2.45	2.86	3.27	3.68	4.09
2.67	3.56	4.44	5.33	6.22	7.11	[illegible]00	8.89
0.28	0.37	0.47	0.56	0.65	0.74	[illegible]84	0.93
0.61	0.81	1.01	1.21	1.42	1.62	[illegible]82	2.02

MASS BREAKDOWN

(kg)

6	8	10	12	14	16	18	20
3.27	3.27	3.27	3.27	3.27	3.27	3.27	3.27
0.91	0.91	0.91	0.91	0.91	0.91	0.91	0.91
0.91	0.91	0.91	0.91	0.91	0.91	0.91	0.91
0.68	0.68	0.68	0.68	0.68	0.68	0.68	0.68
1.13	1.13	1.13	1.13	1.13	1.13	1.13	1.13
10.32	11.11	11.91	12.70	13.49	14.29	15.08	15.88
6.80	9.07	11.34	13.61	15.88	18.14	20.41	22.68

2.72	3.63	4.54	5.44	6.35	7.26	[illegible]	9.07
2.08	2.08	2.08	2.08	2.08	2.08	[illegible]	2.08
1.35	1.45	1.54	1.61	1.67	1.73	[illegible]	1.83
1.35	1.45	1.54	1.61	1.67	1.73	[illegible]	1.83
0.42	0.42	0.42	0.42	0.42	0.42	0.42	0.42
2.99	2.99	2.99	2.99	2.99	2.99	2.99	2.99
0.21	0.21	0.21	0.21	0.21	0.21	0.21	0.21
0.80	1.06	1.33	1.60	1.86	2.13	2.39	2.66
0.62	0.62	0.62	0.62	0.62	0.62	0.62	0.62
0.67	0.67	0.67	0.67	0.67	0.67	0.67	0.67
0.62	0.62	0.62	0.62	0.62	0.62	0.62	0.62
0.83	0.83	0.83	0.83	0.83	0.83	0.83	0.83
0.62	0.83	1.04	1.25	1.45	1.66	1.87	2.08
2.70	2.91	3.12	3.33	3.53	3.74	3.95	4.16
0.62	0.83	1.04	1.25	1.45	1.66	1.87	2.08
42.63	47.69	52.72	57.72	62.70	67.67	72.64	77.59

5.01	5.40	5.78	6.17	6.55	6.94	7.33	7.71
0.41	0.55	0.69	0.83	0.96	1.10	1.24	1.38
0.90	1.20	1.50	1.80	2.10	2.40	2.69	2.99
0.82	1.09	1.36	1.63	1.91	2.18	2.45	2.72
2.21	2.74	3.24	3.71	4.17	4.60	5.03	5.44
4.05	5.02	5.93	6.80	7.64	8.44	9.22	9.98
0.90	1.12	1.32	1.52	1.70	1.88	2.05	2.22
0.74	0.98	1.23	1.47	1.72	1.96	2.21	2.45
1.60	2.13	2.67	3.20	3.73	4.27	4.80	5.33
1.96	2.27	2.53	2.78	3.00	3.20	3.40	3.58
1.88	2.33	2.75	3.15	3.54	3.91	4.28	4.63
2.72	3.63	4.54	5.44	6.35	7.26	[illegible]	9.07
3.18	3.18	3.18	3.18	3.18	3.18	3.18	3.18
1.58	1.58	1.58	1.58	1.58	1.58	1.58	1.58
1.58	1.58	1.58	1.58	1.58	1.58	1.58	1.58
0.54	0.72	0.90	1.08	1.26	1.44	[illegible]	1.80
4.07	5.43	6.79	8.14	9.50	10.86	12.21	13.57
31.63	37.60	43.39	49.06	54.62	60.11	[illegible]	70.89
32.98	39.39	45.64	51.75	57.77	63.71	69.58	75.39

0.33	0.39	0.43	0.47	0.51	0.55	0.58	0.61
1.13	1.31	1.46	1.60	1.73	1.85	1.96	2.06
1.64	1.89	2.12	2.32	2.50	2.68	2.84	2.99
0.21	0.24	0.27	0.30	0.32	0.35	0.37	0.39
0.37	0.43	0.48	0.53	0.57	0.61	0.65	0.68
0.06	0.06	0.07	0.08	0.09	0.09	0.10	0.10
0.45	0.45	0.45	0.45	0.45	0.45	0.45	0.45
0.91	0.91	0.91	0.91	0.91	0.91	0.91	0.91
0.04	0.05	0.05	0.06	0.06	0.07	0.07	0.07
1.13	1.13	1.13	1.13	1.13	1.13	1.13	1.13
0.45	0.45	0.45	0.45	0.45	0.45	0.45	0.45

3.29	3.29	3.29	3.29	3.29	3.29	3.29	3.29
1.88	1.88	1.88	1.88	1.88	1.88	1.88	1.88
11.90	12.49	13.00	13.47	13.90	14.30	14.67	15.03
2.16	2.68	3.17	3.63	4.08	4.51	4.93	5.33
2.92	3.14	3.32	3.48	3.61	3.74	3.85	3.95
3.08	3.56	3.98	4.36	4.71	5.03	5.34	5.63
0.58	0.62	0.65	0.68	0.71	0.74	0.76	0.78
5.74	10.00	11.13	12.16	13.11	14.01	14.87	15.69
6	8	10	12	14	16	18	20
11.90	12.49	13.00	13.47	13.90	14.30	14.67	15.03
31.63	37.60	43.39	49.06	54.62	60.11	65.53	70.89
32.98	39.39	45.64	51.75	57.77	63.71	69.58	75.39
42.63	47.69	52.72	57.72	62.70	67.67	72.64	77.59
4.50	4.50	4.50	4.50	4.50	4.50	4.50	4.50
8.74	10.00	11.13	12.16	13.11	14.01	14.87	15.69
99.41	112.27	124.73	136.90	148.84	160.60	172.21	183.69
100.76	114.07	126.98	139.59	151.98	164.19	176.25	188.19

POWER BREAKDOWN

(W)

6	8	10	12	14	16	18	20
442.20	589.60	737.00	884.40	1031.80	1179.20	1326.60	1474.00
961.31	1281.74	1602.18	1922.61	2243.05	2563.49	2883.92	3204.36
1538.09	2050.79	2563.49	3076.18	3588.88	4101.58	4614.28	5126.97
32.50	35.00	37.50	40.00	42.50	45.00	47.50	50.00
30.00	30.00	30.00	30.00	30.00	30.00	30.00	30.00
50.00	50.00	50.00	50.00	50.00	50.00	50.00	50.00
100.00	100.00	100.00	100.00	100.00	100.00	100.00	100.00
754.70	804.60	954.50	1104.40	1254.30	1404.20	1554.10	1704.00
1773.81	1496.74	1819.68	2142.61	2465.55	2788.49	3111.42	3434.36
2550.59	2265.79	2780.99	3296.18	3811.38	4326.58	4841.78	5356.97

LAWS-A STUDY
LMSC/TDS Design

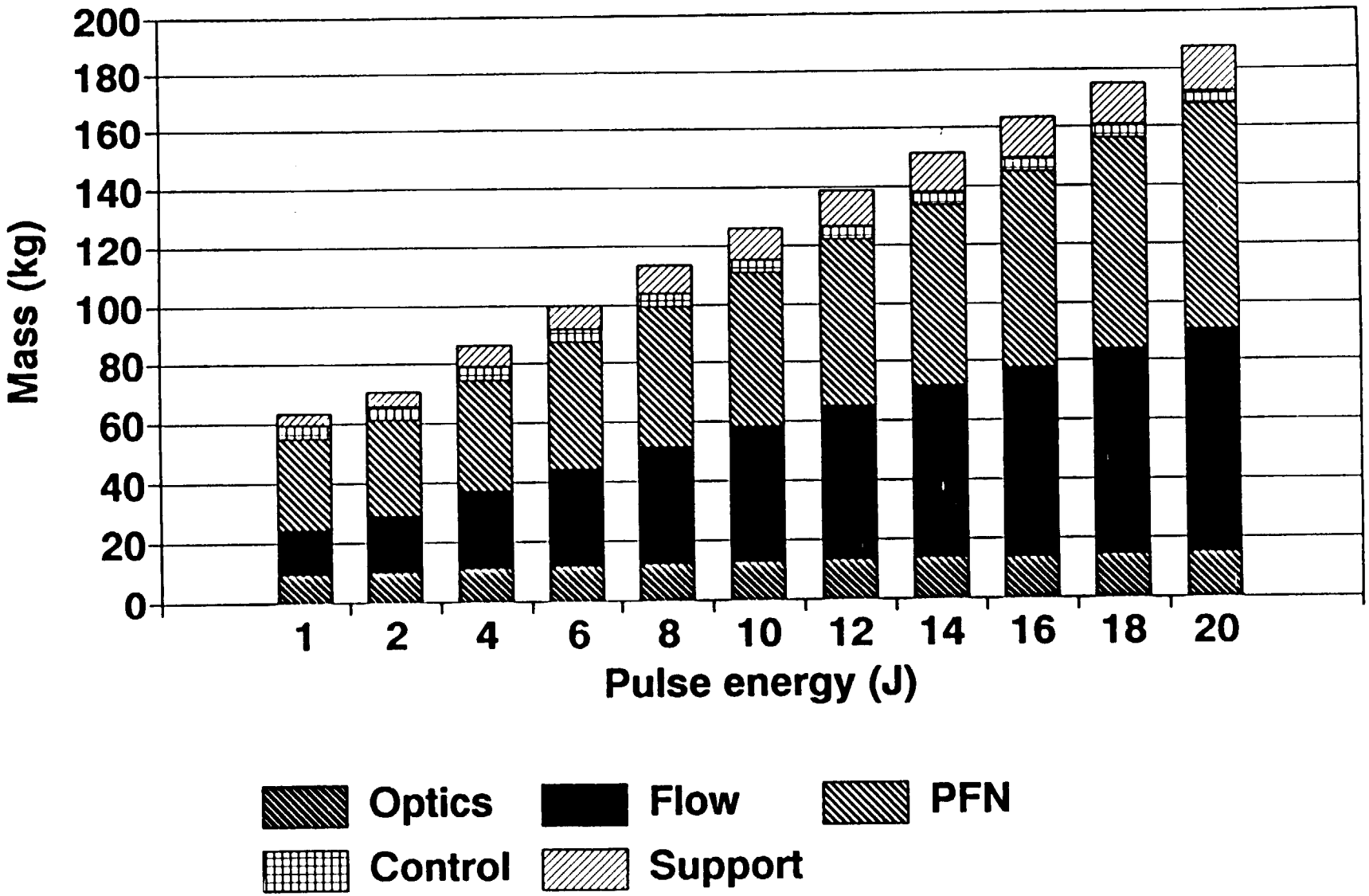

LAWS-A STUDY
LMSC/TDS Design

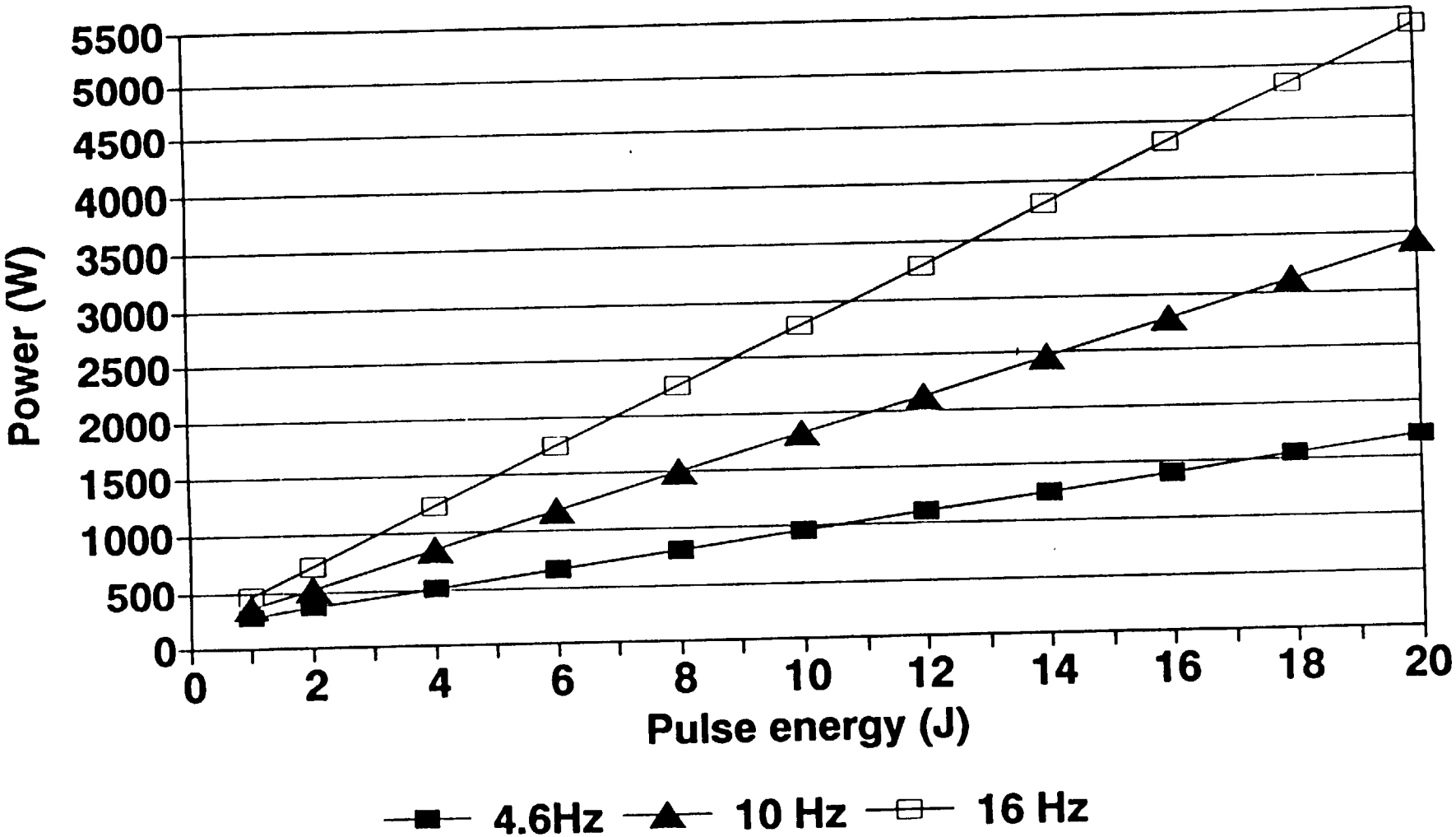

LAWS-A STUDY

LMSC/TDS Design

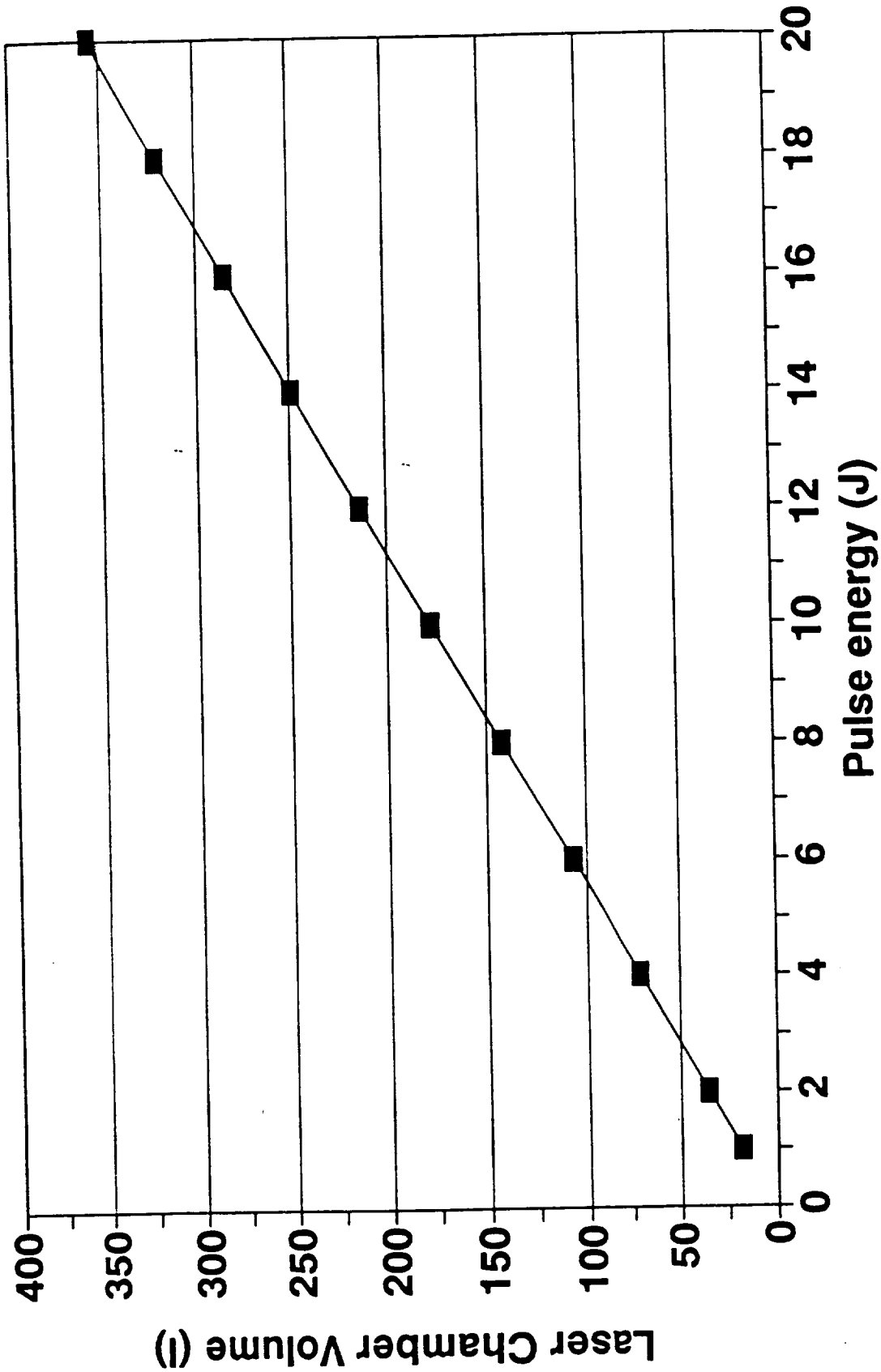

5 Discharge Circuit Components for LAWS

5.1 Introduction

This chapter is based on a memo addressing the issues associated with the high voltage components in the LAWS laser device. High voltage pulse circuits consist basically of capacitors, inductors and some form of switch, all of which have been specifically designed for the voltage of interest. Conventional electronic circuits are used to form additional control circuitry. Obviously with pulsed high voltage there is the potential for considerable RFI contamination. This can be overcome through the use of screening. The screening is usually some form of metal container for the circuitry.

5.2 Switching Devices

The requirements of the pulse required to form the discharge are severe, typically the discharge pulse must provide ~30-40 kV at 3-4 kA in a pulse of duration 1-3 μs with leading edge voltage rise times of the order of ~300 ns. This corresponds to a rate of rise of ~100 kV/μs! Originally spark gaps were used as the switching device, but these have a limited lifetime and have been replaced by thyratrons in most applications. Recently solid-state switching devices have become available. Thyratrons and solid-state switching technologies are discussed below.

5.2.1 Thyratrons

Thyratrons are the most common high voltage switching device in pulsed gas lasers and they have been well tried and tested. The main market for thyratrons has traditionally been radar modulators and these radar thyratrons were a little too small for switching large lasers of the LAWS type. The manufacturers have increasingly been observant of the growing laser market (particularly excimer) and now offer a range of tubes suited to laser switching. The development of ceramic and metal envelope technology has made modern thyratrons mechanically durable over their glass predecessors. For example, English Electric Valve (EEV), probably the major world manufacturer, offers tubes capable of switching voltages up to 100 kV with peak currents up to 20,000 A and average currents of up to 15 A.

A schematic of a thyratron is shown in figure 6.1. It can be seen that the thyratron is basically a simple device. A low pressure gap between the cathode and anode holds off the voltage until a trigger pulse appears on the control grids causing the gap to breakdown and provide a conducting path. Following the discharge pulse the electrons and ions in the gas must recombine before the tube will again hold off a

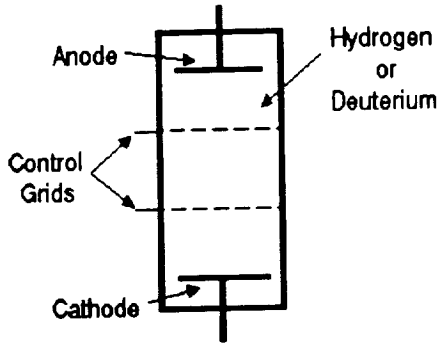

Figure 6.1 Thyratron Schematic

voltage. This limits the pulse rate of the tube. By reverse biasing the control grids, the recombination time can be reduced and the hold-off voltage increased slightly. The practical limit to the pulse rate is ~100 kHz and is not a limitation for the LAWS device. As the discharge is essentially an avalanche type, voltage and current rise times are generally limited by the external circuitry rather than the tube and rise times of 1-5 ns are possible.

As a consequence of the avalanche discharge there is a tendency for the discharge to constrict and this is limited by operating the tube at pressures below the knee of the Paschen breakdown curve. The gas chosen to fill the tube depends on the application. Hydrogen recovers more quickly than deuterium whilst deuterium can hold-off higher voltages.

To ensure consistent operation the tubes are supplied with heaters. The cathode heater provides enhanced thermionic emission, thereby ensuring a more homogeneous breakdown and the gas reservoir heater ensures that the tube pressure is maintained at an optimum value. The reservoir is a solid capsule which holds the reservoir gas in a temperature dependant bond. This enables the gas to be released in a controlled manner. Adjusting the electrical power supplied to the reservoir enables some variation in the tube characteristics to be obtained. To ensure consistent tube operation the power supplies for the reservoirs need to be well regulated, typically providing ~ 6 V at 20 - 40 A for the cathode heater and ~ 6 V at 7 - 10 A for the reservoir heater. This represents a considerable power loss (~ 200 W for the thyratron chosen by AVCO).

Of particular concern for laser devices is the potential for large reverse voltage swings which can damage and eventually destroy the anode. This has been overcome by using either double ended (double cathode) or hollow anode thyratrons.

The lifetime of the thyratron is obviously a concern for the LAWS instrument. Life tests of thyratrons in copper vapour lasers have been carried out by Lawrence Livermore Laboratories in conjunction with EEV. Life tests in excess of 10^9 pulses have been obtained, although no statistics on the distribution of the tube failures has been presented. It should also be noted that Cu vapour lasers operate in a different voltage/current regime to carbon dioxide lasers and at much higher pulse rates. It is more instructive to look at excimer lasers, which operate at lower electric field strengths than CO_2 lasers but much higher current densities. Both Lumonics and Lambda Physik have demonstrated modified commercial excimer lasers with extended life times (~10^{10} pulses) although no statistical data is available. These schemes typically employ a thyratron in combination with a magnetic compression circuit. The magnetic compression circuit enables the current density in the thyratron to be reduced and as the life time appears to be predominantly determined by the peak current value, the lifetime is lengthened. The major thyratron manufacturers (EEV, EG&G and ITT) were also contacted for lifetime information. EEV feels that the 10^9 pulse lifetime should be acheivable but they have no life data - very few people have had a need for the lifetimes and reliability that will be required from the LAWS laser. EG&G has no life data available, they let their customers do the life testing, allthough they did mention that as deuterium has a half life (although not to mine or anyone elses knowledge!), deuterium filled thyratrons have a shelf life and may be unsuitable. Deuterium filled thyratrons are primarily supplied by one of their competitors. ITT had very little comment to make, again they like the other manufacturers have little or no long life data.

It should be noted that as the tube ages (w.r.t. no. of pulses) the gas pressure fluctuates resulting in increased time jitter of the switching point (from ~ 1 ns to 10 - 20 ns) although increasing the heater power may offset this.

As the conductive medium is a gas, this provides the tube with a degree of self healing capability should a fault occur.

It seems likely that a thyratron will provide the required lifetime if the peak current value is kept below the maximum recommended for the tube. Obviously the degree of derating has to be determined, although as there are tubes capable of switching voltage and current combinations much greater than that required by LAWS, simply using an over sized tube could help to solve much of the life problems, although at a power

,weight and volume expense. The use of magnetic compression techniques in conjunction with the thyratron would also appear to be desirable.

5.2.2 Solid-State Devices

All published reports of solid-state device laser switching have used high power thyristors and this section will address these devices. STI Optronics is looking at the possibility of using breakover diodes to form the switch, although energy losses in these switches appears to be high.

There has been considerable development in high power thyristor development over the last few years particularly with respect to phase control and voltage switching requirements. A typical off the shelf thyristor from International Rectifier is capable of switching up to 2 kV with peak currents of up to 53500 A and average currents of 3060 A.

The main problem with these devices stems from their low maximum hold-off voltage and slow voltage and current rise times. Typically a device will have a maximum voltage risetime of 500 V/μs. Thus to switch the maximum voltage a rise time of 4 μs is required compared to a LAWS voltage risetime (AVCO spec.) of ~(0.3 - 0.4) μs, a factor of ten slower. Whilst stacking devices in series will enable the required voltage to be held-off directly (~(15 - 16) devices for the LAWS voltages specified by AVCO), the rise time is still too long. Additionally, for devices stacked in series the triggering is crucial as any failure to switch the devices simultaneously will result in the probable destruction of at least one of the devices. To reduce the voltage risetime, magnetic compression stages can be used.

An alternative to the series switching of many devices is to switch a single or several parallel devices at the 2 kV maximum. This low voltage pulse is then passed through a high voltage step-up transformer to obtain the required voltage. The design of a suitable high voltage transformer is difficult as the inductance must be kept low to ensure a fast transfer time, and this could lead to saturation of the core material. Biasing the core and using a high ΔB material such as an amorphous metal will enable the core volume to be kept relatively small whilst maintaining as short a transfer time as possible. Following the transformer, some degree of magnetic compression would be required to sharpen the voltage risetime and shorten the pulse.

Figure 6.2 shows a schematic of a thyristor. It can be seen that the gate or trigger electrode is a ring structure around the edge of the device. This means that when the device is triggered, conduction occurs progressively from the outside towards the center. Until the device is fully conducting across its whole surface, the current through the device must be limited. This can be achieved by using a suitable value of saturating inductor to limit the current to a minimum until the voltage has risen to a maximum. At this point the inductor saturates to provide a low inductance thereby enabling the current pulse to rise.

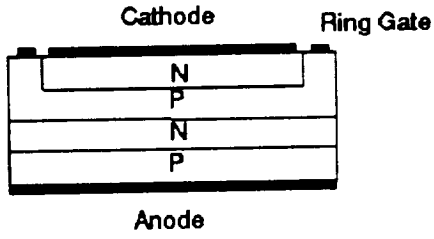

Figure 6.2 Thyristor Schematic

It is apparent from the forgoing descriptions that the thyristor is not ideally suitable for laser switching but that techniques to overcome its limitations have been developed. The reason for this development is the potential weight and volume saving obtainable over using a thyratron switch. Unfortunately, the magnetic control and compression stages require biasing, which is an additional energy loss and the magnetic stages themselves tend to be ~(70 - 95) % efficient depending on the exact design requirements. Thus it is highly likely that a thyristor/magnetic circuit for LAWS would be unable to achieve better than ~(70 - 95) % transfer efficiency from the storage capacitor to the discharge. Without a detailed design, it is difficult to specify this more accurately. As developments in this area occur constantly, this may change.

STI is investigating the use of breakover diodes as a solid state switch candidate. These would have a fast risetime and may prove more suitable than thyristors, however STI has already indicated that the devices have higher energy losses than expected. I await their results with interest!

5.3 Capacitors

Maxwell Laboratories Inc. are probably the major supplier of high voltage low impeadance discharge capacitors for lasers. They typically quote lifetimes in charge/discharge cycles assuming 90 % survivability with < 20 % voltage reversal for

the maximum voltage and peak/RMS current ratings specified in their product guide. Whilst 90 % survivability is probably not sufficient for the LAWS project, if the capacitors are derated, the lifetime and survivability will increase. A telephone call to Maxwell confirmed that given an energy storage requirement they could produce a capacitor with the required lifetime and essentially any required survivability at the expense of weight and volume. This was based on the considerable body of statistical data that they have accumulated. They will be happy to supply this statistical data, however it depends strongly on the capacitor type and model selected and could only be provided after a final decision on the capacitors has been decided.

It should be noted that STI has mentioned the use of ceramic capacitors in their solid state design. These have a considerable capacitance variation with age. Whilst considerable improvements in stability have been made this effect should be considered.

5.4 Magnetic Components

There is little to go wrong with these components other than the failure of the windings or the interwinding insulation due to repetitive stresses and this mechanism is well understood. Similar mechanisms must be considered for any amorphous metal cores which also utilise a tape wound construction.

5.5 Summary

The following table summarises the advantages and disadvantages of each type of component.

5.6 References

Motorola "Thyristor Device Data" Handbook DL137 Rev. 2.

International Rectifier "Power Semiconductors - 1990 Product Digest" Short Form Catalog 90.

International Rectifier "Power Products - Rectifiers & Thyristors" Catalog I-10189.

Maxwell Laboratories Inc. "Capacitor Selection Guide".

EEV Inc. "Hydrogen Thyratrons".

Telephone discussions were also held with EEV, EG&G, ITT, Lambda Physik, Lumonics and Maxwell Laboratories.

Device	Advantages	Disadvantages
Thyratron	Simple circuitry. Self healing. Devices much larger than required available. Lifetimes of 10^9 - 10^{10} demonstrated.	Heaters require considerable power. Bulky and heavy. Little life data available.
Thyristor	Small and compact. Potential overall weight saving.	Require many devices to holdoff full voltage. Not self healing. Complex circuitry to compensate for device limitations. No known life data.
Capacitor	Good statistical database available from manufacturer. 10^9 possible with derating.	Derating increases weight and volume.
Magnetics	Generally required when thyristor switching used. May also be required with thyratron to limit current in thyratron to ensure lifetime requirement met. Rugged, simple component.	Design difficult. Bulky and heavy. Tend to be lossy.

Table 6.1 High voltage component summary.

6 Appendix 1: LAWS Memos

6.1 Introduction

This appendix consists of memos relevant to the LAWS program generated by the author during the period of the contract. This is not a complete listing of the memos, only a listing of the more important ones. The date on each memo is the date it was originally printed.

6.2 Comments from June 1991

Questions for NASA

Page	Comments
	The power and weight constraints are based on the Japanese Polar Orbiting Platform (JPOP), as this platform is no longer being used are these constraints valid? For example if LAWS uses a dedicated platform, the power available is likely to be greater than on the JPOP which was also occupied by other instruments. How valid can the final designs be when the eventual platform is unknown?
JP3	The GE/STI review indicates that the Science Team requested a variable pulse rate with a maximum of 15.7 Hz and an average over one orbit time (93 mins presumably assuming JPOP) of 4.3 Hz. Obviously energy will have to be stored during low pulse rate operation to be available during high pulse rate operation. The Science Team evades this issue by stating that the high pulse rate time of operation be determined by the platform power requirements. Is this energy storage facility to be part of the LAWS device or to be assumed to be on the platform? Additionally the period of time at which the laser will operate at high pulse rates, and the frequency of these periods will influence the flow loop, catalyst and heat exchanger requirements thus some determination of these values is required. The Science Team recommends two modes of operation, a Survey Mode at an average of 4.3 Hz and a High Repetition Rate Mode at an average of 10 Hz. Obviously no combination of these two modes will provide an overall average pulse rate of 4.3 Hz unless either the high rep. mode is never used or the laser runs at 0 Hz for a period equal to the time of operation in the high rep. mode. Was this their intention?

Comments Concerning the Textron LAWS Laser Breadboard Initial Design Review

Page	Comments
1-9	Gas life tests of 2×10^8 and 1×10^8 pulses for the standard and isotopic gases respectively.
1-11	This chart illustrates 3 months for the non-isotopic gas life test and 1.5 months for the isotopic gas mix. At 20 Hz these represent ~1.55×10^8 and ~7.5×10^7 pulses respectively (assuming 30 day months). These figures are only ~75% of the values given above.

For the life tests envisaged, assuming a linear decrease of pulse energy with pulse number, the pulse energy will be 90% of the initial pulse energy for the $2x10^8$ test and 95% for the $1x10^8$ test assuming a final pulse energy of 50% of the initial value. These changes will be detectable, but because of likely noise on the signal it will be difficult to extrapolate out to 10^9 pulses. A more accurate technique would be to monitor the gas composition to assist in an extrapolation. This is particularly true as 50% energy at 10^9 is probably too much of a drop off. Ideally a value for the pulse energy after 10^9 shots should be given to the contractors.

1-14 The lifetime indicated in this table of $3x10^8$ pulses is for components only, not the gas mixture as this will be changed.

1-21 The Ernst profile is based on the assumption of the electrodes in isolation with no nearby dielectrics or conductors. The insulated wall will modify the electric field, so that under ideal conditions the profile of the cathode should be modified from the Ernst profile. the preioniser is stated as being made from mycalex (with a possibility of being relaced by zerodur). I am unfamiliar with mycalex and information concerning its mechanical and electrical properties would be most useful. No indication is made of the preioniser discharge circuitry and so it is assumed that it is connected to the main discharge circuit, the standard approach for corona preionisers. this should however be clarified.

1-22 Breadboard energy loading of 80 J/L-Atm with 1:1:3 gas mixture.

3-5 The energy loading is defined as being high, however the value given is typical of TE CO_2 lasers and may even be considered to be on the low side of average energy loading values. High energy loading values are typically of the order of 400 J/L-Atm. Perhaps 'optimum energy loading' would be more appropriate.

3-9 STI has undertaken studies of the isotopic gas mixture and the results of these studies are available. This work was carried out for the Geophysics Laboratory, Air Force Systems Command, United States Airforce, Hansom air Force Base, Ma. 01731-5000 between September 1988 and August 1989.The report number is GL-TR-89-0292 and is approved for public release with unlimited distribution. If this report is considered inadequate, some indication as to why this is the case would be appreciated.

Questions for GE/STI concerning Phase II Quarterly Review, March 6, 1991

Page	Comments
JP5	The contractors suggest a baseline laser design of 15J with a 1.5 m aperture telescope, this being the maximum due to weight constraints. However the Science Team indicates a maximum pulse rate of 15.7 Hz whilst the contractor has chosen 20 Hz. Why?
JP7	The beam truncation optics consist of a simple 2 element off-axis beam expander. Such devices introduce coma and astigmatism in to the beam unless critically aligned.
JP7	The contractors indicate that the laser energy can be increased from 15J by increasing the laser gain length for the same beam size with the same flow loop. If the gain length is increased, the discharge cross-section will increase requiring an increase in the flow loop cross-section at the laser head. Additionally an increase in the laser energy results in an increased load for the heat exchanger which has previously been optimised for 15J laser operation. The increased energy input into the discharge to enable the increase in output energy will result in greater dissociation during the discharge pulse resulting in the need for a greater quantity of catalyst. A larger discharge power supply would also be required, resulting in an increase in weight.
AW8	The contractor indicates that the shutter to protect the receiver during the output pulse remains closed for ~4 mS. When opened, the immediate signal will represent that from a target ~600 km ie presumably the ground return, however surely signal is required prior to this?
TRL3	Mike, the issues in this paragraph have been raised with the contractor and are being addressed. I have included them for your information. The laser sub system contains coated flat ZnSe windows on the discharge chamber rather than Brewster angle, presumably for space saving constraints however durability of coatings needs to be addressed. Similar concerns exist for the intra-cavity lens and the graded reflectivity output coupler. Work at RSRE has shown such output couplers for CO2 use to be easily damaged and to have reflectivity profiles which only loosely follow the specified profile. Additionally the center reflectivity was found to be much lower than that indicated by the manufacturers. Since this report considerable inprovements have been made in the design of these elements and STI is very confident that they are adequate for the task. Personally during my involve-

ment with the ESA Lidar project during 1989 two of the other contractors procured and tested these elements, both found that they were damaged within a few hundred shots at high pulse energies (~10 J) whilst at low pulse energies (~1J) they were adequate. Unfortunately neither contractor supplied energy density values which would have been more useful. I believe that STI's experience is limited to pulse energies in the 1 J region.

TRL3 TRL11 TRL12 The IO/LO trades indicate a preference for the Synrad laser. This laser has not been sold in a frequency tunable, yet alone stabilised configuration. STI indicated that these changes are being carried out by the manufacturer. Success in stabilising the laser to the degree required has to be demonstrated. Page TRL3 shows the cw laser as line center locked, this technique has generally been considered to be less accurate than opto-galvanic stabilisation. Opto-galvanic stabilisation however requires a dc discharge and hence can not be used with rf excited lasers. The lifetime issue of these lasers must also be addressed, even with two lasers, each is required to have a life of at least 13000 hrs assuming that the lasers are on continuously during a three year mission life.

TRL31 TRL32 The contractor indicates a pulse energy of 15 J in the FWHM of the pulse shape, neglecting the gain switched spike and tail of the pulse. This is then called the useful pulse energy. However in their loaded cavity calculations they indicate that in the far field 85 % of the energy is available giving a useful pulse energy of 12.75 J in the far field. It must be determined whether the output energy is to be specified at the exit of the laser cavity or in the far field. Obviously if at the laser exit this is satisfactory however if specified in the far field this design is deficient.

TRL40 The contractor indicates a corona bar backup geometry. If only one backup is available then each must last $5x10^8$ pulses whereas most existing corona devices have not been tested beyond the 10^7 level and most of these have failed.

No discussion of the laser discharge circuit is provided, allthough there are lifetime issues concerned with the high voltage components, especially the switch.

6.3 Breadboard Reviews

MEMO

To: Mike Kavaya

From: Gary Spiers

Subject: Breadboard Reviews

Date: July 3, 1991

General Comments for NASA

The two contractors are using different definitions of the pulse width. STI takes the FWHM, excluding the gain switched spike whilst AVCO includes the gain switched spike, although not using the spike as the maximum. Complementary to this is the definition of the pulse chirp. Both contractors have a tail on their optical pulses which is excluded from the energy consideration as these tails are outside the FWHM pulse definition. However these tails are transmitted and will contain frequency chirp, which appears to have been excluded from the chirp figures provided.

It can be argued that because of the relatively low intensity of these tails, they will be sufficiently attenuated by the atmosphere such that they will not be seen by the receiver and can hence be discounted. I am not aware of any quantitative work to verify this apparently reasonable assumption.

An additional chirp problem is encountered in the gain switched spike which can exhibit considerable frequency chirp. This occurs because the frequency of the laser can be considered to be in the process of selection during the spike. Injection locking should reduce the chirp in this spike significantly. Again no quantitative information has been provided. This problem has been avoided by STI by choosing to define the pulse to exclude the spike, however it is transmitted and unlike the tail has significant intensity.

A major concern is the approach the contractors will take to the limited amount of life testing possible within the current schedule. Subjectively, STI appears to have a program to eliminate possible failure mechanisms as soon as their potential to limit the lifetime becomes evident. AVCO appears less decided on the best means to proceed with these tests. Clarification from both contractors would be beneficial.

From the point of view of a laser physicist, the logical choice for the breadboard pfn is a thyratron switched unit. This enables the required voltage and current pulses to be obtained quickly and reliably so that other aspects of the laser design can be investigated. Thus both contractors have chosen this route. Alternative long term solutions can then be developed off line without sacrificing other aspects of the laser program. I will address details of the pfn decisions on my return from Colorado. However I should point out that both capacitors and thyratrons are available which greatly exceed the LAWS requirements if a power, weight and volume penalty is accepted. The real decision for LAWS is not if the pfn will last but what trade offs in power, weight and volume are available for a given projected life that would be acceptable from a risk reduction point of view. Solid state switching on the other hand has potential weight, volume and power savings but has not been demonstrated at the LAWS requirements.

Both contractors intend to use research detectors rather than established technology. Some means of verifying the life of these detectors must be decided upon.

Preionisers have traditionally been 'designed' to produce as much preionisation as possible to enable high energy loading densities to be achieved. This creates large stresses which lead to failure of the device. In the LAWS device high energy loading densities are not required and consequently the preioniser has to produce much less preionisation thereby enabling a reduction in the stresses on the preioniser. Additionally the traditional approach to preioniser 'design' has been a try it and see technique without consideration of all the requirements, it being easy to replace a preioniser if it fails.

Both contractors have developed numerical models of the laser, and the AVCO comparison between experiment and theory highlights the limitations of their model. The STI model is probably limited in the same manner as these models are extremely complicated. It should be noted that the experimental and theoretical pulse shape comparison provided by STI is for an X-ray preionised device, not the LAWS device. Thus both contractors will be approaching the breadboard as an experimental device for firming up the LAWS parameters. They will be reluctant to tie down their breadboard design completely to enable changes to be made during the initial experimental work. Whilst this approach may be difficult to accept, it is probably the safest approach. It is unlikely that any of the major design parameters will be changed, but things such as the gas composition and pressure and in particular the voltage and current loading are likely to be modified. This explains the current lack of definite information on the pfn designs.

Both contractors need to address the long term reliability of the local oscillator as well as the main laser.

In the following comments, the bulk are addressed towards aspects of the AVCO design. This occurs simply because at this point they have provided more detail than STI and consequently are more open to analysis. However in conversations with both contractors my subjective feelings were that STI was much more on top of the project than AVCO who appear to be understaffed, poorly supported by the parent company and appear to suffer from last minute design changes handed down from Lockheed without prior warning.

Comments on the AVCO breadboard.

Testing

The contractor proposes to use thermal paper to determine the beam uniformity and has shown a comparison (page 3-20) of a burn pattern and a theoretical calculation. Thermal paper has a very limited dynamic range, requiring that the beam be attenuated by various factors so that an intensity map of the beam has to be built up over many shots. The linearity and uniformity of the thermal paper is unknown. Additional their may be variations in the beam profile on a shot to shot basis. Finally to interpret the burn pattern a densitometer is usually used to determine the shading of the burn. This technique obviously requires considerable care and effort if some degree of quantification is to be obtained. The alternative of using a matrix beam profiler on a single shot basis is obviously much easier, simpler and more reliable. Beam profilers are however expensive.

The second testing issue concerns the longlife testing. When I enquired how they intended to proceed with the life tests ie how to identify potential problems and eliminate them before failure set in, I was left with the (subjective) impression that they had not considered this issue in detail. It should be noted that the test equipment listed in the Initial Design Review makes no mention of the gas analysis techniques to be used. These techniques however are probably essential to identify potential problems early on. Traditional techniques of waiting for a change in the optical output or the voltage and current characteristics of the laser may require too many shots before problems are apparent. It would appear important to obtain clarification of the tests proposed from the contractor.

Preioniser

I am unfamiliar with mycalex (perhaps it has another name in the UK) and can not at this point comment on it. However zerodur appears to have the characteristics to make a very durable preioniser, provided that it will produce sufficient preionisation.

Isotopic gas studies

The contractor indicates the desire to undertake tests to characterise the gain characteristics of the isotopic gas mixture. This appears to repeat the measurements previously made by STI. However there is a gain limiting mechanism within the gas kinetics such that as the energy pump level increases the gain does not continue to increase with increasing pump power but levels off and eventually falls. Several mechanisms have been proposed for this in the literature and AVCO undertook a DOD study to identify the correct mechanism. This work is classified, however I believe I know which of the mechanisms is most likely to account for this gain fall off. For accurate modeling of the laser this mechanism must be included for high input energy densities. The STI study did not address such high energy loadings and thus the required information is not available. However LAWS is not a high energy loading device and the relevant rate constants for this process may not be required any way.

Thermal Lensing

STI have calculated that at high pulse rates the average intensity will be sufficiently high to cause thermal lensing in transmissive optics in their laser system. As the AVCO design has similar maximum energy and pulse rate requirements but with a smaller beam cross-section, this will be more of a problem for their design, although they have as yet to make any mention of it. To compound this problem they are using partial reflectors for the beam turning mirrors which are more prone to damage than simple metal reflective optics.

Resonator Design

The contractor is using injection through one of the turning mirrors which potentially leads to the damage problem outlined above. The alternative technique is to use injection off the zeroth order of the grating (as STI) however AVCO has mounted their pzt cavity adjustment on the grating so that the injection source would have to track the grating movement if they were to revert to this arrangement. This would be difficult and provide additional complexity. If however the pzt was mounted on the back of the primary mirror this would then become possible. The disadvantage is the increased size and mass of the primary mirror over that of the grating.

Modeling

The modeling results provided in the Initial Design Review provide only general agreement with the experimental results. Specifically (page 6-9) the predicted output energy is higher than that obtained to date and the comparison of theoretical and experimental pulse shapes (page 6-10) concludes agreement, however analysis shows that although the laser turn on times are the same (a difficult quantity to predict accurately), the ratio of the gain switch spike to the next peak is ~2 theoretically and ~3 experimentally whilst the FWHM of the theoretical and experimental pulses is ~3μs and ~2μs respectively. Thus the actual pulse length is 2/3 of the predicted pulse length, a considerable difference.

Comments on the STI Breadboard.

Preioniser

STI have chosen barium titanate for their preioniser material. I have had some experience with this material as an electrode structure in a capacitively ballasted discharge device. Although it has excellent electrical characteristics, it is brittle and may powder after repeated cycling. Vibration shock during launch may also be a problem for the material. STI admits that it has only had limited life testing so far. The epoxy used to mount the preioniser (page TED 57) appears to be in contact with the laser gas and potential outgassing must be considered.

Resonator Design

I have expressed my concerns about the damage thresholds of graded reflectivity materials previously and in view of improvements in their manufacture must await the results of testing. If the optic fails the life test, it could be replaced with a scraper mirror and conventional reflector without too much difficulty at the breadboard stage.

Gain length

Some concern has been expressed over STI's decision to increase the breadboard gain length over that originally specified. Whilst this appears a drastic change, the investigative nature of the breadboard is probably better served by this change as it enables a wider discharge loading parameter space to be addressed. This unfortunately has some effect on the gas loop design.

Pulsed Power

As discussed above a thyratron switched pfn is a good starting point for the breadboard. The solid state route being taken by STI must be considered fairly high risk, with potential large gains if successful. It should be pointed out that the thyratron system can be designed as a backup for the solid state

system rather than as an interim solution. Discussions with STI indicate that this is their intention. As mentioned above I will comment further on the two switching technologies at a later date.

Modeling

The comparison of experiment and theory presented (page CHF 49) are NOT for the LAWS device or breadboard.

Local Oscillator

The manufacturer of the local oscillator does not have a commercially available grating tuned laser, let alone a frequency stabilised cw oscillator. Therefore this is presumably a special order item. The benefits of this manufacturers laser is its ruggedness, however at this point it has completely unproven frequency performance. Most conventional frequency stabilised cw lasers use the opto-galvanic technique to provide the stabilisation feedback. Being an rf discharge device, this is not possible and hence a line center locking technique. Within my limited experience this technique is less sensitive than the opto-galvanic method and therefore may require verification.

6.4 LMSC DR-13, DR-5, DR-7, DR-10, Risk Retirement Plan

MEMO

To: Mike Kavaya

From: Gary Spiers

Subject: LMSC DR-13, DR-5, DR-7, DR-10, Risk Retirement Plan

Date: July 25, 1991

Mike,

These comments may be completely stupid but here goes:-

Laws Risk Retirement Plan

It seems odd that LMSC has no tasks under the risk reduction plan, despite being one of the prime contractors.

DR-13 Error Budget Analysis

On the error budget analysis too many of the other unit values don't have units, for example on view BR F312481 -03 the laser jitter is specified as 0.60, presumably with units of μrad to give a velocity error of 0.004 m/s. However on the same view graph the orbit position is also given to 0.6 units (again I assumed μrad) but a velocity error of 0.04 m/s! Similarly the azimuth uncertainty is given as 1.01 (μrad?) for a velocity error of 0.004 m/s as per the laser jitter. If these are all in μrad then there appears to be an inconsistency here?

DR-10 Prime Equipment Specification

There are a lot of TBDs in this report, in addition to the following comments:-

Page	Section	REQID	Comment/ Question
9	3.2.1.2.8	LAS00090	This indicates a laser chirp of 200 kHz is required but by the contractors own error budget analysis a laser chirp of 100 kHz is now required.
10	3.2.1.2.2.20	LAS00220	This states that the output energy after 10^9 shots should be < 20 % down from the initial output energy. Was this figure given by the science team or derived by the contractor.

11	3.2.1.3.2.5	REC00060	This gives the quantum efficiency of the detector as >30 % @1.4 GHz. This is low compared to the 47 % used in the error budget calculations.

DR-7 Systems Engineering and Integration Requirements

The weight table on page 36 contains an error. It states that the Laser Controls/Power will have a weight of 550 kg, this should be 50 kg based on the weight table in the Prime Equipment Specification (page 34). It should be noted that whilst both of these tables have the same total weight, the distribution of the weights between some of the individual components is different.

6.5 GE/STI Breadboard Frequency Chirp

MEMO

To: Bob Jayroe, Randy Baggett & Michael Kavaya

From: Gary Spiers

Subject: Frequency chirp in the STI Optronics laser design.

Date: August 5, 1991

Summary of Available Information.

On 7/25/91 I contacted Rhidian Lawrence at STI Optronics in regard to aspects of the frequency chirp of their laser design. He told me that the chirp had been based on an assumption of a linear chirp of 50 kHz/μs. The frequency chirp has two main components,

1) Plasma chirp due to the electron density in the discharge and

2) Laser induced medium perturbation (LIMP) due to heating of the laser gas as a consequence of the laser action. It has been well established through work carried out at RSRE that the LIMP chirp has a nonlinear time dependence, (t^2 for short pulses and t^3 for long pulses). When I mentioned this, he indicated the NOAA laser as an example of the linear dependence and suggested I contact M.J. Post who has carried out a detailed characterisation of the laser. He also indicated that no plasma chirp would be present as the discharge pulse is over before the laser optical pulse starts. I gained the impression that STI had not done any detailed modeling of the chirp and had relied on experience to estimate the value.

I contacted M.J. Post on 7/26/91 and he provided me with a reference of a paper containing details of the NOAA laser characterisation. This clearly indicated a nonlinear LIMP chirp as well as the presence of some plasma chirp. I again contacted M.J. Post who faxed me a large copy of the original diagram so that the time dependence could be determined. The calculation of the LIMP chirp in the paper was incorrect and on recalculating the expected LIMP chirp, I obtained a value of ~340 kHz compared to the experimental value of ~300 kHz. By overlaying the calculated result on the experimental result provided by M.J. Post it was found that the experiment very closely fitted the expected t^3 dependence. A copy of my calculation was faxed to M.J. Post. It should be noted that the plasma chirp on this pulse was ~300 kHz within the first ~2 μs.

I recontacted Rhidian Lawrence on 7/26/91 and told him of my findings. He indicated that the laser recently supplied to GE was much better than the NOAA laser and that he would fax me available results and some form of justification for the chirp value provided for the LAWS device.

On 7/29/91 I recontacted Rhidian Lawrence to determine when I would receive the faxed information. I was left with the impression that they had done most of their chirp work in the early 80's and were not aware of some of the more recent papers. Rhidian indicated that even if the laser produced 300 kHz of chirp, it was probable that someone like Bob Lee would say that this was acceptable for wind measurement (Michael Kavaya contacted John Anderson who refuted this argument). Rhidian indicated that I would receive a fax of the requested information by the end of the day.

I received the fax midday on 7/30/91. The fax outlined the approach used by STI to decide on the value of the LAWS chirp. This used a scaling relationship derived by a former employee in the early 80's. This relationship involves a t^2 relationship which was unfamiliar to me, although it bore some similarities to the early published theory of Willetts and Harris. Unfortunately they could not provide a derivation of this equation. Preliminary measurements of the chirp on the GE device were supplied as evidence of the low linear chirp dependence. Rhidian indicated that these were measurements carried out during a quick testing of the laser and that the energy was thought to be ~1.5 J. It should be noted that the output from this device is still only 75 % of the design energy. The oscilloscope photographs provided are not suitable for an accurate determination of the frequency chirp, particularly as Rhidian indicated that the frequency chirp would vary from pulse to pulse, sometimes being below 50 kHz and sometimes above 150 kHz. I am uncertain if these chirp values were for the whole pulse, part of the pulse or per μs. The fact that the value varied considerably from pulse to pulse would seem to indicate either poor frequency stability in the laser or an inadequate measuring system.

Discussion and Conclusions.

At this point I can not say that the STI LAWS breadboard will not meet specifications, however I feel most uneasy with the current state of affairs. Most of these problems arise due to the inadequacy of the available theory. Whilst I have personally found that the improved Willetts and Harris theory provides good agreement with experiment, it does generally provide an upper bound on the value to be expected. If the NOAA device performed as per the specification, I would be much happier in accepting the breadboard design. The failure

of the NOAA device to meet the specification and the failure of the GE device to so far meet its energy specification coupled with my calculations are discouraging for the breadboard. If an accurate measurement of the chirp on the GE device could be obtained, this would enable an additional check to be made on the theory. If this device fits the Willetts and Harris theory then the breadboard is unlikely to achieve the 140 kHz frequency chirp during the required 3 μs. If the chirp of the device is below this value the likelihood of the breadboard achieving the design point is higher. This would also enable verification of the presence or absence of plasma chirp. If plasma chirp is present this would probably also be present in the breadboard device and would ensure failure to meet the design specification. Without detailed knowledge of the voltage and current pulse shapes, a calculation of possible plasma chirp can not be undertaken.

If the GE device measurements can not be made before the breadboard go ahead must be given then I feel that the evidence, being limited in scope, should not prevent the breadboard from proceeding. If the breadboard does fail to meet specifications, the information gained should be sufficient to ensure that the contractor would be able to construct the final LAWS device to specification. This is obviously an unsatisfactory state of affairs and could prejudice the contractor against being selected for the next phase of the contract. If the contractor is made aware of these concerns and their implications and still feels confident that his design is satisfactory then he should probably be allowed to proceed.

6.6 LAWS Breadboard Frequency Chirp Test Plan

MEMO

To: Bob Jayroe, Randy Baggett & Michael Kavaya

From: Gary Spiers

Subject: Breadboard frequency chirp test plan

Date: August 6, 1991

General Overview.

The frequency chirp should be measured by beating the pulsed laser output (p.o.) with a c.w. local oscillator (l.o.) on a suitable detector and the resultant intermediate frequency (i.f.) signal from the detector should be digitised directly for analysis.

Specifics.

Number of samples.

When measurement occurs, a run of 10 or more pulses should be characterised for each pulse energy and beam location. This run should not exclude any 'bad' pulses that occur during the run. Ideally the data should consist of consecutive pulses. If the data collection scheme is incapable of handling the data rate then the data should be collected with as few pulses between samples as possible. Samples should be taken at both the maximum and minimum pulse rates of the device as well as suitable intermediate points.

Complementary measurements.

Simultaneous digitisation of the temporal pulse shape and the frequency chirp should be performed. If this proves difficult then alternate measurements of each may be performed. The total energy in each pulse should also be recorded simultaneously.

Beam sampling.

The measurement of the frequency chirp should be undertaken at the center of the pulsed beam in the far field. If this measurement has to be made in the near field then the measurement should occur in the portion of the beam that has the highest intensity. Additionally the sampling of the frequency chirp at different locations in the beam is encouraged.

Heterodyne detector.

The l.o. and p.o. intensities should be arranged to ensure that the detector is shot noise limited with an ~10 dB shot noise to other noise ratio whilst ensuring linear operation of the detector.

Intermediate frequency.

The i.f. signal should be chosen by tuning the local oscillator such that the digitiser can provide at least 10 digitisation points per i.f. cycle whilst ensuring that the i.f. remains within the bandwidth of the detector. Additionally the i.f. should provide as many cycles as possible during the pulse duration.

Frequency determination.

The temporal evolution of the pulse chirp will be determined by measuring the time between the zero crossing points of the i.f. signal and calculating the corresponding frequency. As there is often an essentially d.c. offset of the beat signal voltage from zero a high pass filter may be placed between the detector and digitiser to remove this offset, provided that it is confirmed that this filter has no effect on the i.f. beat frequency. Alternatively a digital filter may be used, provided the same condition is met.

Output data.

1) The data should consist of frequency as a function of time, f(t) plots. For each plot the pulse rate, pulse energy and time dependent pulse shape should be available.

2) For a given beam location and energy coplots of f(t) should be provided. The plots should represent the typical performance and variation of the output rather than the optimum performance.

3) If possible, Fourier transforms of f(t) should also be provided, where f(t) has a suitable number of leading and trailing zeros added.

4) Statistics on the variation of the energy, pulse length, pulse shape, frequency variation, and frequency of occurence of multimode pulses during the measurement period are also desirable.

5) ASCII files of the raw data should be available to NASA/MSFC if requested.

6.7 Lambda-Physik Longlife Excimer Testing Reports

MEMO

To: Bob Jayroe, Randy Baggett & Michael Kavaya

From: Gary Spiers

Subject: Lambda Physik long life excimer testing reports

Date: August 6, 1991

Whilst much of the reports can not be applied to LAWS, some aspects of the report are valuable. The following points should be noted:-

Discharge Electronics

Although excimer lasers operate at lower electric field strengths than CO_2 lasers, they require much higher operating currents. Thyratron failure is generally due to either the exhaustion of the internal gas reservoir or failure of one of the internal electrode structures. High current density pulses tend to cause more damage to these electrodes and therefore excimer lasers can be considered to provide a more demanding environment than an equivalent CO_2 laser. Lambda Physik use a magnetic saturating compressor (MSC) technique to reduce the peak current through the thyratron. They have a patent on this technique, however, the technique has been used in CO_2 lasers prior to its implimentation in their excimer lasers and so I suspect the patent only covers excimer lasers. What is apparent from their literature is the need for extensive testing to determine which thyratron is most suitable for the required application. Even apparently similar designs from different manufacturers may have very different lifetimes.

The test lasers have low pulse energies of ~13 - 150 mJ, depending on the model tested, which correspond approximately to CO_2 laser pulse energies of ~50 - 1000 mJ. This obviously limits the degree of applicability of these results but still keeps them useful as it demonstrates the feasibility of achieving very long pulse lifetimes.

It should be noted that Lambda Physik has concluded that the other high voltage components (the saturating inductor in the MSC, capacitors and HV power supply) never failed in the tests and they are sufficiently confident of their reliability to have eliminated them from failure and maintenance tables for their lasers.

Electrode Lifetime

They concluded that the final limiting factor on their laser lifetime occured due to erosion of the electrode leading to distortion of the electric field profile and hence arcing. As CO_2 lasers operate at much lower current densities than excimers, this is much less of a problem in the CO_2 case and thus the electrodes should have an even longer life than that demonstrated here.

Radio Frequency Interference

It should be noted that despite considerable effort to eliminate RFI, Lambda Physik found that the lasers automatic control system would occasionally crash due to RFI. To eliminate this problem they have introduced fiber optic connections between the diagnostic and control elements of their most recent laser designs. This has some implications for the LAWS design.

6.8 LAWS Laser Breadboard - final design reviews

MEMO

To: Bob Jayroe, Randy Baggett and Michael Kavaya

From: Gary Spiers

Subject: LAWS laser breadboard - final design reviews

Date: September 13, 1991

General Comments

It should be noted that although these were final design reviews neither of the two contractors had completed all of the details of their breadboard design. All of the major issues had been considered and it was mainly the fine mechanical detail of the designs that had to be completed. An impression was obtained that AVCO was closer to completion of their design than was STI.

The frequency chirp for both of the laser designs is anticipated to be higher than that required by the LAWS device to be constructed in phase C/D. This reflects the uncertainty in the current theory and is a concern. Hopefully both contractors will obtain sufficient information to ensure an adequate design for phase C/D.

As part of the overall design, AVCO appears to have considered the need for electrical screening more thoroughly than STI. Their consideration of attenuating the electrical noise escaping from the laser windows illustrates their experience with much larger lasers where this is a severe problem. Additionally as part of the life testing they are covering their laser optics and using dry filtered nitrogen or air to prevent contamination. This again would appear to be an outgrowth from their previous large laser programs where even single dust particles on an optic can result in destruction of the optic. Some consideration of these problems by STI would seem desirable.

The documents provided by both contractors were well presented, however the concerns expressed in the AVCO portion of this document illustrate the difficulty of providing a thorough assessment of the contractor until the experimental phase is entered. As STI has not really entered this phase yet a comparison is difficult at this stage.

It should be noted that AVCO refers to energy loadings with units of J/l whilst STI uses units of J/l-atm. As the AVCO device operates at 0.5 atm., an AVCO energy loading of 80 J/l is the similar to an STI energy loading of 160 J/l-atm.

STI Optronics

On page CHF48 STI presents discharge voltage and current pulses together with a photograph of a discharge obtained using a 1:1:8 CO_2:N_2:He gas mixture and an energy pump loading of 125 J/l-atm. Presumably this information was provided to demonstrate the ability of their preioniser to successfully preionise a discharge, however it should be noted that this test was run at an energy density less than that specified for the breadboard (~160 J/l-atm.) and with a gas mix containing a smaller proportion of molecular components than the baseline breadboard design (1:2:3 CO_2:N_2:He). These changes make achievement of a stable discharge much easier than for the breadboard device and do not necessarily demonstrate the ability to achieve a stable discharge in the breadboard device.

The data presented on pages CHF52-CHF56 were collected on an x-ray preionised device as part of an earlier program and are not results of the LAWS program. X-ray preionisers usually produce very uniform but weak preionisation and this tends to limit both the maximum energy pump loading possible and the proportion of molecular species in the gas. Consequently all of the results presented in these pages are for energy pump densities less than that required by the breadboard. This is unfortunate, as at higher energy loading a saturation effect tends to occur limiting the gain available. It should be noted however that for conventional gas mixtures this saturation limit is generally higher than the 160 J/l-atm. required for the breadboard and is unlikely to be a problem.

My concerns over the chirp to be expected from this device have been expressed previously however my calculation falls within the pass/fail criteria specified by STI. It is understood that in an effort to obtain a more accurate estimate of the limp chirp, STI will be developing a more complete numerical model of the process during this phase.

During the laboratory tour it was not possible for STI to run the COLT device at a pulse rate greater than 39 Hz due to restrictions in the pulse generator. At this pulse rate I did see some weak filamentation of the discharge. Filamentation is usually a precursor to the formation of an arc at higher pulse rates and could potentially result in the inability to achieve 50 Hz operation in the device, although I feel this is unlikely to occur.

It should be noted that the question raised by M.J. Post at the AVCO review concerning dither synchronisation is also valid for the STI design.

During a presentation of IR&D work on the pulsed power switching for LAWS, the comment was made that the thyratron was not suitable as it would not achieve the life requirements. They felt that based on information provided by one of the thyratron manufacturers that the cathode would evaporate within the operational lifetime of LAWS. When I contacted the manufacturers, non of them were able to confirm this and all felt that this would not be a problem if managed correctly. On checking back with STI, it became apparent that they had been provided with incorrect information by EG&G although part of the decision to eliminate the thyratron had been based on an apparent political belief that NASA did not want to use thyratrons. After assurances that we have no preference for a switching device other than that it should satisfy the project requirements they are in the process of reassessing their design.

AVCO/Textron

The failure to obtain an energy loading of greater than 80 J/l with the long electrodes may indicate several possibilities. Firstly that the preionisation is weak and/or non-uniform and secondly that the electrode alignment tolerances are not tight enough. Whilst using two short electrodes overcomes this problem (as STI have done with their discharge from the onset) it raises some concern. During the laboratory tour I was left with an unsatisfactory feeling concerning the tolerances used in aligning the electrode pair and the lack of flatness on the grid electrode. AVCO are used to building large devices in which these effects are small fractions of the discharge cross-section and can be ignored. However on smaller devices such as LAWS (and Lowkater) these considerations become important. It should also be noted that most of AVCO's experience has been with electron-beam pumped devices and they have essentially only the Lowkater self-sustained experience prior to LAWS. My concerns over the engineering aspects of the design seen during the tour were also expressed to me by M.J. Post and C. Freed.

AVCO also showed a thyratron test bed where a previously used thyratron had been tested for ~10^4 pulses. The apparent purpose of this test was to ensure that a thyratron would last whilst switching the required LAWS load. The value of this test is doubtful as there has been no attempt to monitor the thyratron to see if its switching characteristics (eg turn-on point wrt trigger) are changing with number of pulses. The thyratron manufacturers recommend using very stable dc supplies for the heaters to enable accurate control of the device

switching point. By running these heaters at the minimum consistent with reliable switching and gradually increasing the heater power with time ensures a consistent switch point and a prolonged life. No attempt was made in the above test to do this and simple ac heater supplies were used.

During the meeting M.J. Post raised concerns over the synchronisation of the cavity locking technique with the injection oscillator dither to ensure accurate location of the line center. AVCO will assess this situation.

AVCO have chosen Maxwell capacitors for their breadboard. These are industry standard capacitors that have developed a very high reputation for consistency and reliability, however in assessing the amount of derating required to achieve an $8x10^8$ pulse lifetime, AVCO has used the manufacturers stated lifetime which only has a 90 % probability of being achieved. If the probability of achieving the life is to be increased, then further derating will be necessary.

Using the data presented by AVCO on page 9-10 we see that for 30 Hz operation of the laser, each fan will have a gas flow of 342 cfm and a pressure drop of ~0.72 in. H_2O. From the graph at the bottom of page 9-10 we see that this just falls within the fan operating capability. Obviously a detailed calculation of the pressure drop is needed rather than the approximation used to calculate it above and the mechanical stresses on the laser due to the increased speed of the fans may need to be considered, however it would appear that 30 Hz operation from the fans is feasible.

6.9 LaRC Workshop on CO-oxidation catalysts for CO_2 Lasers and Air Purification, October 29-30, 1991

MEMO

To: Michael Kavaya, Jim Bilbro, Bob Jayroe, Randy Baggett, Rex Geveden

From: Gary Spiers

Subject: LaRC Workshop on CO-Oxidation catalysts for CO_2 Lasers and Air Purification, October 29-30, 1991

Date: November 6, 1991

The first day of the meeting was taken up with talks, whilst the second (half) day was occupied with a discussion between the Army and the LaRC catalyst group over funding for the forthcoming year.

During the flight to LaRC, I was accompanied by Shelby Kurzius of Lockheed who allowed me to read a preliminary copy of the AVCO chirp results. Whilst this draft lacks some information, further comment should wait until the final report is obtained.

DAY 1

The two catalysts under discussion at the workshop were the $Pt:SnO_2$ with or without promoter and the $Au:MnO_2$. The following points can be summarised:-

$Au:MnO_2$ no promoter	Higher activity than promoterless $Pt:SnO_2$ but less than $Pt:SnO_2$ with promoter. Requires no pretreatment with a reducer (CO) and has a half life of ~12.5 yrs for low CO_2 concentrations. Unfortunately in gas mixtures with CO_2 levels equivalent to that in a laser, the activity falls drastically and the decay rate is ~6-9 months.
$Pt:SnO_2$ no promoter	This catalyst is optimised for 17%-20% Pt proportions. The catalyst activity improves in the presence of ~0.1% H_2O which can be achieved by using a silica base for the catalyst. Pretreatment of the catalyst using a reducer greatly increases the activity of the catalyst. The half-life of the catalyst is ~6 months but degrades with time. Two causes for the decay in activity have been identified, the first occurs due to CO_2 capture at the catalyst surface blocking CO access to the reaction sites. This can be prevented by allowing the catalyst to outgas for ~1 hr periodically. The second decay mechanism occurs as a reversal of the pretreatment. High CO_2 concentrations have little or no effect on the catalyst activity. Opening a laser containing a pretreated catalyst to air will reverse the pretreatment, although it may be possible to self pretreat the catalyst in a laser by using a CO rich gas mixture.
$Pt:SnO_2$ with promoter	This is the most active catalyst to date and patents have been filed. Until this process is complete, the promoter can not be revealed. This will probably be possible early in 1992. The promoter is used with a 13% $Pt:SnO_2$ combination and has successfully been placed on Corderite monoliths of 3" diameter and 1/2" thickness. The monolith has a BET of 1 m^2g^{-1} which is increased to >200m^2g^{-1} by etching with nitric acid. No shake and bake tests have been performed on the monolithic catalyst, although a rubbing test was performed to attempt removal of catalyst material. This removal was found to be

difficult. Isotopic labeling of the catalyst has occurred. To prepare for labeling the catalyst surface is initially reduced to remove existing O^{16}. At 225 °C >75% reduction occurs whist at 125 °C <50% reduction occurs. Reduction is considered complete when no further O^{16} is detected at a mass spectrometer downstream of the catalyst. O^{18} in He is then passed over the surface. When the stoichiometric ratio of O^{18}:He downstream of the catalyst becomes constant, the surface is assumed to be labeled. The labeled catalyst has a slightly lower activity than the unlabeled catalyst. To date only a short (5 day) isotopic integrity test has been performed. No scrambling was seen, although this test did not recycle the gas to allow build up of O^{18} to occur if scrambling is present.

$Au:MnO_2$ with promoter — At present no promoter has been found for this catalyst although investigations are continuing. It is thought highly probable that a promoter can be found.

The mechanism by which oxidation of the CO occurs is under investigation by analysis of the catalyst surface during catalytic activity. This has centered on the $Pt:SnO_2$ catalysts. Without the promoter, there appears to be two states of Sn on the catalyst surface, which appear to be SnO_2 and Sn respectively. The Sn appears to be present as a Pt:Sn alloy. When the promoter is present, all the Sn appears to be present as SnO_2 thereby ensuring a larger amount of Pt available as CO absorption sites which leads to the increased activity.

Preliminary Monte-Carlo analyses of the catalytic activity seem to imply that the catalyst should not be uniform but have 'clumpiness' or 'islands of Pt in a sea of SnO_2'. A uniform distribution will tend to lead to catalyst poisoning.

A list of attendees at the meeting is enclosed. Most of these people left before the end of the talks preventing much discussion.

A meeting entitled "Longlife CO_2 Laser Technology" will be held at RSRE, Malvern, U.K. in late October or early November of 1992.

DAY 2

The meeting on the second day was primarily to determine the funding to be provided by the Army to LaRC. Present were:-

Billy Upchurch, NASA LaRC

Dave Schryer, NASA LaRC

Kirkman Phelps, US Army CRDEC

Jay Fox, US Army CNVEO

Cynthia Gaiter Swim, US Army CNVEO

John Finn, NASA Ames

Gary Spiers, UAH/NASA MSFC

Kirkman Phelps expressed interest by a 3rd party in obtaining some catalyst for use in 'physical protection'. The intention of the 3rd party is to compare Billy's catalyst with the hopcalite they are currently using.

Jay Fox requires catalyst for a laser being developed by Hughes. He has no need of a monolith structure and would be satisfied with having the catalyst coated onto a flat plate. They intend to compare the performance of the LaRC catalyst against that of commercial catalyst from Phillips. The laser uses a 13% CO_2 rich gas mixture at a pressure slightly above 1 atm and operates at 200 Hz. An energy of 6 J is deposited into the discharge which is ~15 in. long. The laser uses corona preionisation, which appears to be weak as they require an ionisable additive to maintain a stable discharge. The nature of the additive is secret, which causes Billy some concern as he can not predetermine the effect it will have on the catalyst. The laser has been run with the Phillips catalyst (which poisons in air) at catalyst temperatures of 40-50 ^{o}C. The need to be able to field service the laser is strong leading to a preference for the Au:MnO_2 catalyst if possible. The laser must last for 10^8 pulses with initial tests to $5x10^7$ pulses.

Funding for LaRC Catalyst Effort

FY91 budget

US Army CRDEC	115K
NASA	130K
IR&D Div. Office	15K
FED Div. Office	15K
Total	275K

Proposed FY92 budget

Anticipated expenditure

UFLA	30K
UCASD	30K
Contractors	150K
Research Supplies	30K
Travel	5K
Sub-total	245K
Tax	40K
Total	285K

Known income

NASA (MSFC)	140K

Outstanding Balance

To find(!)	145K

Notes

1) This does not include deliverables to the Army (35K) or NASA.

2) No discretionary funding is likely this year.

3) The Army is satisfied with the catalyst as is and they are not prepared to fund in excess of FY91 levels. They are somewhat upset at the lack of NASA support for one of its own programs, particularly as they (the Army) regard the program as very successful.

4) If there is a funding shortfall, funding to one or both of the universities will be stopped.

5) There is growing interest in the use of catalysis to eliminate organics from the atmosphere (e.g. space station) and some funding may be possible by switching the emphasis to air pollution control.

6.10 Reasons for maintaining both laser houses.

21 January, 1992

Benefits in maintaining both laser houses under one prime contractor

Gary Spiers

PRELIMINARY

The two laser houses have significant differences in their designs. At this point the preferred design could well prove to be a combination of the two designs rather than either one on its own. Only with testing of both designs is it possible to verify the pros and cons of each design. For example:-

Laser Design Feature	TDS design	STI design
Resonator	Conventional hard edged scraper mirror.	Unstable resonator with a super-gaussian reflectivity profile output coupler.

The conventional hard edged unstable resonator has a long history and can be considered to be well understood and to be constructed from durable components ie it is a 'safe' design. The super-gaussian unstable resonator is a more recent technology and has the potential to increase the amount of useful energy available in the far field compared to a conventional unstable resonator. There is however some concern over the durability of the coatings used to form the output coupler profile. This concern and others are being addressed by the STI breadboard design.

Discharge Cross-Section	4.2x4.2 cm^2	5x5 cm^2

The use of a smaller discharge cross-section enables a lower high-voltage design to be implemented, which may make eventual space qualification of the high voltage elements of the LAWS design easier. However a small discharge cross-section increases the frequency chirp of the laser pulse. As the contractors have each chosen a different discharge cross-section this will provide a good data base for optimising the discharge cross-section of the phase C/D device to enable the required pulse chirp

	characteristics to be obtained whilst simultaneously keeping the discharge voltage as low as possible.	
Preioniser Material	Micalax	Barium Titanate
	The life of the preioniser has been identified as one of the key concerns to be addressed by the breadboards. By maintaining both contractors two different preioniser materials (and designs) are able to undergo extensive testing under LAWS type conditions, a procedure that would not be possible if only one laser manufacturer was carried forward.	
Flow loop	Uses a symmetric flow loop with two discharge arms, two fans, two catalyst beds and two heat exchangers.	Uses an asymmetric flow loop with one discharge arm, one fan, one catalyst bed and one heat exchanger.
	The TDS design provides potential redundancy in all the major flow loop components. The STI design is much simpler and easier to implement but provides for little redundancy. Much of the TDS flow loop design has been inherited from company and defense agency funded programs.	
PFN design	Monopolar design	Bipolar design
	The TDS design is simple and easy to implement whilst the STI design provides the potential for redundancy in the preioniser (by reversing the voltage on the electrodes), the high voltage switch (two are in the current design) and the potential for elimination of a high voltage switch for the main discharge pulse(company funded investigation).	

6.11 Comments on GE and LMSC DR-8 and DR-9

Comments on GE DR-8 LAWS Preliminary Design Document

Gary Spiers,UAH

March, 1992

Page	Section/Fig.	Para.	Comment
1	1.1-1		Change velocity estimation box to that decided at Science Team Meeting Jan 92?
2	1.1	1	As above comment.
2	1.1	1	Pulse length should be μs not msec.
2	1.1	2	Wrong units for pulse length again!
2	1.1	3	Modify power available statement to match definition written by Dave Emmett?
2	1.2-1		Useable pulse energy 27.5 J ??
2	1.2-1		Efficiency misspelled.
2	1.2-1		Degrees misspelled.
2-3	1.2		The contractor specifies removing the energy in the pulse spike and tail to provide 15 J useable energy, but useable energy is in the far, not near field so is a further reduction necessary or has this been included. Additionally whilst the energy in the pulse tail will fall within the 10 MHz bandwidth, the science team has indicated (John Anderson Jan 92 meeting) that the energy in the pulse tail is generally undesirable.
3	1.2	2	Burst is misspelled.

3	1.2		A nominal 20 J pulse at 5 % efficiency gives a stored energy of 400 J. Charging 400 J in 50 ms requires a power of ~8 kW. This is more than the maximum power available from the solar panels. Presumably the energy storage and smoothing capacitors in the high voltage power supply are being utilised in some fashion to allow this power consumption?
4	3.3-1		Figure is missing.
7	4.1.1.2		This definition of spectral width is not realistic as the whole pulse is transmitted, not just the portion defined as useful. Is this a NASA or contractor derived requirement?
7	4.1.1.4		The 20 Hz power problem again.
7	4.1.1.5		Due for modification?
14	4.2.2.1-1		The cw laser is missing a power feed.
14	4.2.2.1	1	Strictly speaking the grating is not a Littrow grating but a grating mounted at the Littrow angle.
15	4.2.2.1-2		Injection beam is labeled as injection via higher grating order. This should perhaps be changed to indicate zeroth order injection as per the text on page 14?
15	4.2.2.1-2		The output coupler is labeled as parabolic, although the current choice is super-gaussian.
15	4.2.2.1	2	HV power supply- last sentence has redundant "of the".
16	4.2.2.1	3	Ambiguity in the meaning of the phrase 'length of the laser'. In view of the length provided (75 cm) this would appear to be the 'discharge length'.

18	4.2.2.1	2 & 3	Paragraph repeated.
20	4.2.5	1	"schematically is Figure 4.2.5-1" should be "schematically in Fig...."
31	4.3.1.4	1	Duplicated "and" in last sentence.
34	4.3.1.5.2-1		This table appears to be missing.
34	4.3.1.5.2-2		This table appears to be missing.
34	4.3.1.5.2	1	"Cryocooler" misspelled.
35	4.4.1.1	3	"Telescope" misspelled in last sentence.
45-46	4.4.1.7.1-3		The time dependant form of the frequency chirp shown here is unlike anything documented in the literature which has generally shown a quadratic or cubic dependence on time. Whilst it is appreciated that STI feels they have an understanding of the cause of this behaviour, I would prefer to reserve judgement on this issue until a measurement has been made on the breadboard device. The use of a RSS technique to obtain the spectral standard deviation also causes concern. As the contractor has the intensity and frequency time dependence plotted in the figure, a preferable way to obtain the spectral width would be to calculate the complex electric field, $E(t) = \sqrt{I(t)}.e^{\int \omega(t).dt}$ where $I(t)$ is the time dependent intensity and $\omega(t)$ is the time dependent frequency variation. The power spectral density is then obtained by taking the square of the magnitude of the complex fft of $E(t)$.

48	4.4.1.7.3		The equation for the atmospheric coherence radius appears to be in error. See for example Eqn. 165 of Frehlich and Kavaya, Appl. Opt., v30,5325-5352,(1991).
49-53	4.4.1.7.3.1-2		Whilst considerable effort has gone into determining possible sources of angular error which can result in an error in the collocation of the signal and lo beams on the detector, it is not clear that the possibility of wavefront error (even for correctly positioned beams) has been considered although such a wavefront error between collocated signal and lo beams can significantly affect the mixing efficiency on the detector.
53-54	4.4.1.8		This section needs revising to include latest information.
55	4.4.1.9		Where does the high voltage electronics fall, in the laser subsystem or the electrical subsystem.
58	4.4.2.1.1	2	Fig. 4.4.2.1.2-1 can not really be considered to show two laser profiles as only the gain loaded profile can be achieved in a physical system, the passive case only demonstrates what is achievable using a laser with a resonator and no gain to perturb the beam profile formation. Obviously in a practical laser without gain, no laser beam is formed in the first place!
66	4.4.2.2.3		Concerns over this modelling have been expressed earlier in this document.

C.2

67-68	4.4.2.2.4		Whilst the mode profiles shown are for a cavity with a graded reflectivity mirror (grm), they are not calculated for the grm to be used in the LAWS device.
72	4.4.2.2.6	2	repeat of the word vibrational in N_2 vibrational temperature. Relaxation also repeated two sentences further on.
80	4.4.2.3.1		Was the graded reflectivity profile used the correct profile, or the parabolic profile shown earlier? If the parabolic was used, shouldn't this be recalculated for the super gaussian that will actually be used?
84	4.4.2.3.3		If the baseline LAWS receiver required 140 W with 80 W going to the cooler, why does the table show 200 W of power for cooling and a receiver total of 280 W? Additionally 100 W is allocated for the IO/LO laser and servo-loop electronics, yet the table shows 50 W for this purpose? Has the need for a considerable increase in the cooling of the IO/LO laser and modulators been accounted for in the option 1 and 2 cooling budgets. It is appreciated that option 2 has a larger IO/LO laser to offset increased optical losses and therefore probably has larger modulator crystals which require more power to drive them, yet a 100 % power increase for the RF frequency synthesis from option 1 to option 2 seems large?
86	4.4.2.3.2.4		This table appears to contradict that on page 84. Clarification please!

86	4.4.2.3.2.4		Conclusion no.2 indicates that the IO/LO laser for the back-to-back modulator approach is the same as for the present (presumably meaning baseline) design, yet the baseline design uses a 5 W optical power laser whilst the back-to-back option uses a 55 W optical power laser!
90	4.5.1.2		Presumably these figures are for the baseline receiver configuration. They need reconciling with the receiver figures mentioned earlier. For example the receiver cooling requires 200 W yet the total system thermal requirements is only 200 W?!
90	4.5.1.3		This paragraph states an input power requirement to the coolant system of 240 W yet the table above shows 200 W?
105	5.1.1.2.2.1		If both of the main laser resonator elements have moved during launch then whilst adjustment of just one of them will probably be sufficient to attain lasing, it may not be possible to fully optimise the laser.
107	5.1.1.2.3.1		Is a quad detector sufficient to monitor the mode profile?
FEM	Fig.4		Although I have little or no knowledge of design reduction for FEM purposes, this does seem to be an over simplification of the telescope mirrors as it assumes they are perfectly rigid.

Comments on GE DR-9 LAWS Interface Requirements Document

Gary Spiers,UAH

Page	Section/Fig.	Para.	Comment
Most			Lots of TBD again!
7	3.2.2.4	1	If the local oscillator and gain module interface is not considered here, where is it considered?
8	Fig.3.2.2.4-1		This shows a beam generated using a parabolic profile output mirror of order 2 rather than with the 8^{th} order supergaussian profile the contractor intends to use.
10	3.2.2.4	6	The hill-climbing servo-loop to operate the local oscillator must be locked to something, usually the power or discharge current. Which is it in this case?

Comments on LMSC DR-8 and DR-9 LAWS Documents

Gary Spiers,UAH

Michael, I found these reports very frustrating, whilst LMSC gives great detail on administrative details, the actual hardware design details are presented in such a fashion that the information presented is sufficient to indicate that they have been working but insufficient to critically assess the status of the design! The following applies to the DR-8 report. I have no comments on the DR-9 report!

Page	Section/Fig.	Para.	Comment
205	4-106		Update SNR eqn to that of Frehlich & Kavaya?

7 Appendix 2: Computer Modeling of Pulsed CO_2 Lasers for Lidar Applications

7.1 Introduction

The following article was published in the NASA/MSFC FY91 Global Scale Atmospheric Processes Research Program Review, NASA Conference Publication 3126. The presentation made at the review is also included for completeness.

7.2 Published Paper

TITLE: Computer Modeling of Pulsed CO_2 Lasers for Lidar Applications

INVESTIGATORS: Gary D. Spiers, Center for Applied Optics, The University of Alabama in Huntsville, Huntsville, Al. 35899, (205) 895 6030/(205) 544 3213.

Martin E. Smithers, NASA Code EB23, Marshall Space Flight Center, Huntsville, Al. 35812, (205) 544 3477.

Rom Murty, School of Engineering and Technology, Alabama A&M University, Normal, Al. 35762, (205) 851 5581.

SIGNIFICANT ACCOMPLISHMENTS:

Allthough this modeling effort has only recently commenced, the experimental results obtained during the past year will enable a comparison of the numerical code output with experimental data to be made. This will ensure verification of the validity of the code. The measurements were made on a modified commercial CO_2 laser, the PSI LP-140. Results obtained included:-

1) Measurement of the pulse shape and energy dependence on gas pressure.

2) Determination of the intra-pulse frequency chirp due to plasma and laser induced medium perturbation effects. A simple numerical model showed quantitative agreement with these measurements. The pulse to pulse frequency stability was also determined.

3) The dependence of the laser transverse mode stability on cavity length. A simple analysis of this dependence in terms of changes to the equivalent fresnel number and the cavity magnification was performed.

4) An analysis of the discharge pulse shapes enabled the low efficiency of the laser to be explained in terms of poor coupling of the electrical energy into the vibrational levels. This analysis also provided estimates of the electron drift velocities and number densities.

5) The existing laser resonator code has been modified to allow it to run on the Cray XMP under the new operating system.

FOCUS OF CURRENT AND PLANNED RESEARCH:

A numerical model of a pulsed transversely excited (TE) CO_2 laser is being developed to enable the performance of such devices to be predicted prior to construction. This is of particular benefit to the LAWS contract where two contractors are providing alternative laser configurations.

Although numerical models of TE CO_2 lasers have been used in the past these models have normally been constructed as several computer programs, each addressing a particular feature of the laser. Although a limited degree of feedback is available between these programs each is essentially a stand alone program and this lack of interaction between the modules resulted in limitations on the predicted output. This approach was necessitated by the considerable run time required by each of the programs. With the availability of much greater computing power, it has become possible to integrate all these modules into a single program where they can interact with one another.

The model addresses the transfer of stored electrical energy into the vibrational and rotational levels of the molecular gas species present in the laser gas and the subsequent conversion of the energy in these levels into the optical output pulse. The electrical to vibrational energy conversion will be modeled by solution of the Boltzmann equation with the inclusion of superelastic and electron-electron collision processes which are normally excluded from the simpler models. Additionally a multi-line multi-mode gain distribution will be used to determine the optical output as opposed to the normal single-line single-mode approximation. The inclusion of hot band contributions to the gain together with modeling of the gas thermodynamic effects will enable the frequency content and stability of the output pulse to be determined as well as the output amplitude and pulse shape.

The model will be verified by comparison with experimental results obtained within the laboratory and from the published literature.

PUBLICATIONS:

1) Jaenisch, H.M. & G.D. Spiers,"Modifications to the LP-140 Pulsed CO_2 Laser for Lidar Use", SPIE High Energy Lasers Conference, Los Angeles California, Jan 24, 1991.

2) Spiers, G.D.,"Discharge Circuit Considerations for Pulsed CO_2 Lidars", To be presented at the OSA Coherent Laser Radar: Technology and Applications Topical Meeting, Snowmass Colorado, July 8-12, 1991.

7.3 Presentation Material

Modeling of Pulsed CO_2 Lasers.

- Gary D. Spiers
  Center for Applied Optics
  University of Alabama in Huntsville
  Huntsville
  Al. 35773
  (205) 895 6030 / (205) 544 3213

- Martin E. Smithers
  Optical Systems Branch
  Mail Code EB23
  Marshall Space Flight Center
  Huntsville
  Al. 35812
  (205) 544 3477

- Rom Murty
  School of Engineering & Technology
  Alabama A&M University
  Normal
  Al. 35762
  (205) 851 5581

Layout

- Background
- Objectives
- Work completed
- Work in Progress

Background

- The design of lasers for use in Lidar devices has tended to consist of one of two approaches.

  1) Modification of an existing design that has undergone considerable testing.

  2) Construction of a preliminary breadboard to enable assessment of the design.

- These approaches have been used because of the difficulty in predicting the exact output characteristics at the preliminary design stage.

Objectives

- To develop a detailed numerical model of a pulsed CO_2 laser that will enable the determination of a laser's output characteristics without the need to resort to the construction of preliminary breadboard designs.

- The model will be verified by comparison of the output results with those obtained experimentally and from the published literature.

- The model will be used to compare the relative performance of the two lasers proposed for the LAWS project.

Work Completed

Experimental results obtained on a modified commercial CO_2 laser, the PSI LP-140.

- Modified to provide single line output.
- Transverse mode stability improved.
- Pulse frequency chirp measured and a reasonable agreement with theory seen.
- Laser discharge characteristics measured.

Discharge Characteristics

- LP-140 consists of eight cathodes arranged around a common anode so as to provide a folded optical cavity.
- Each 'electrode pair' is driven by it's own discharge circuit.
- All circuits use a common high voltage power supply and a single thyratron discharge switch.
- Analysis of digitised voltage and current pulses enables the determination of properties important for the modeling of the discharge kinetics.

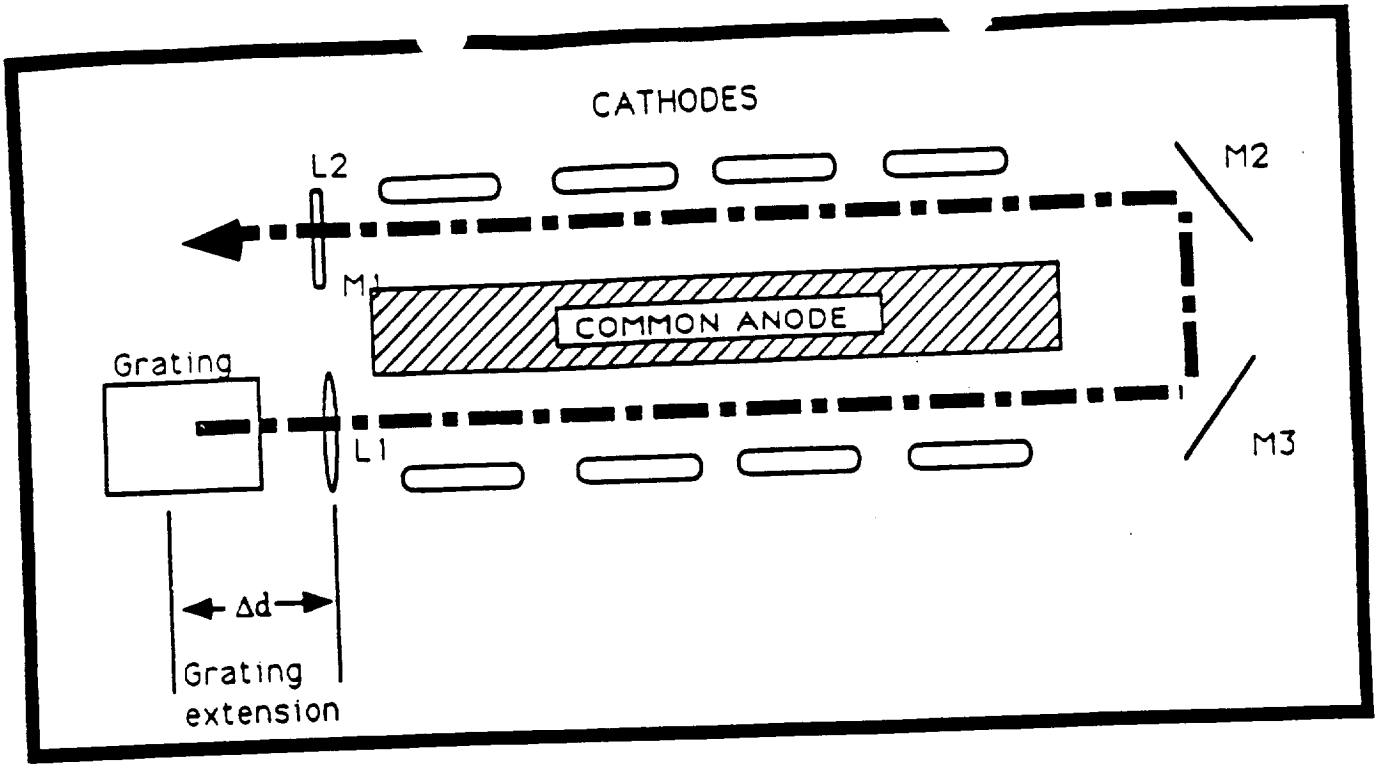

LP-140 Schematic

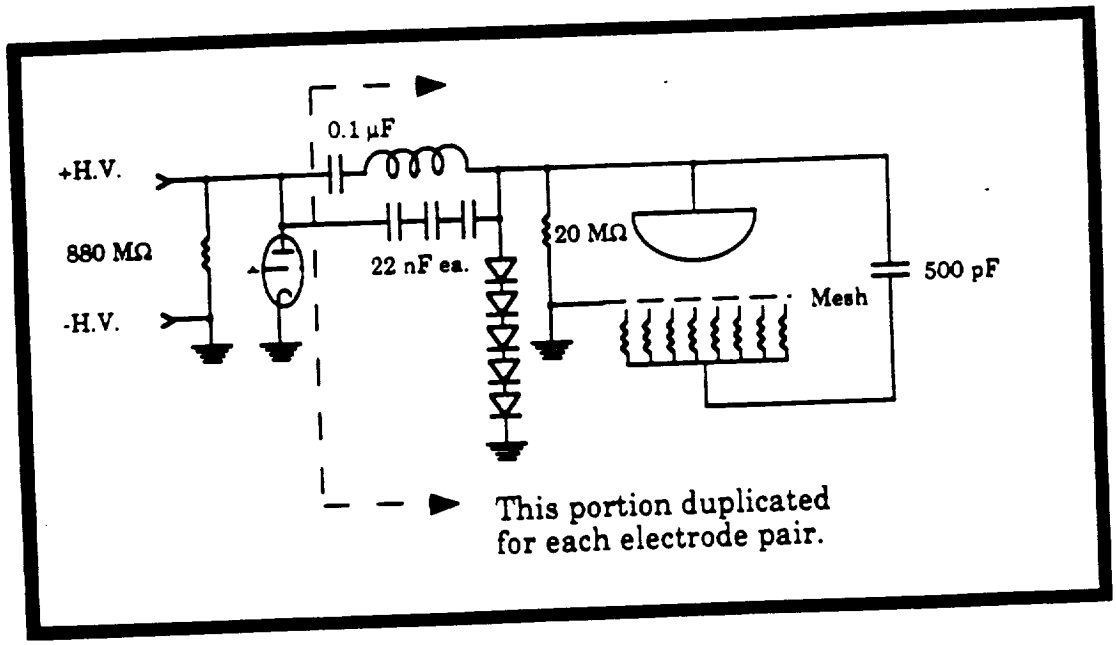

Single Electrode Pair Discharge Circuit

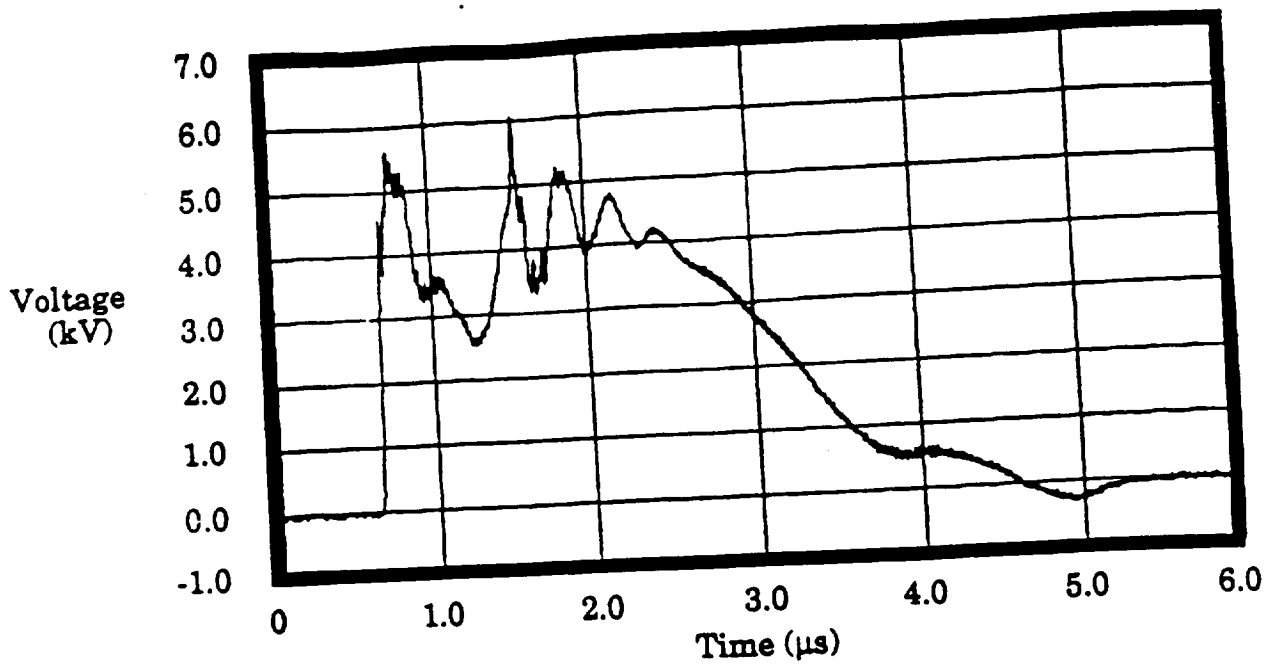

LP-140 Discharge Voltage Pulse

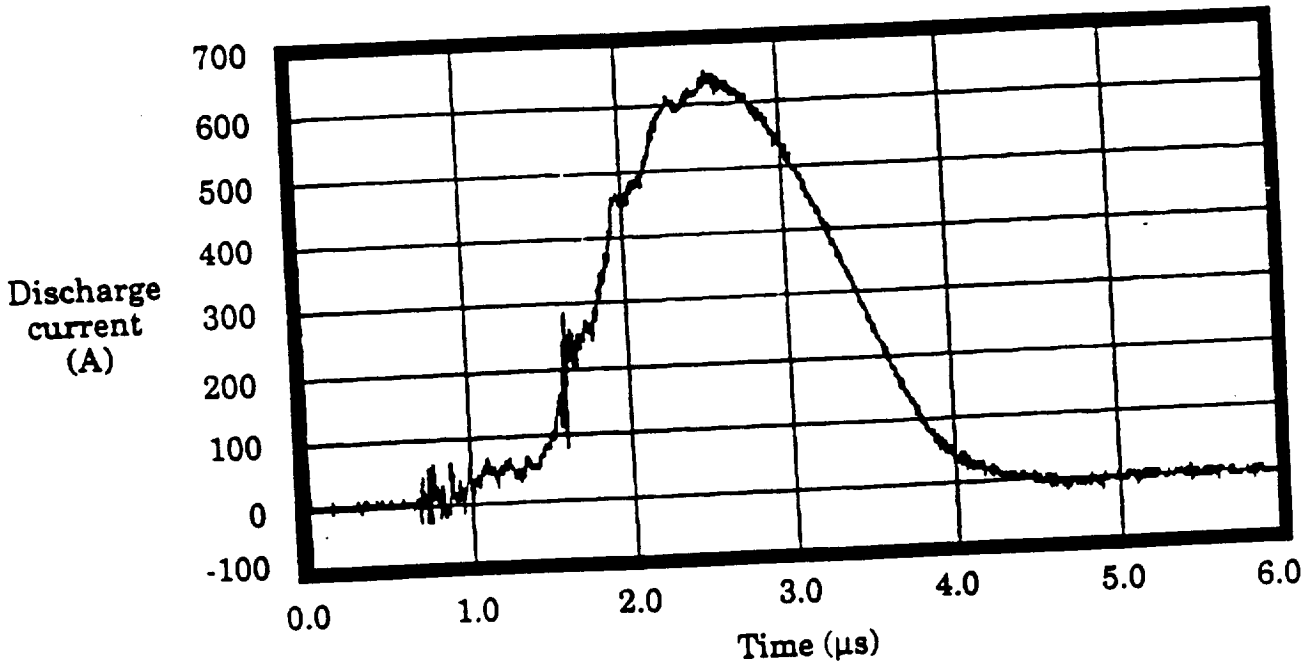

LP-140 Discharge Current Pulse

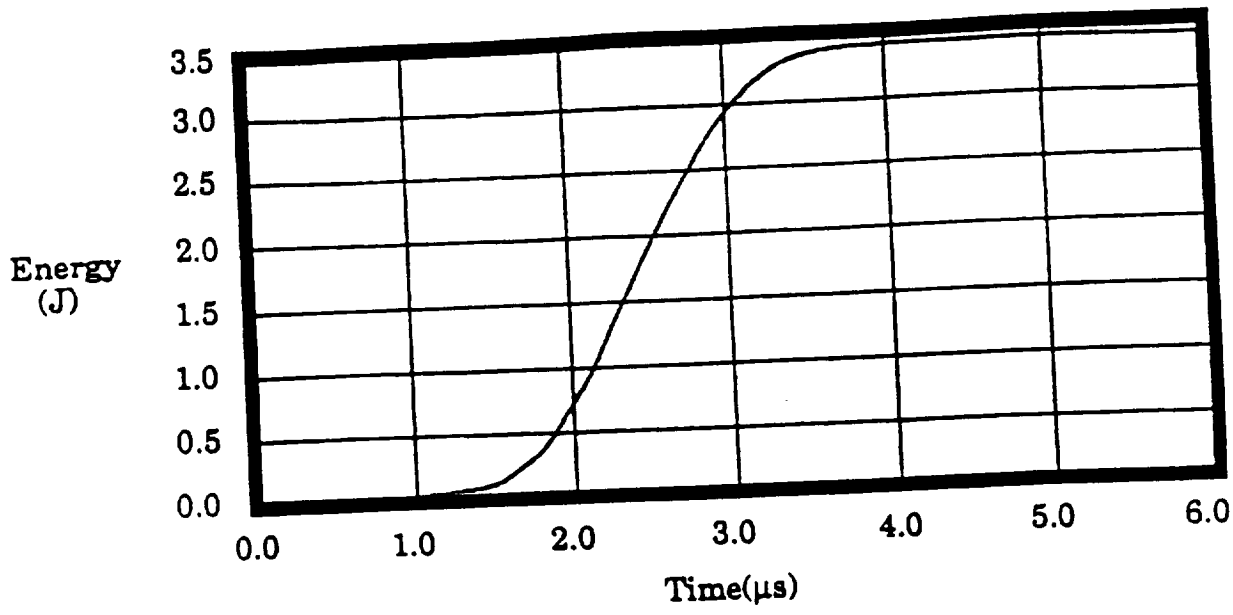

The Time Evolution of the Deposition of Energy into the Discharge

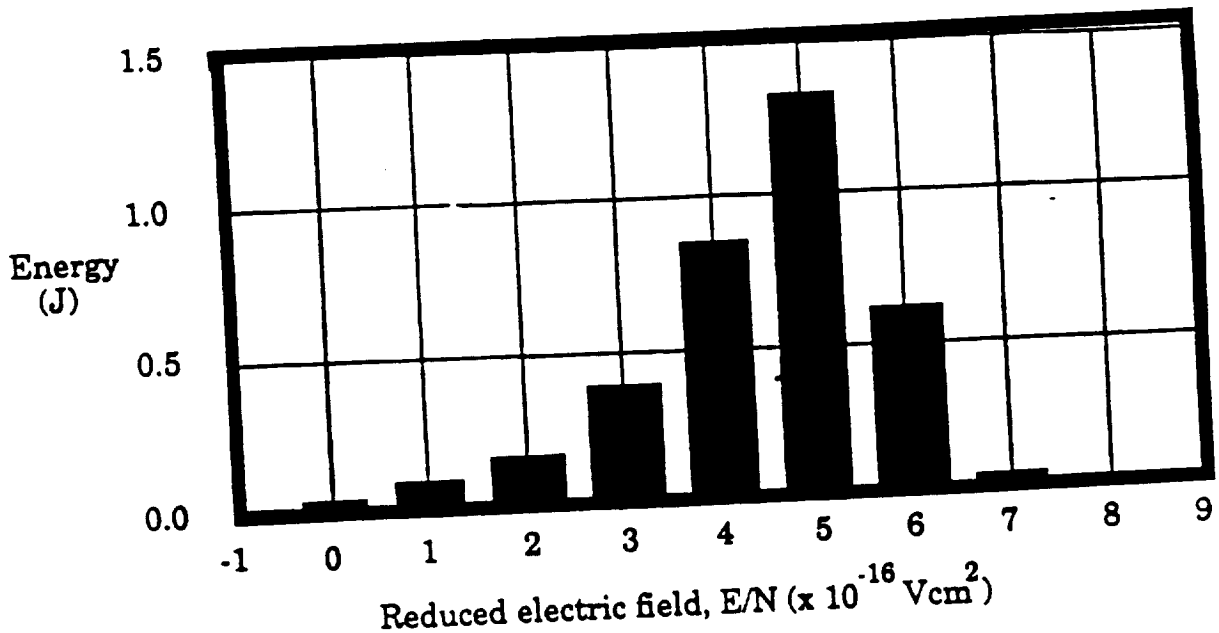

The Distribution of the Deposited Energy as a Function of the Electric Field

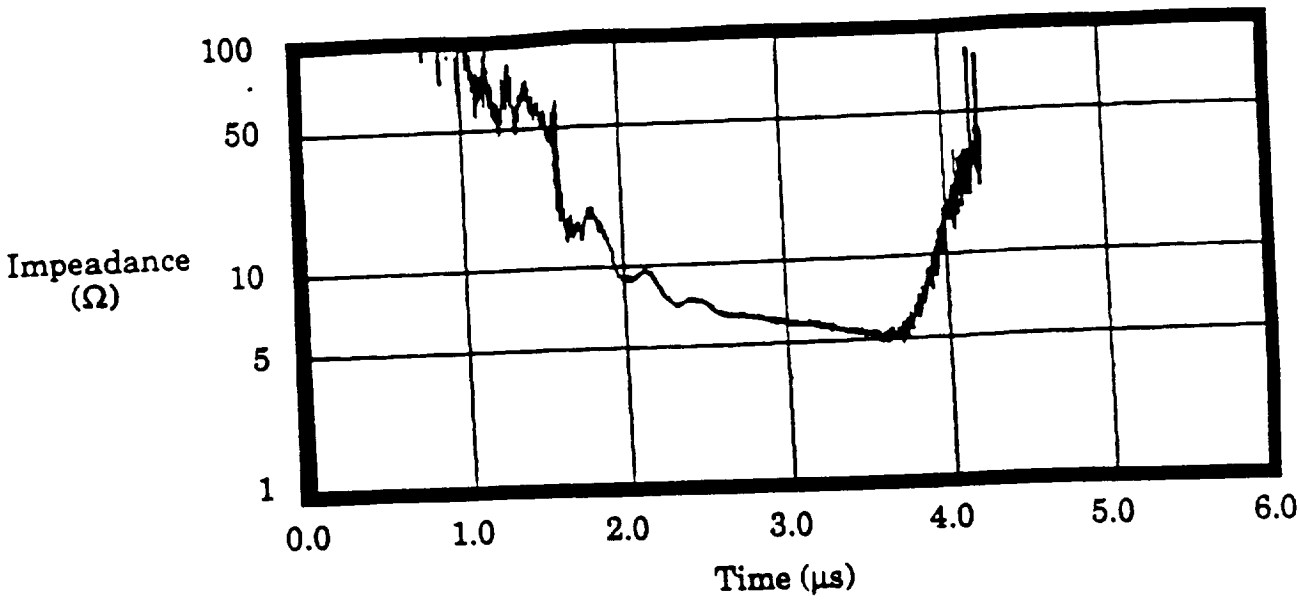

The Time Dependence of the Discharge Impeadance

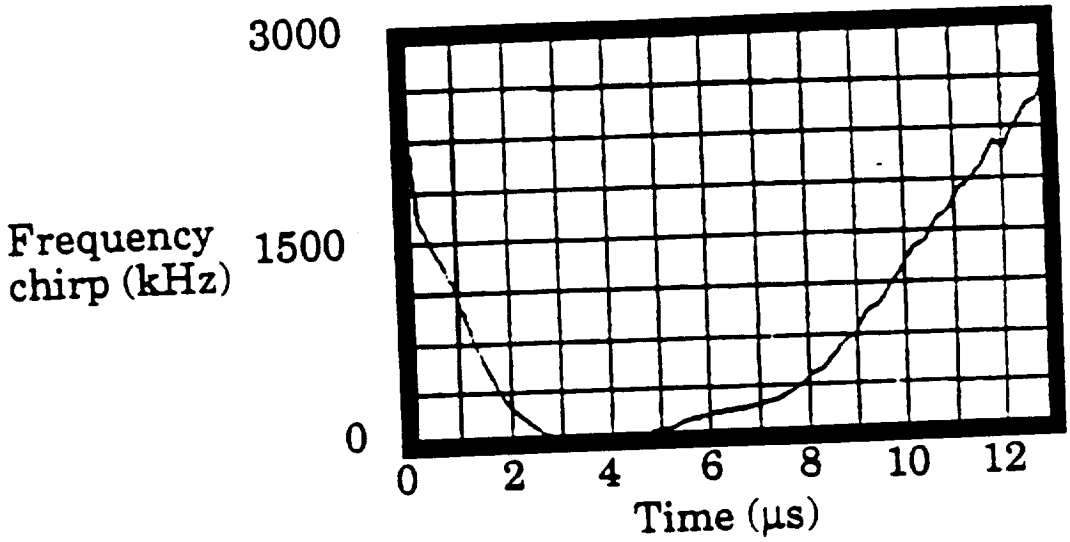

The Frequency Chirp of the Laser Pulse

Model Overview

- Segment the laser into multiple smaller boxes and solve the system of equations for each box.

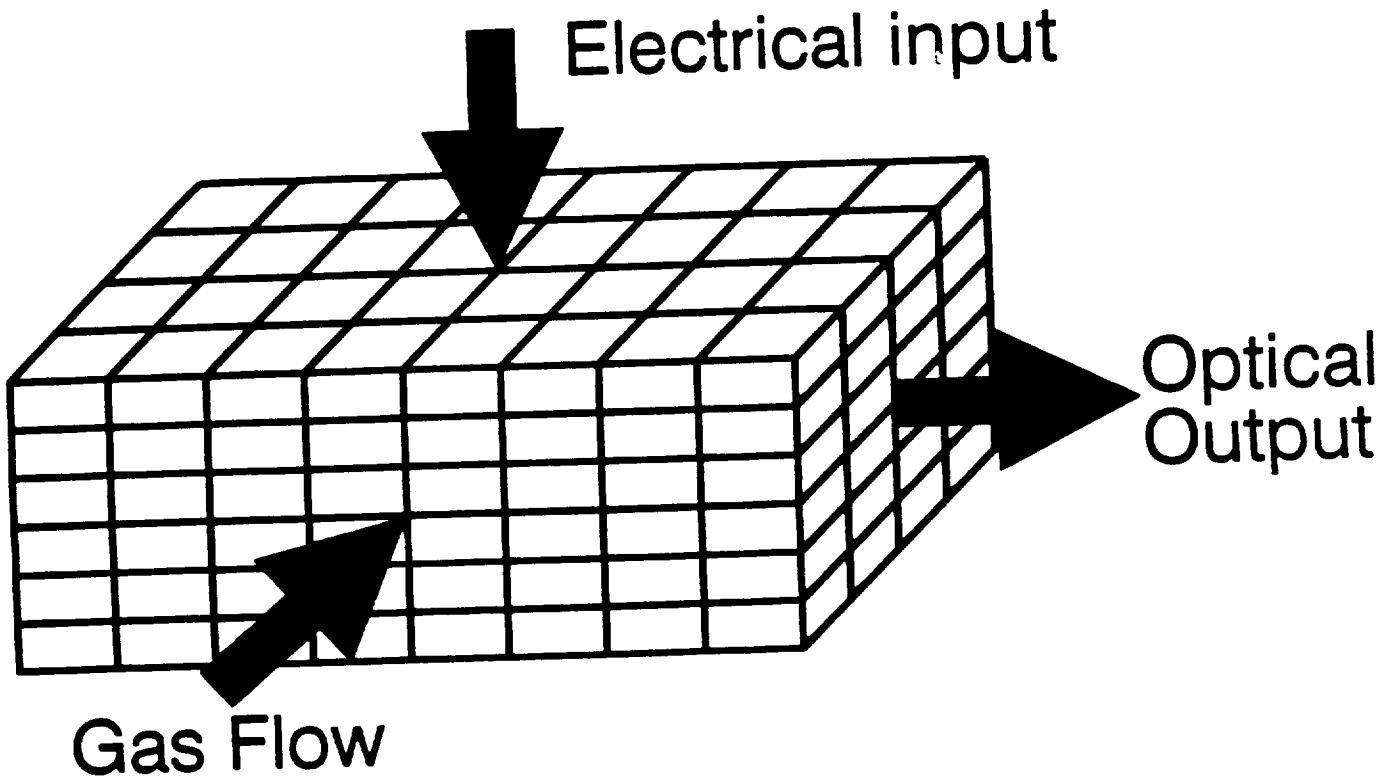

- Not necessarily a uniform grid.

Interaction Diagram

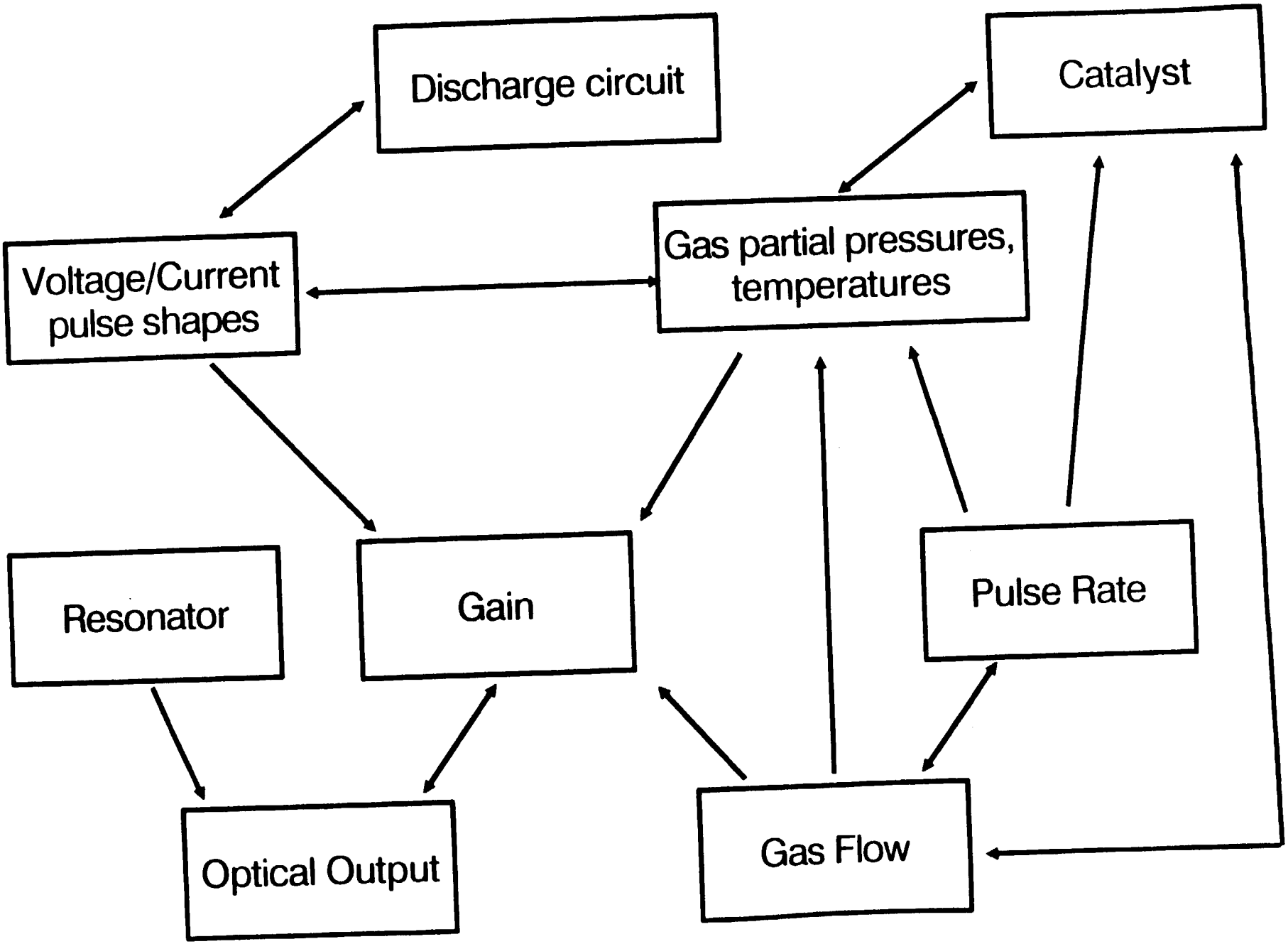

Program Flowchart

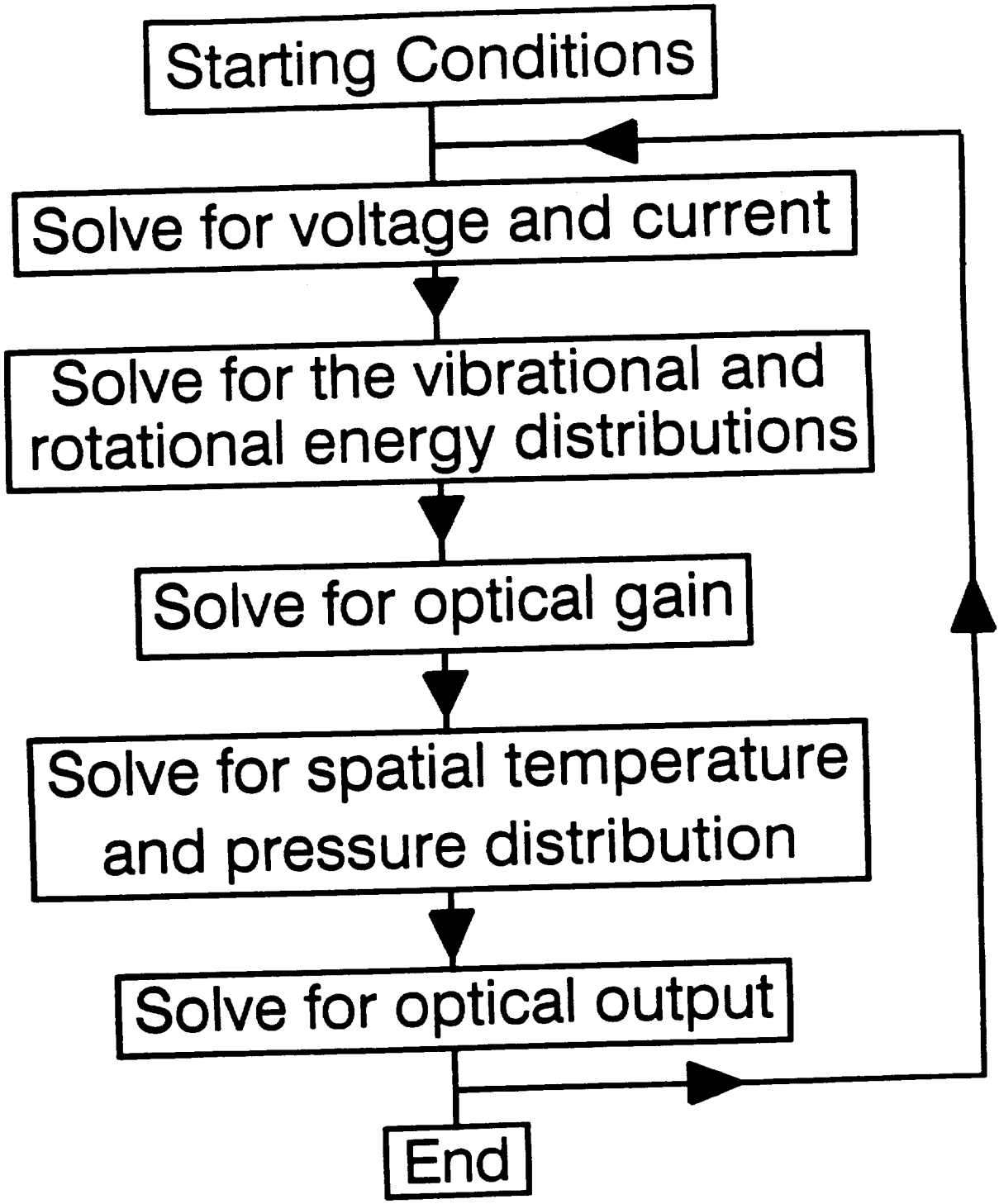

- The remainder of this presentation will be concerned with the gas kinetics.

Starting Conditions

- Bulk:
  Gas constituents.
  Gas temperature and pressure distributions.

- Individual molecular species:
  Number density.
  Vibrational and rotational energy distribution.

- Resonator configuration

- Initial distributions determined by solution of equations under the assumption that the system is in equilibrium at some temperature, T, usually taken to be room temperature.

Voltage and Current Determination

- Use two sources:

  1) Initially use experimentally determined voltage and current pulses.

  2) When rest of code has been verified then include calculation of voltage and current pulses.

- Existing non-proprietary codes assume a constant voltage and the linear deposition of energy into the discharge.

- A better model requires modeling of the discharge circuit and pfn as well as the gas discharge.

Vibrational / Rotational Energy Distribution

- Solve the Boltzmann equation to determine electron excitation rates.
- Use these rates to solve for the vibrational energy distribution using a temperature model.
- The rotational energy distribution within a vibrational level is given by a Boltzmann distribution.

The Boltzmann Equation

- The Boltzmann equation is used to calculate the electron distribution function in a plasma in the presence of an electric field and allows for the impact of elastic and inelastic collisions of the electrons.

- Code to solve the Boltzmann equation is available from the Air Force Weapons Laboratory.

- However, most Boltzmann solvers for the CO_2 laser consider only the upper and lower laser vibrational levels and neglect superelastic electron scattering losses which can be important at high input energy loadings.

- The A.F.W.L. code has these limitations and is being modified.

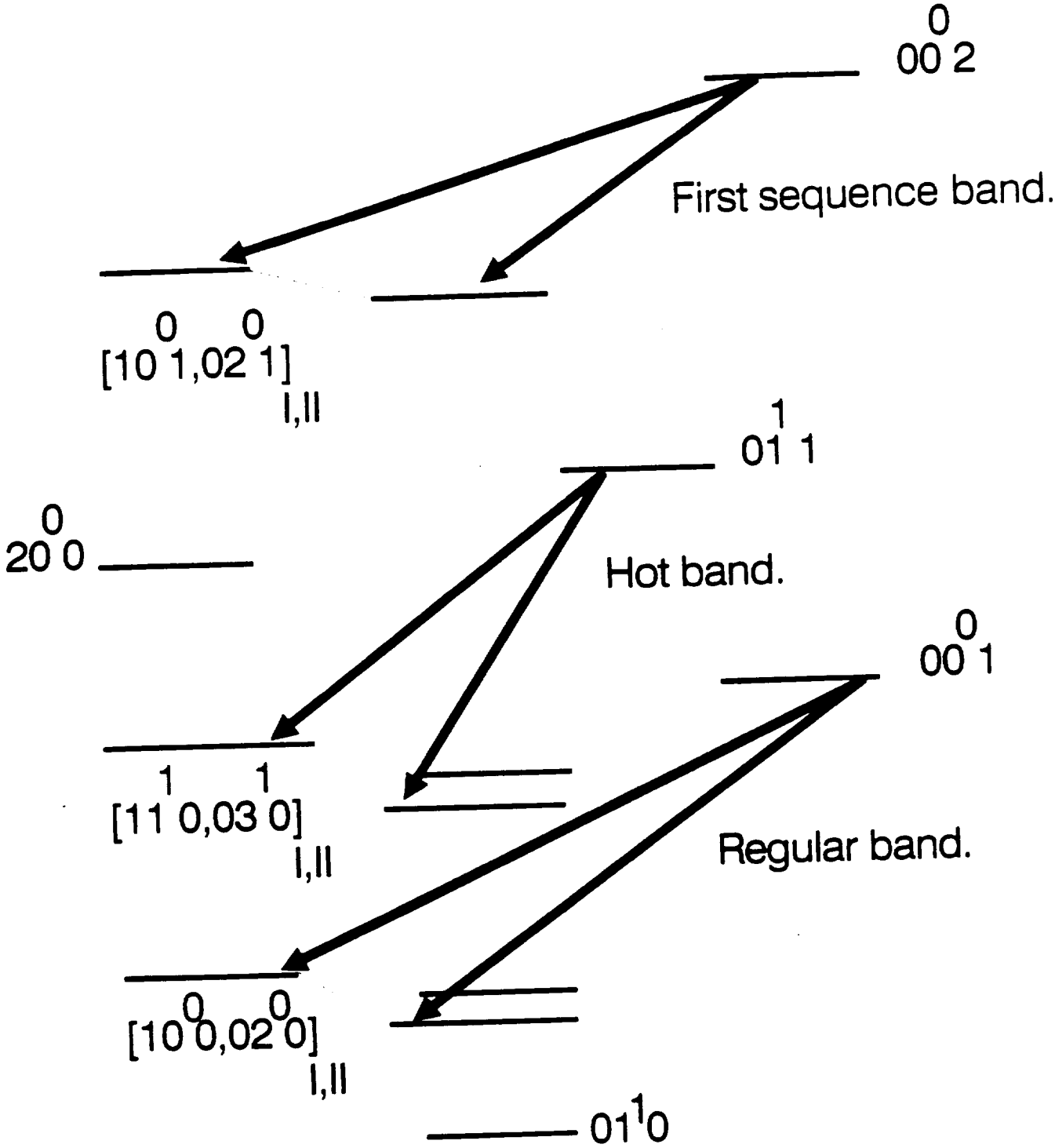

Lower Vibrational Levels of the CO_2 Molecule

The Temperature Model

- Each vibrational level can be considered as having a characteristic temperature. The population change in each level is given by a first order differential equation which includes terms for:
  a) electron processes.
  b) energy exchange between vibrational levels.
  c) Vibrational to translational energy exchange.

- For a pulsed laser a minimum of five temperatures is considered:
  1) 001 upper laser level.
  2) 020 lower laser level.
  3) 100 lower laser level.
  4) Nitrogen V1 level.
  5) Rotational and translational temperature.

Optical Gain

- Once the energy in each of the rotational / vibrational levels has been found the gain is determined from the populations of the upper and lower levels of the lasing transition, the Einstein B coefficient and the line shape.

- The line shape is a function of the gas composition and pressure and is dominated by collision broadening for pressures above 50 torr.

- Existing codes assume single mode operation. The inclusion of the energy distribution for the rotational levels enables line competition effects during gain build-up to be modeled and also allows for the modeling of injection seeding.

Summary

- Experimental measurements have been made on a pulsed CO_2 laser.

- A numerical model of a pulsed CO_2 laser is under development. The model will incorporate many of the smaller effects ignored by previous codes in an effort to be able to model the spatial, temporal and frequency variations of the pulsed laser output.

- The model will be verified by comparison with both the published literature and the experimental data collected previously.

- The model will then be used to compare the lasers proposed for the LAWS project.

8 Appendix 3: Discharge Circuit Considerations for Pulsed CO_2 Lidars

8.1 Introduction

The following paper was presented as a poster at the OSA Coherent Laser Radar: Technology and Applications Conference in Snowmass, Colorado July 8-12, 1991. This form of the paper was published in the OSA 1991 Technical Digest Series Volume 12.

8.2 Published Paper

Discharge Characteristics of the LP-140 Pulsed CO_2 Laser.

Gary D. Spiers

Center for Applied Optics
The University of Alabama in Huntsville
Huntsville, Al. 35899
(205) 895 6030

Introduction

The LP-140 is a low pressure pulsed transversely excited CO_2 laser manufactured by PSI(9.1). The laser has a folded cavity construction and each arm of the cavity contains four discharge sections. The eight cathodes are placed on the outer edges of the cavity arms so that they can share a single large wire grid anode. Eight additional electrodes each consisting of a potted array of resistively ballasted pins are located behind the grid anode directly opposite each of the cathodes. The sympathetic discharge used in the LP-140 relies on a preliminary discharge between the anode and these pin electrodes to preionise the main discharge volume. Each electrode pair has a discharge volume of 280 cm^3. The discharge circuit is arranged such that each electrode pair has its own energy storage capacitors and pfn (fig. 9.1.) but all share a common thyratron and HV supply. The capacitors are charged to 9 kV. The dc HV supply consists principally of a large HV step-up transformer with no regulation or adjustment of the output voltage possible without modification.

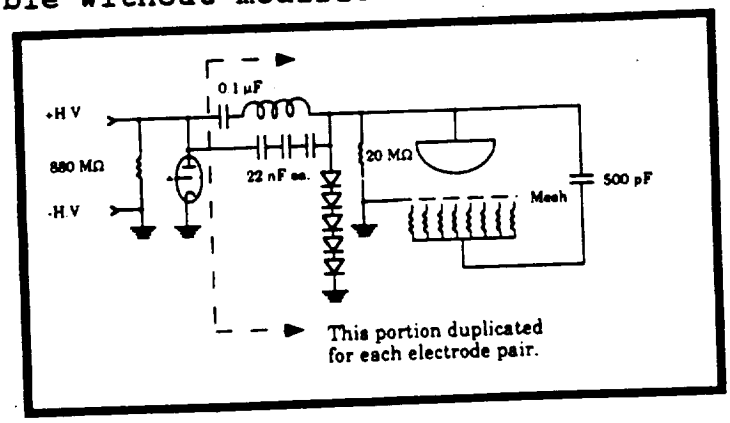

Figure 9.1. The discharge circuit for one of the electrode pairs.

There are essentially two discharge circuits in this circuit, the first is the main discharge circuit consisting of the 0.1 μF capacitor and the second comprises the three 22 nF capacitors. As there is an inductor in series with the 0.1 μF capacitor, this circuit will have a large time constant with respect to the 22 nF discharge circuit. When the thyratron is triggered, the 22 nF circuit provides a low energy fast rise-time voltage pulse across the laser head. This pulse breaks down the gap between the grid and the pin electrodes to provide a preliminary preionising discharge. When the slower main discharge pulse arrives at the laser head, the main discharge gap is preionised and homogeneous breakdown occurs. The small 500 pF capacitor prevents energy from the slower main discharge pulse from being deposited into the preionisation discharge.

Voltage and current pulse measurements

The voltage pulse was measured using a Tektronix P6015 high voltage probe connected to a LeCroy 9450 dual 350 MHz digitising oscilloscope. The discharge current pulse was measured simultaneously using a Pearson Electronics Model 110 induction coil. After being digitised by the oscilloscope, the pulses were either ported to a plotter or to an IBM compatible computer for analysis. Figures 9.2 and 9.3 show representative voltage and current pulses from one of the electrode pairs.

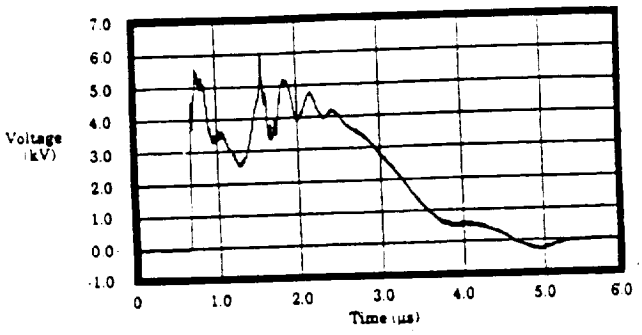

Figure 9.2. The discharge voltage pulse.

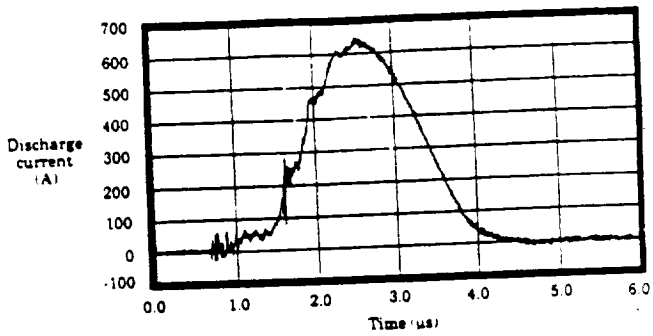

Figure 9.3. The discharge current pulse.

Results and Analysis

It can be seen from the voltage pulse that there is an initial sharp voltage pulse rising to ~4.5 kV. This is the preionisation pulse and it is immediately followed by the main discharge pulse which rises to ~5.5 kV. The voltage pulse then proceeds to ring across the discharge with an approximate average value of ~4.5 kV which is half of the initial capaci-

tor charging voltage, as would be expected. This ringing, although undesirable is not excessive. The current pulse rise is delayed with respect to the voltage rise. This is to be expected as the discharge impeadance is required to fall before a significant current flow can be obtained. The current peaks at a value of ~650 A as the voltage pulse starts to fall.

Further analysis of the discharge was carried out to enable the discharge impeadance, electron concentration, electron drift velocities and energy deposition to be determined as a function of time.

The energy deposited into the discharge was obtained by integrating the digitised current and voltage pulses (fig. 9.4). It can be seen that a total of ~3.4 J is deposited into the discharge. This provides a total of 27 ± 3 J deposited into all eight pairs of electrodes compared to a total nominal energy of 32 J stored in the capacitors. The considerable variation on the total energy is due to voltage variations arising from the unregulated power supply. For a nominal optical output of 1 J this provides an electrical to optical conversion efficiency of 3.7 ± 0.2 %, a pfn transfer efficiency of ~84 % and a stored energy to optical energy conversion efficiency of ~3 %. This figure does not include the conversion efficiency of the dc HV supply. It can be seen that the optical to electrical efficiency is low compared to a potential efficiency >10 %.

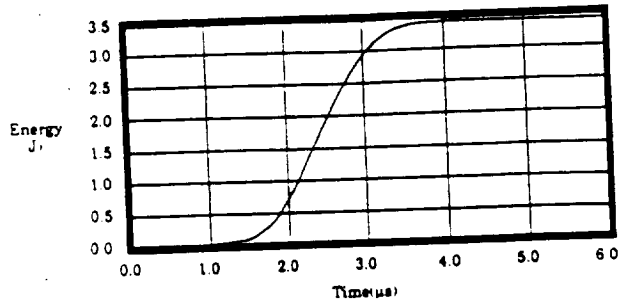

Figure 9.4. Energy deposition into the discharge.

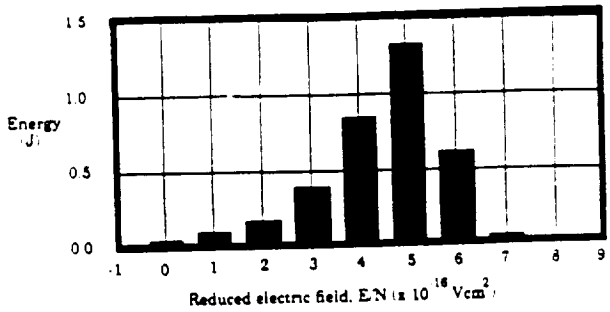

Figure 9.5. The energy deposition dependence on E/N.

Only the energy deposited into the $CO_2(001)$ and the $N_2(v=1-8)$ vibrational energy levels is useful for lasing action. Lowke et al.(9.2) have shown that the optimum excitation of these vibrational levels occurs for values of the reduced electric field, E/N of ~$(1-3)x10^{-16}$ Vcm^2. The

range of E/N values during the discharge pulse was divided into intervals of $1x10^{-16}$ Vcm^{-2} and the energy deposited into each of the intervals calculated (fig. 9.5). It can be seen that most of the energy is deposited in the $(4-6)x10^{-16}$ Vcm^{-2} region and this accounts for the low electrical to optical conversion efficiency obtained.

Ideally to maximise the pfn transfer efficiency the circuit impeadance should match that of the discharge. However the discharge impeadance is a complex non-linear function dependent on both the discharge waveforms and the gas composition. An estimate of this impedance was obtained by dividing the voltage by the current (fig. 9.6). It can be seen that the discharge impeadance during the bulk of the energy deposition varies between 5 Ω and 10 Ω. This variation suggests an optimum value of ~7 Ω for the circuit impeadance. It should be noted that the discharge impeadance will vary with gas composition and optimisation of the discharge circuit should be undertaken after a final gas composition is chosen.

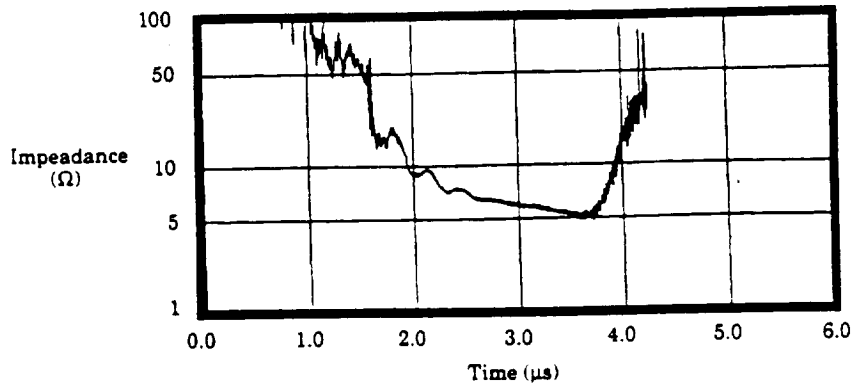

Figure 9.6. The discharge impedance.

Summary

Voltage and current pulse measurements of the LP-140 discharge were obtained and from these were derived the electrical energy deposited into the gas, the electrical to optical conversion efficiency, the input energy dependence on E/N and the discharge impeadance. It was found that 3.4 J was deposited into each discharge, which had an impeadance of (5-10) Ω. A poor electrical to optical conversion efficiency of ~4 % was found to be due to the electrical energy being deposited at too high a value of E/N for efficient excitation of the relevant CO_2 and N_2 vibrational levels.

References

(9.1) Pulse Systems, Inc., 140 Meadow Lane, Los Alamos, New Mexico 87544

(9.2) Lowke, J.J., A.V. Phelps & B.W. Irwin; "Predicted electron transport coefficients and operating characteristics of CO_2-N_2-He mixtures"; J. Appl. Phys.; **44**; 4664 (1973)

9 Appendix 4: Presentation made at the Code RC Review

CODE RC REVIEW

Optical Systems Branch
Marshall Space Flight Center
Huntsville, Al. 35812

Wednesday 18th. September 1991

LAWS Breadboard Status

Gary D. Spiers

Center for Applied Optics
University of Alabama in Huntsville
Huntsville, Al. 35899

LAWS BREADBOARD

NASA
MSFC EB-23

Requirements

The laser breadboard is to be built such that the following performance parameters can be measured and evaluated for both isotopic and non-isotopic gas mixtures:

1. Pulse Repetition Frequency
2. Pulse Energy
3. Absolute Frequency and Frequency Stability (Interpulse and Intrapulse including mode stability and chirp)
4. Beam Quality
5. Efficiency
6. Pulse Temporal Profile
7. Life testing and analysis to project component lifetimes to 10^9 pulses

LAWS BREADBOARD

NASA
MSFC EB-23

Requirements

The breadboard does not have the same requirements as the space unit. It is designed to address any outstanding laser design issues to ensure a solid data and knowledge base for Phase C/D.

- The laser heads are similar to the proposed LAWS designs.
- Auxilliary units are not optimised to enable the contractors to use existing equipment.
- Differences from the expected Phase C/D design must be traceable to that design e.g. the contractors are measuring extraction efficiency rather than wall plug efficiency to enable existing high voltage charging supplies to be used.

BREADBOARD TARGETS

NASA
MSFC EB-23

	TDS	STI
Pulse Energy (J)	15-20 (Near Field)	15-20 (Far Field)
Pulse Width (uS)	2.5-3.0	3.0
PRF (Hz)	10 (Life Test at 20)	20 (@ reduced o/p)
Beam Quality	1.1	1.2
Wavelength (um)	9.11 & 10.6	9.11 & 10.6
Beam Mode	SLM & STM	SLM & STM
Chirp (kHz)	200	< 250
Efficiency (%)	>9 (Extraction)	8 (Intrinsic)
Lifetime (Pulses)	10^8	$> 10^7$

COMPETITION SENSITIVE

TDS LASER COMPARISON

NASA
MSFC EB-23

	LAWS Device	Breadboard
Pulse Energy (J)	>15 (Far Field)	15-20 (Near Field)
Pulse Width (us)	>2.5	2.5-3.0
PRF (Hz)	10 (Avg.)	10 (Life Test @ 20)
Wavelength (um)	9.11	9.11 & 10.6
Beam Mode	STM & SLM	STM & SLM
Chirp (kHz)	100	200
Beam Quality	1.2	1.1
Lifetime (Pulses)	10^9	10^8
Weight (kg)	200	N.A.
Efficiency (%)	> 5 (Wall Plug)	> 9 (Extraction)

COMPETITION SENSITIVE

STI LASER COMPARISON

NASA
MSFC EB-23

	LAWS Device	Breadboard
Pulse Energy (J)	15 (Far Field)	15-20 (Far Field)
Pulse Width (uS)	3.0	3.0
PRF (Hz)	10 (Avg.) 20 (Max.)	20
Wavelength (um)	9.11	9.11 & 10.6
Beam Mode	SLM & STM	SLM & STM
Chirp (kHz)	< 150	< 250
Beam Quality	< 1.1	1.2
Lifetime (Pulses)	10^9	$>10^7$
Weight (kg)	< 165	N.A.
Efficiency (%)	> 6 (@ 10 Hz)	> 9 (Intrinsic)

COMPETITION SENSITIVE

BB. DESIGN COMPARISON

NASA
MSFC EB-23

Resonator	Textron	STI
Beam Size (cm^2)	4 X 4	4.6 X 4.6
Cavity Length (m)	3.4	4.8
Gain Length (m)	1.36 (4 sections)	1.2 (2 sections)
Output Mirror	Scraper	Graded Reflectivity
Magnification	2.25	1.35
Neq	1.38	N.A.

STI OPTICAL LAYOUT

NASA
MSFC EB-23

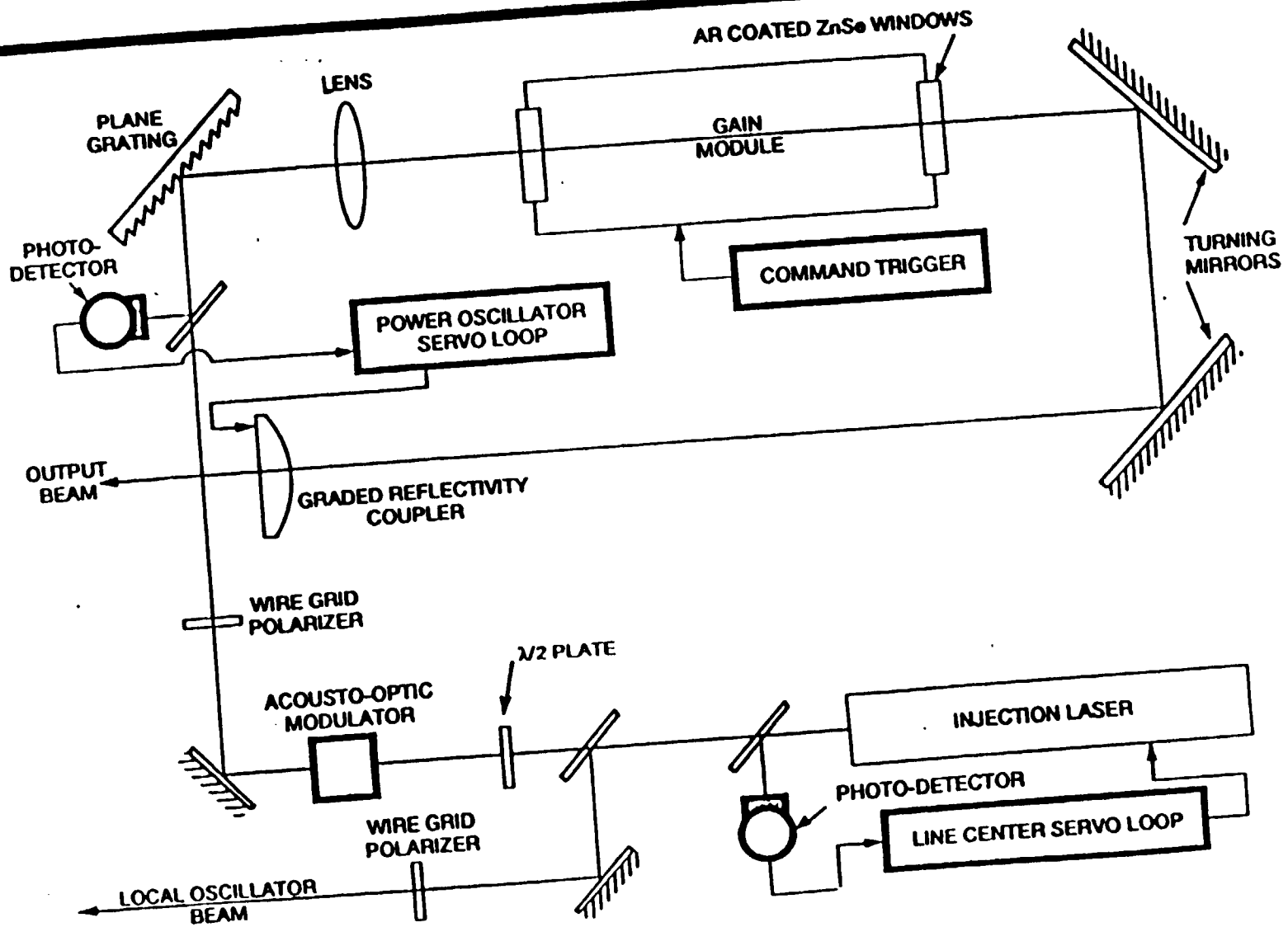

COMPETITION SENSITIVE

TDS OPTICAL LAYOUT

NASA
MSFC EB-23

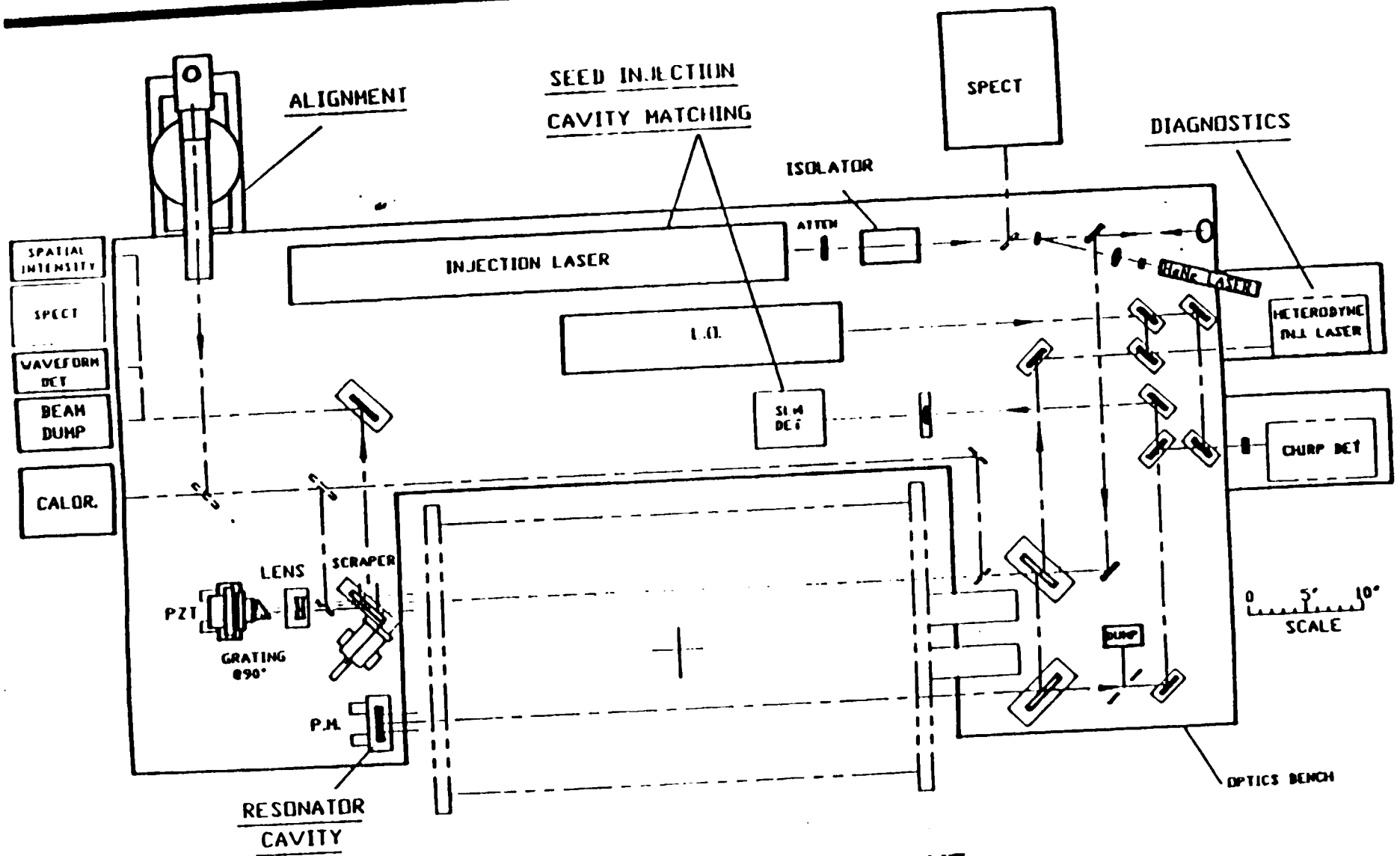

COMPETITION SENSITIVE

GDS BB R.1.0 9/17/91

STI GRM CONCEPT

NASA
MSFC EB-23

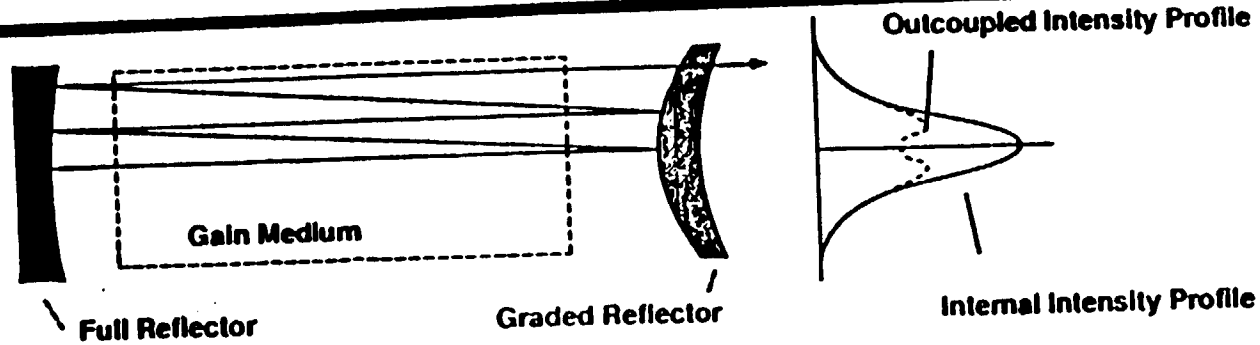

$R(r) = R_0[1 - (r/a)^n]$

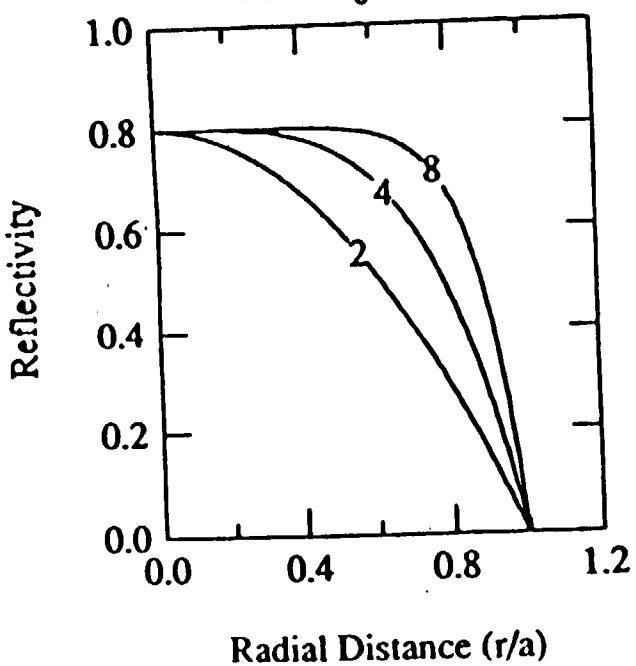

Supergaussian
$R(r) = R_0\exp[-2(r/a)^n]$

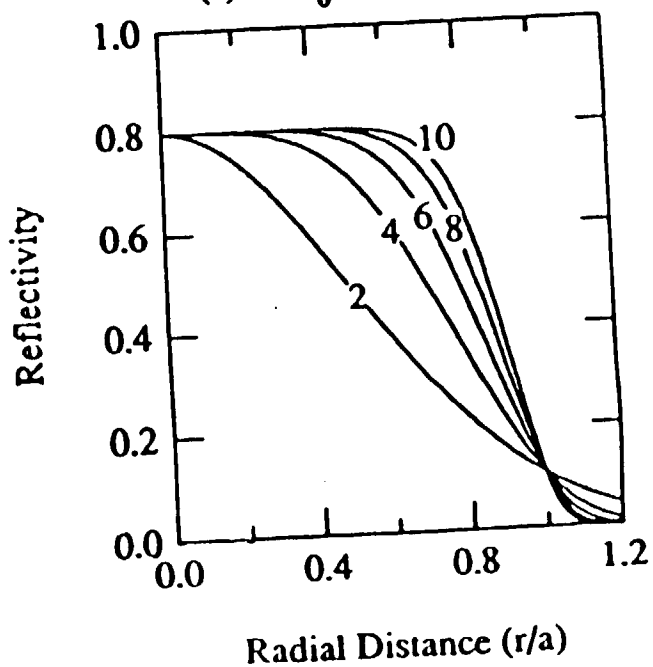

COMPETITION SENSITIVE

STI GRM Vs. SCRAPER

NASA
MSFC EB-23

- Comparison of Graded Mirror and Hard Mirror
- Both Resonators Extract Same Pulse Energy

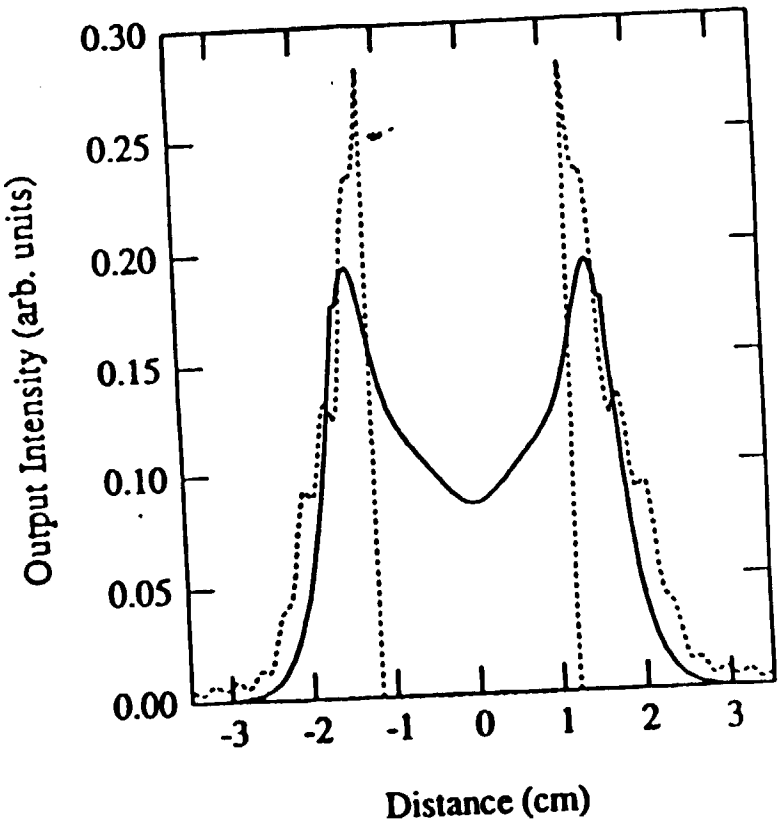

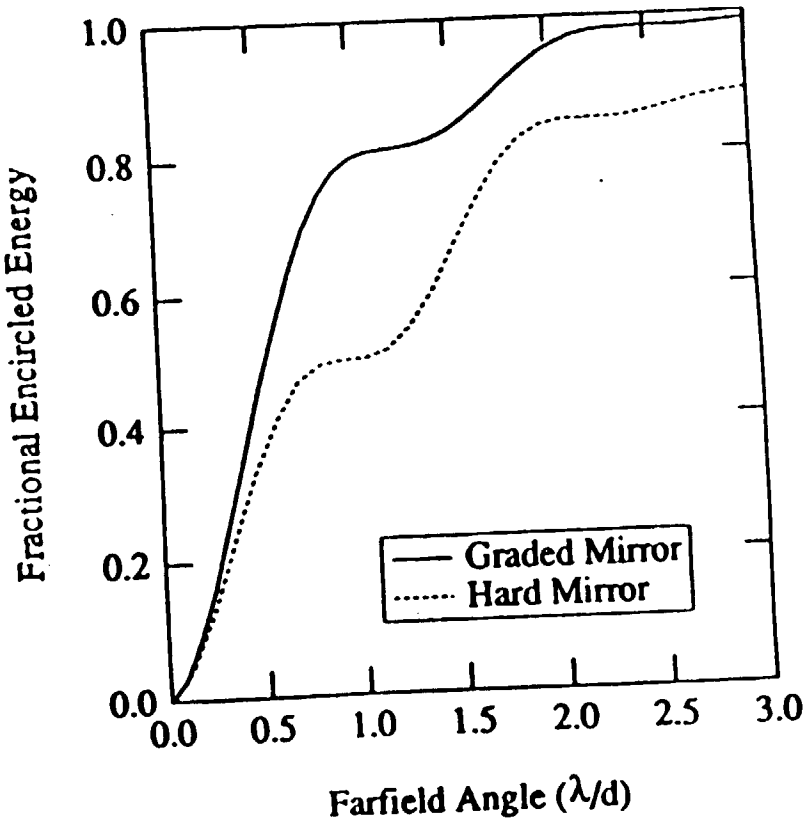

- Hard Edged: $M = 1.9, N_{eq} = 1.5$
- Graded Mirror: $M = 1.35$, Super-Gaussian, $n = 8$

COMPETITION SENSITIVE

BB. DESIGN COMPARISON

NASA
MSFC EB-23

Discharge	Textron	STI
Cross-section (cm^2)	4.2 X 4.2	5 X 5
Discharge Length (m)	1.36	1.2
CO_2 : N_2 : He	1 : 1 : 3	1 : 2 : 3
Gas Pressure (torr)	475	380
Energy Loading (J/l-atm.)	138	160
Discharge Voltage (kV)	20 (40 pk.)	30 (60 pk.)
Discharge Current (kA)	3 (max)	2.4 (Avg.)
Pulse Length (us)	4.5	3.5 - 4.0
Impedance (Ω)	8	12
Preioniser material	Micalax	$BaTiO_3$

COMPETITION SENSITIVE

BB. DESIGN COMPARISON

NASA
MSFC EB-23

Pulsed Power	Textron	STI
Stored Energy (J)	263	190 - 240
PFN Charge Voltage (kV)	40 (max)	+ and - 30
Discharge Current (kA)	3 (max)	2.4 (Avg.)
Pulse Duration (us)	4.5	3.5 - 4.0
HV Switch	Thyratron	Thyratron

STI ELECTRODE GEOMETRY

NASA
MSFC EB-23

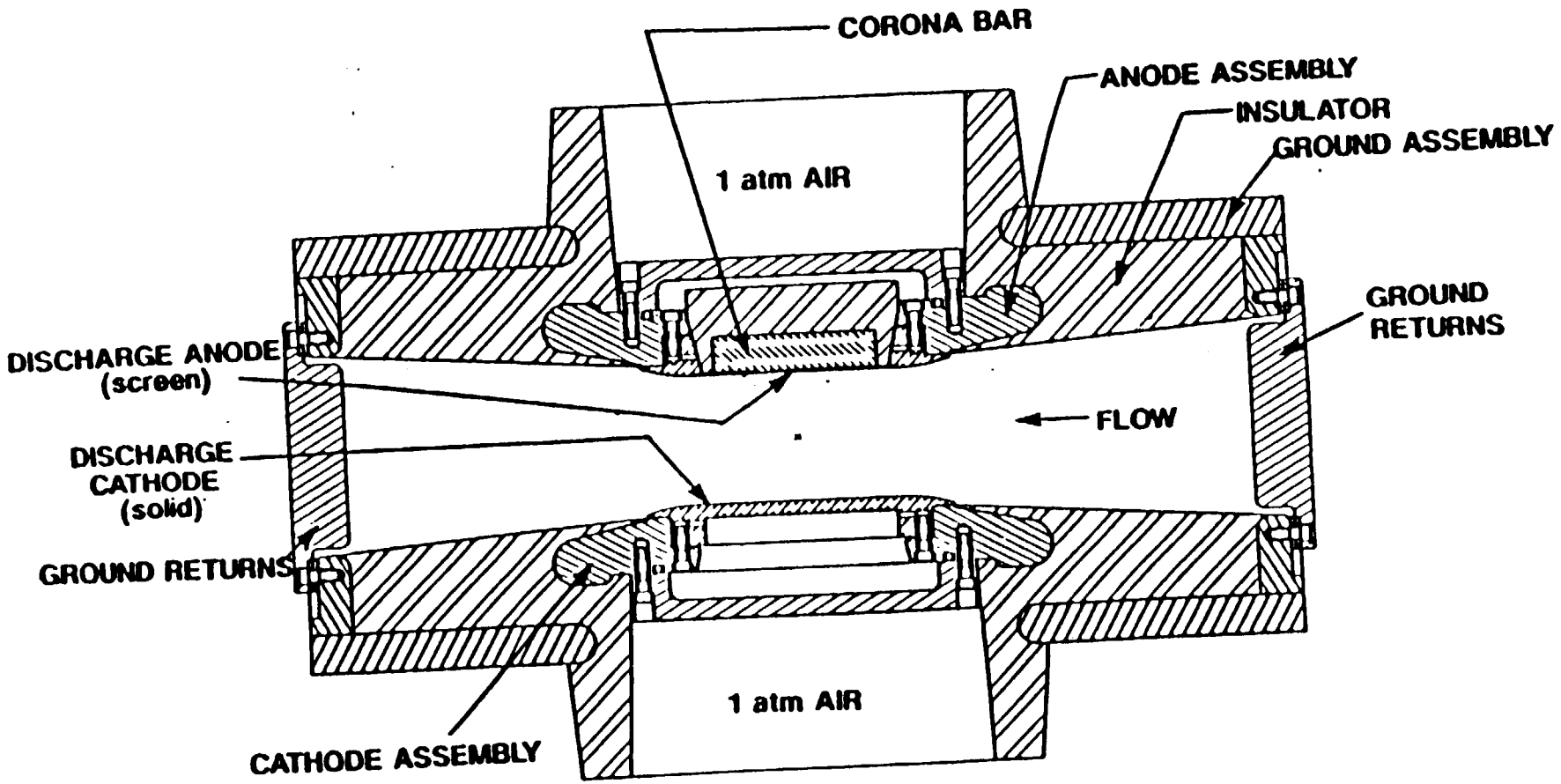

COMPETITION SENSITIVE

GDS BB R.1.0 9/17/91

TDS ELECTRODE CONCEPT

NASA
MSFC EB-23

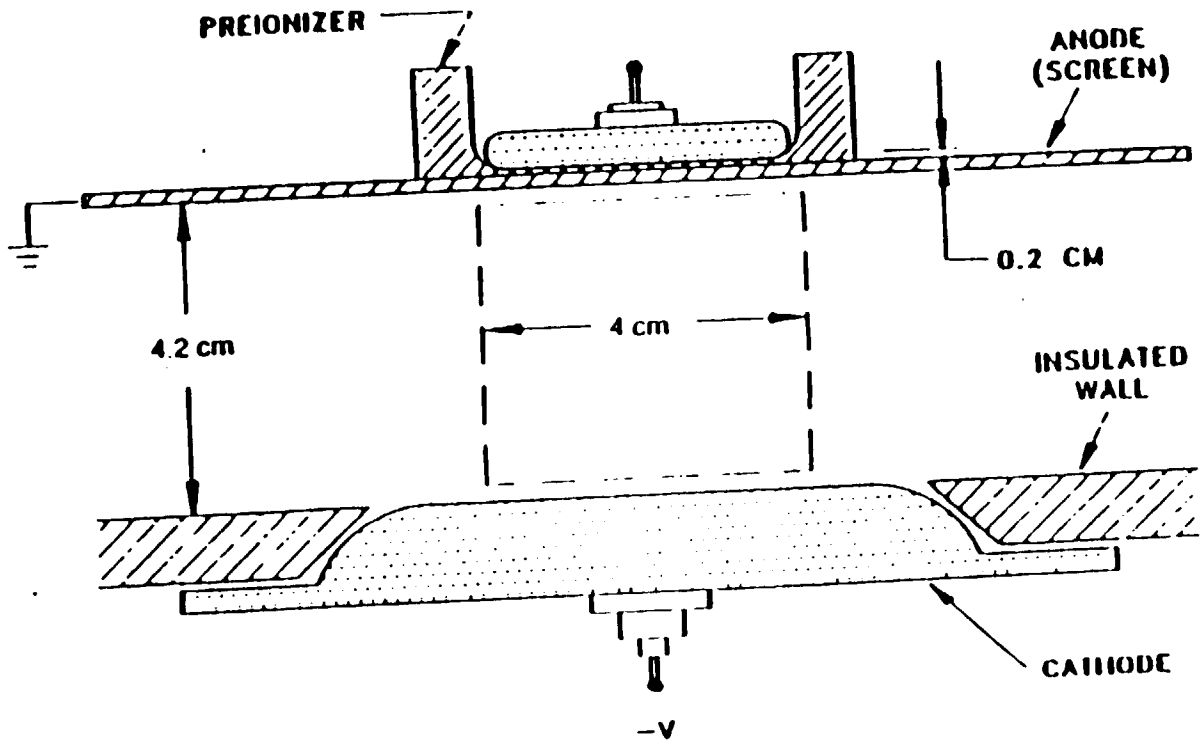

Glow Voltage: 21 kV
Electrode Profile: Modified Ernst

COMPETITION SENSITIVE

TDS DISCHARGE CIRCUIT

NASA
MSFC EB-23

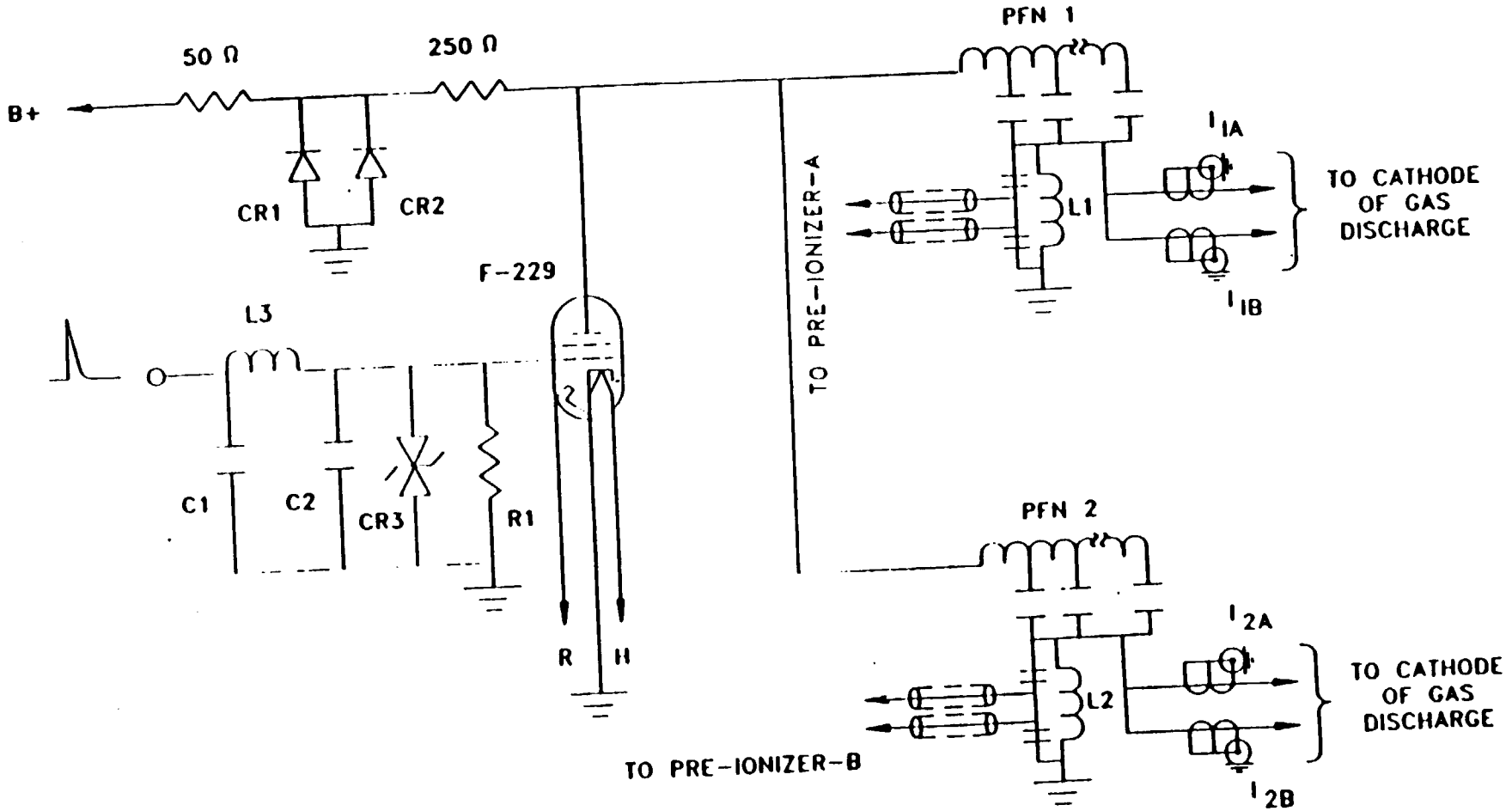

COMPETITION SENSITIVE

STI BIPOLAR DISCHARGE

NASA
MSFC EB-23

- Unipolar

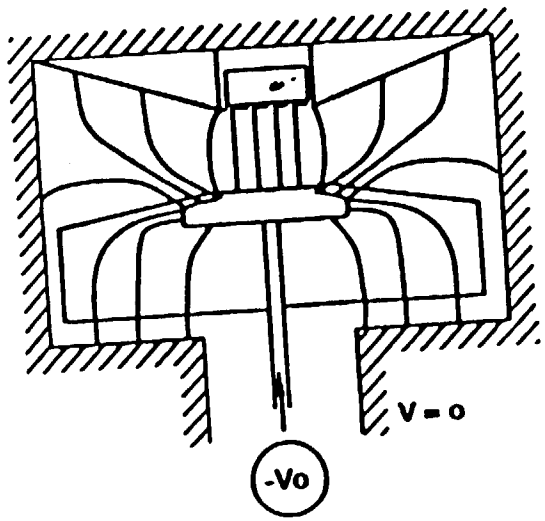

- Bipolar

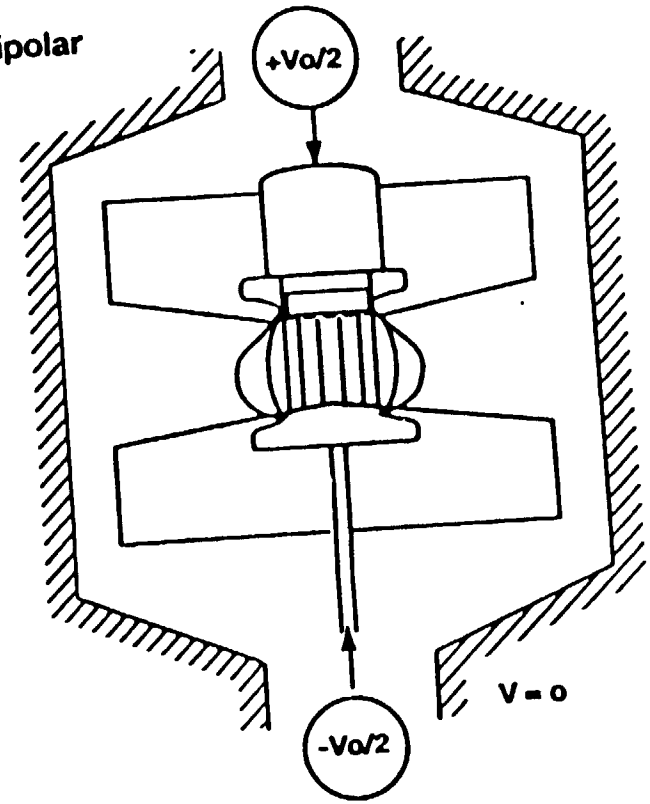

01 10641

- High Fields to Ground (stray)
- Surface Flashover is More Likely
- Higher Voltage Insulator

- Strongest Field is Between Electrodes
- Insulator Stress is Halved
- Voltage is Halved

COMPETITION SENSITIVE

148

STI BIPOLAR DISCHARGE

NASA
MSFC EB-23

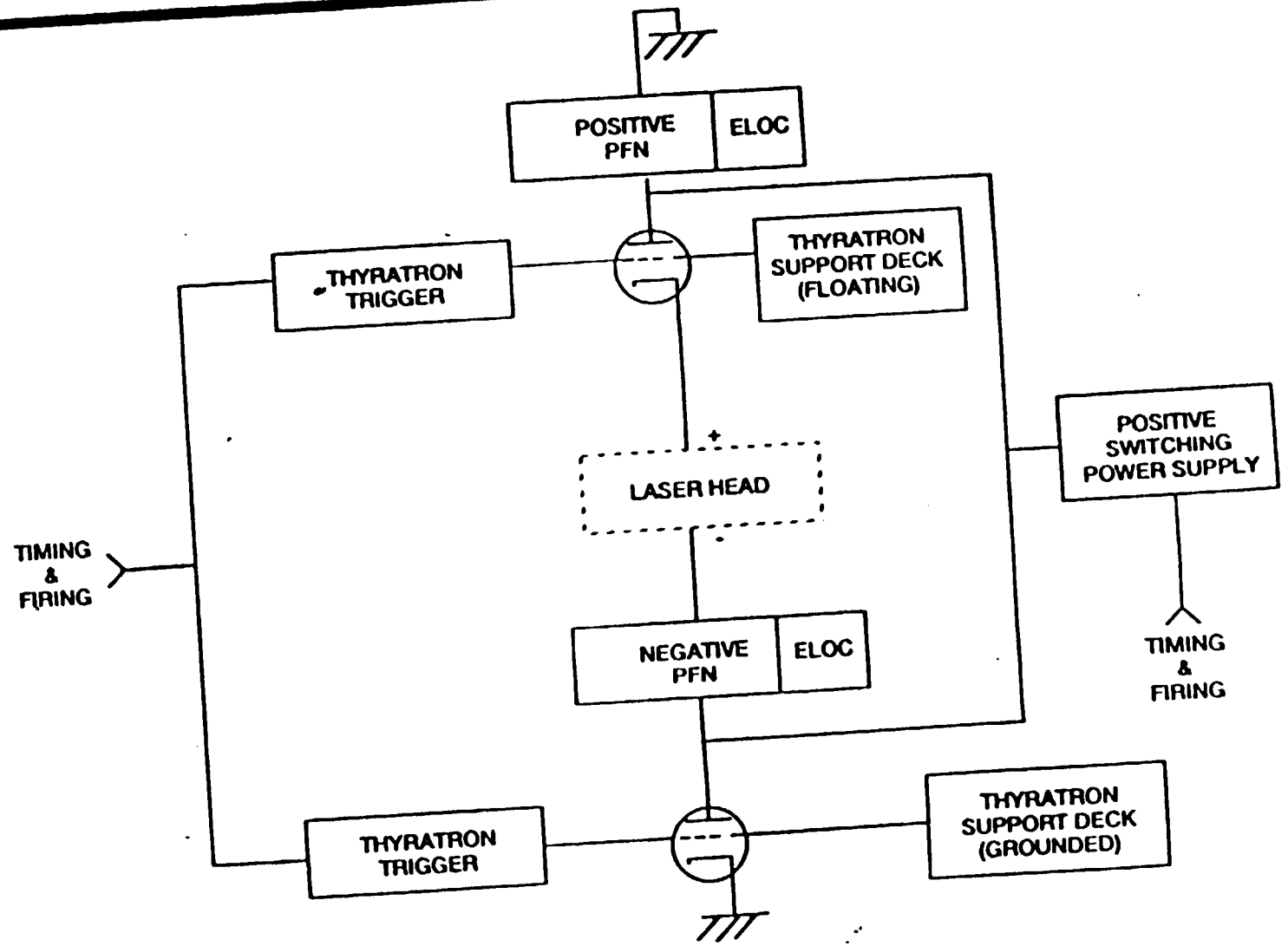

COMPETITION SENSITIVE

GDS BB R.1.0 9/17/91

BB. DESIGN COMPARISON

NASA
MSFC EB-23

Flow Loop	Textron	STI
No. of Fans	2	1
Cavity Flush Factor	3	3
Gas Velocity (m/s)	2.4	3
Fan Speed (RPM)	2400	3000

051-150

TDS FLOW LOOP

NASA
MSFC EB-23

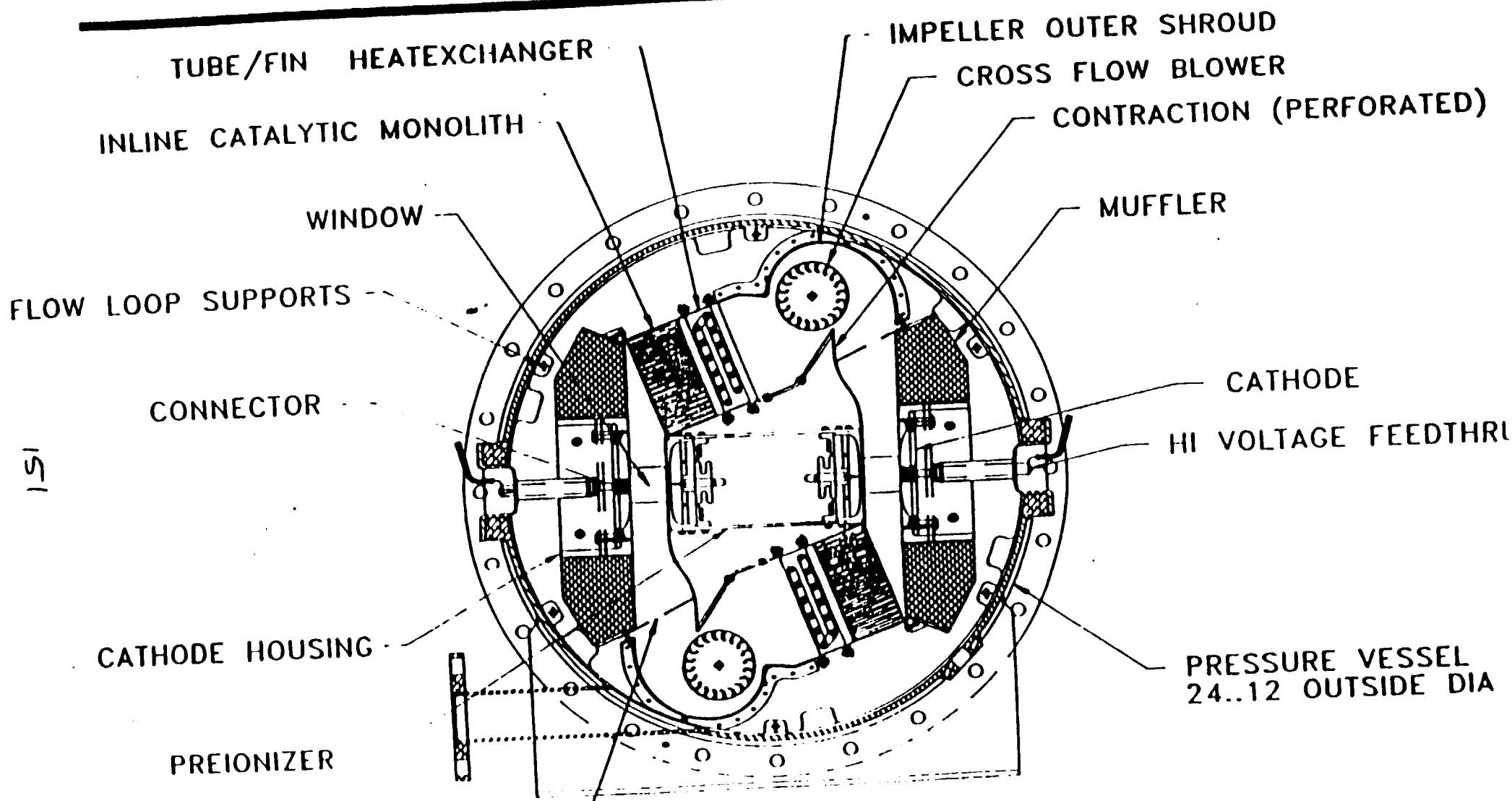

151

COMPETITION SENSITIVE

GDS BB R.1.0 9/17/91

STI FLOW LOOP

NASA
MSFC EB-23

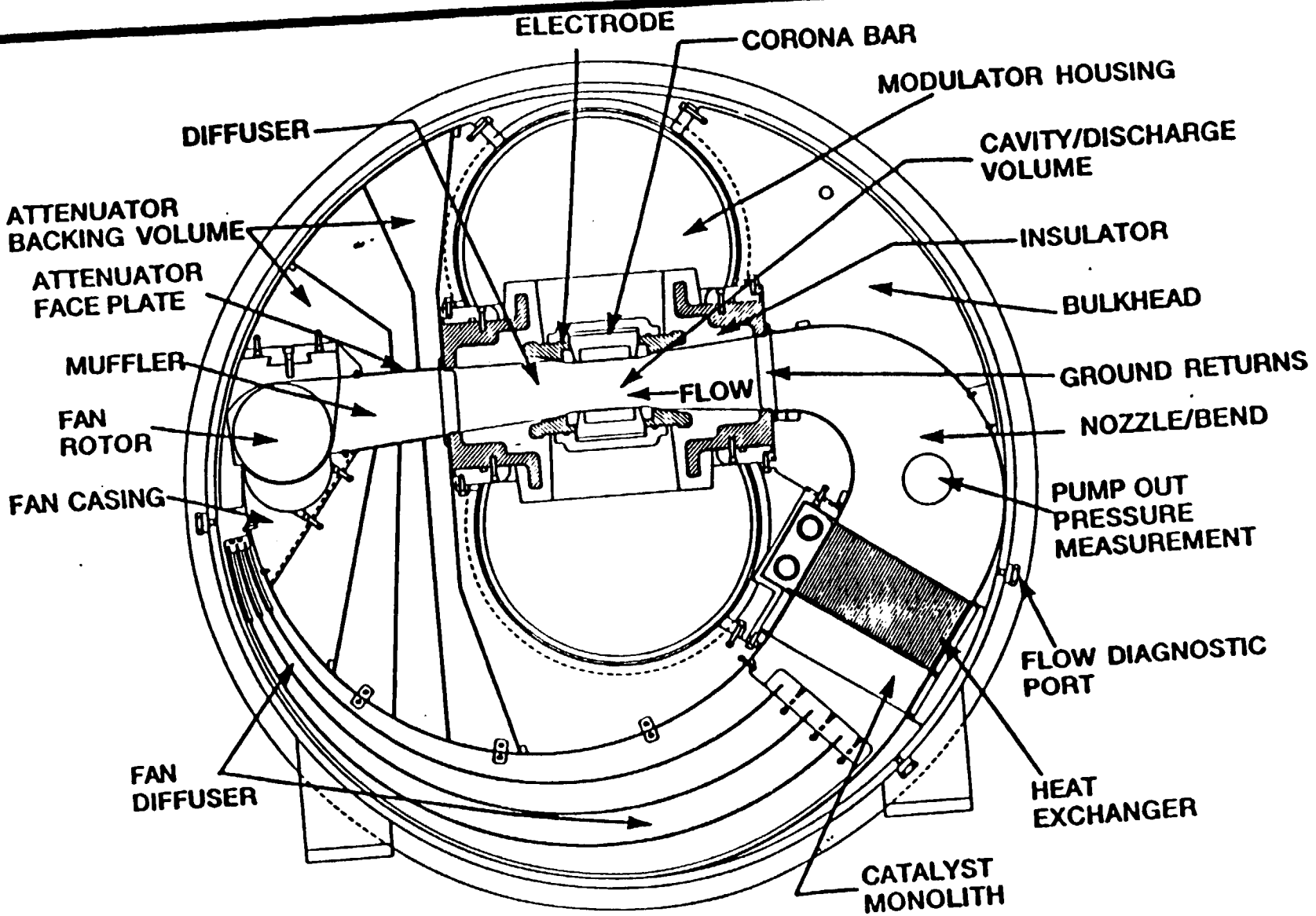

COMPETITION SENSITIVE

LAWS BB. CATALYST

NASA
MSFC EB-23

Catalyst from two sources will be tested in the breadboard devices. These sources are NASA LaRC and UOP.

- UOP is loaning STI some catalyst to use in the COLT life test device. LaRC will also supply catalyst for use in the COLT device to enable a comparison of the two catalysts to be made.

- Life testing of the LaRC catalyst will occur at STI, whilst life testing of the UOP catalyst will occur at TDS.

- In both cases initial tests will be carried out with Oxygen-16 before changing to the Oxygen-18 isotope. These Oxygen-16 tests will go to ~10^7 pulses.

TEXTRON DVTS

NASA
MSFC EB-23

Resonator

- Same resonator geometry as breadboard but shorter gain length (0.67 m).
- Demonstrated cavity matching technique.
- Demonstrated injection technique and obtained SLM and STM operation.

Oxygen-18

- Small DVT to obtain 'hands-on' experience.
- Measure gain and extraction efficiencies.
- Verify 9.11 um line selection using grating.

Discharge

- Study different preioniser materials for reliability.
- Optimise electrode length.
- Accelerated testing of chosen preioniser and thyratron.

TDS RESONATOR DVT

NASA
MSFC EB-23

Demonstration of successful cavity locking and injection to produce SLM and STM

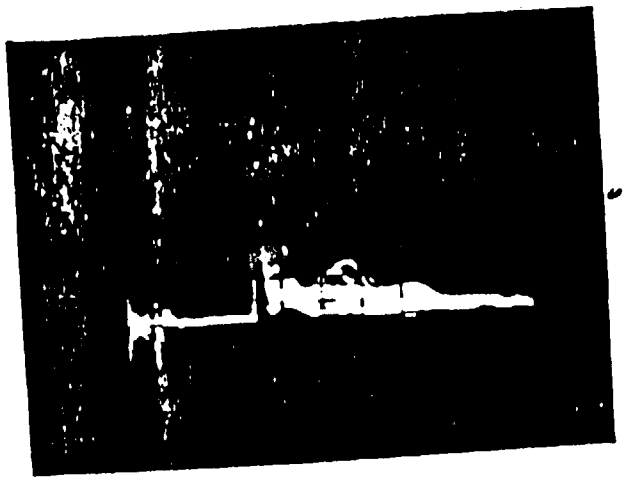

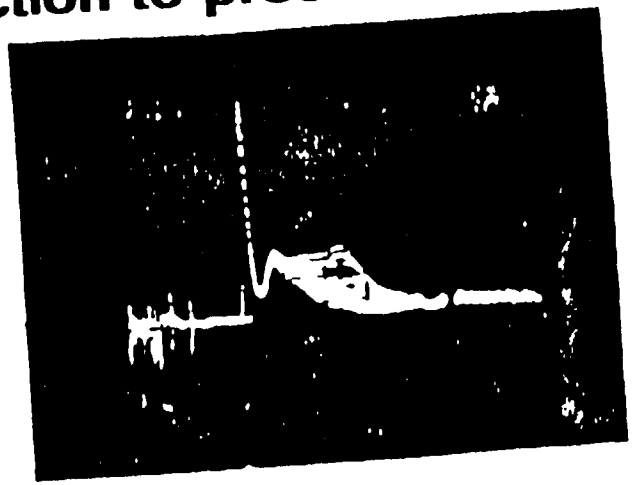

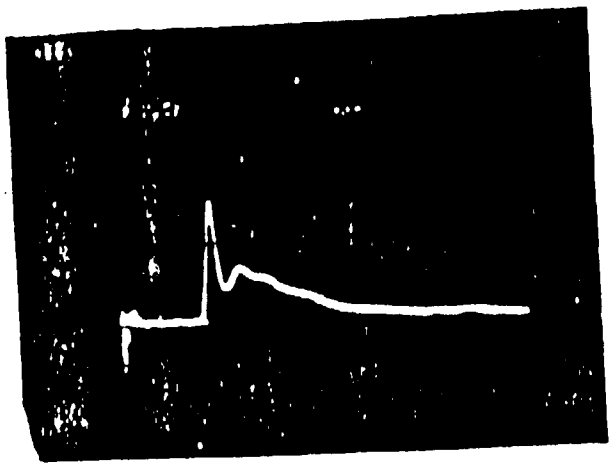

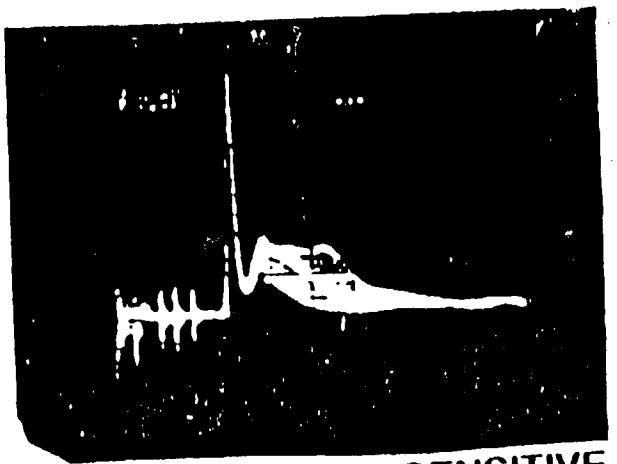

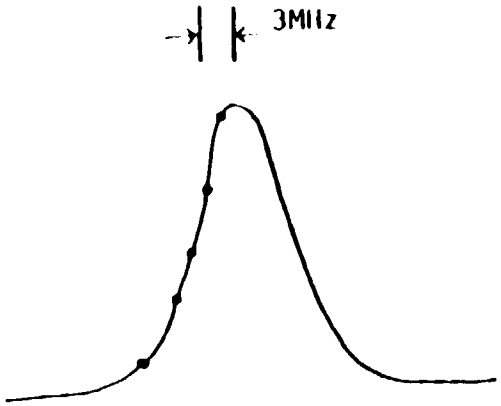

551

COMPETITION SENSITIVE

STI OPTRONICS DVTS

NASA
MSFC EB-23

Life Breadboard

- Using two breadboards one for performance, the other for life testing.
- Uses existing COLT device to do accelerated life testing (50 Hz) of components, gas and materials.

Discharge and Pulsed Power

- Ceramic preioniser selection based on previous DVT work.
- Preioniser life demonstrated $> 5 \times 10^6$ pulses on COLT.
- $> 3 \times 10^8$ pulse life on excimer laser.
- Investigation of bipolar excitation technology.
- Investigating alternative HV switches.

Fan Design

- Based on DVTs conducted for CORA.

COMPETITION SENSITIVE

9.51

STI SCHEDULE

NASA
MSFC EB-23

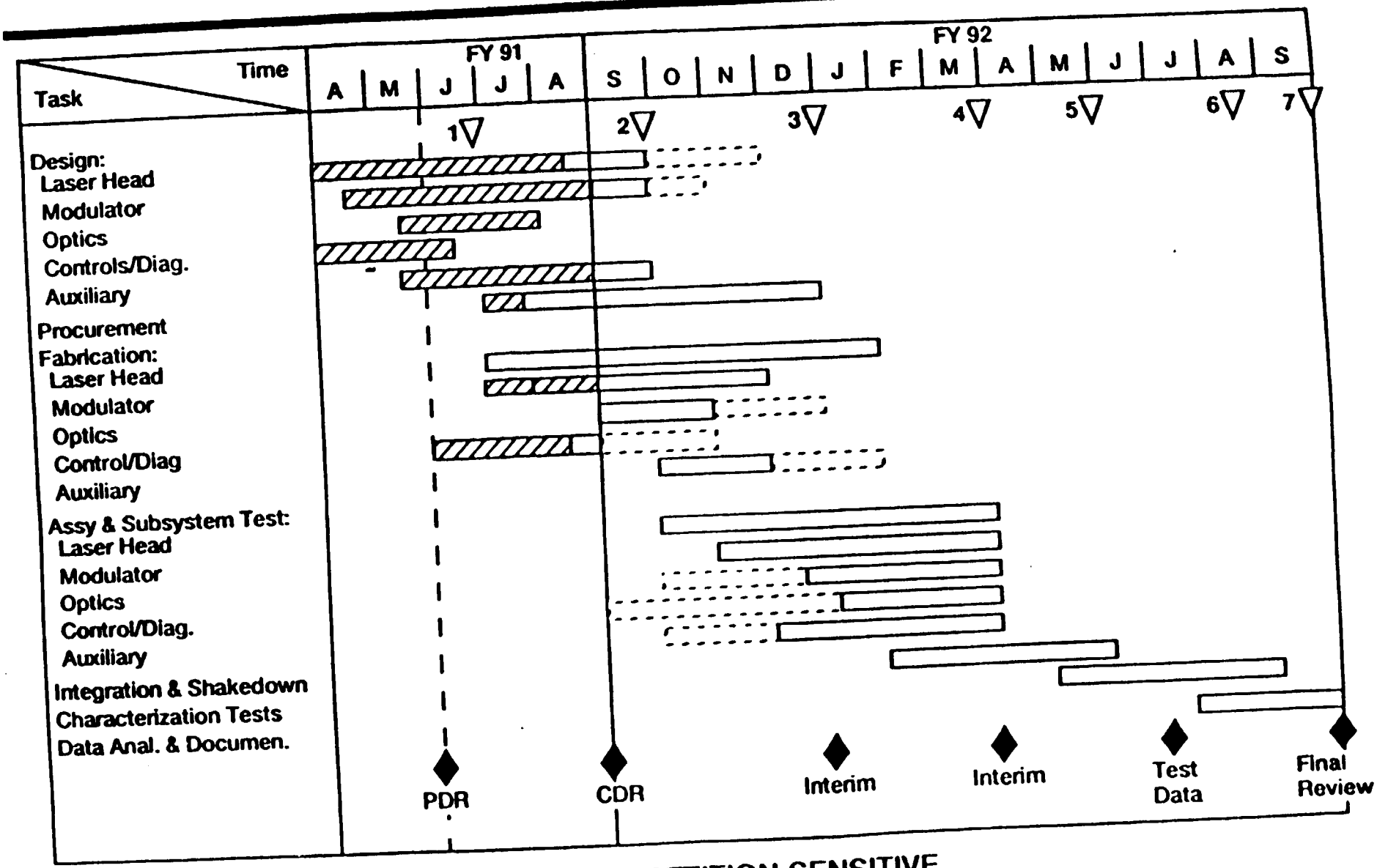

COMPETITION SENSITIVE

GDS BB B 1.0 9/17/91

STI BREADBOARD STATUS

NASA
MSFC EB-23

- STI Breadboard Final Design Review was on 8/27/91.
- Detailed component drawings to be started on some aspects of the laser head.
- Control and modulator systems ~80 % complete.
- .Laser head design 2 - 3 weeks behind schedule.
- Modulator ahead of schedule.
- Heat exchanger and control components purchased.
- Laboratory modifications underway, complete mid to end of September.

TDS SCHEDULE

NASA
MSFC EB-23

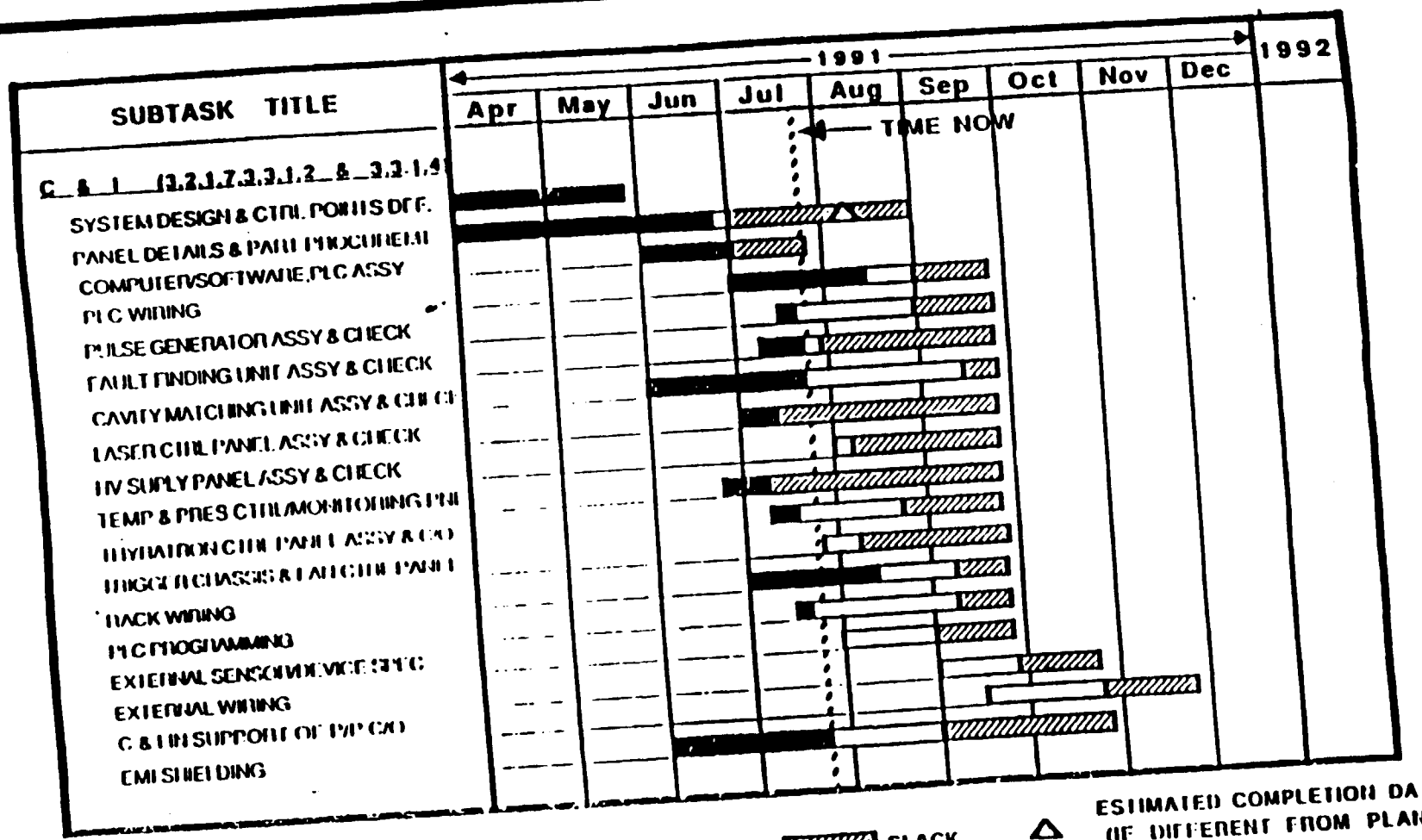

NOTE: BLACKENED AREA IN THE SCHEDULE COMPLETION LINE SPACE FROM TIME NOW LINE APPROXIMATES THE TRUE AHEAD OF/BEHIND SCHEDULE.

COMPETITION SENSITIVE

TDS BREADBOARD STATUS

NASA
MSFC EB-23

- TDS Breadboard Final Design Review was on 9/5/91.
- Subsystems design 80 - 90 % complete. Pulsed power and control systems under fabrication.
- Design will be completed by 9/30/91.
- Major design issues have been resolved by initial DVTs.
- Overall program cost and schedule on target.